SUPPLEMENTARY MATERIAL

Christina Georgakopoulou[a‡], Dimitrios Thomos[a‡], Theodoros Tsolis[a], Konstantinos Ypsilantis[a], John C. Plakatouras[a,e], Dimitrios Kordias[b,c], Angeliki Magklara[b,c,d], ,Constantine Kouderis[a], Angelos G. Kalampounias[a,e], and Achilleas Garoufis[a,e,*]

[a] Department of Chemistry, University of Ioannina, GR-45110 Ioannina, Greece

[b] Institute of Molecular Biology and Biotechnology-Foundation for Research and Technology, 45110 Ioannina, Greece

[c] Laboratory of Clinical Chemistry, Faculty of Medicine, University of Ioannina, 45110 Ioannina, Greece

[d] Institute of Biosciences, University Research Center of Ioannina (U.R.C.I.), Ioannina, Greece [e] University Research Center of Ioannina (URCI), Institute of Materials Science and Computing, Ioannina, Greece

Table of contents

Table S1: Crystal data and structure refinement for complex $(4)(PF_6)_4$.

Figure S15: ^1H NMR Spectra of $d(CGCGAATTCGCG)_2$ in H_2O/ D_2O 9:1 (buffer phosphate 100 mM, pH = 7.0) at 298 K, 500 MHz.

Figure S16: ^1H – ^1H COSY NMR Spectra of $d(CGCGAATTCGCG)_2$ in H_2O/ D_2O 9:1 (buffer phosphate 100 mM, pH = 7.0) at 298 K, 500 MHz.

Figure S17: ^1H – ^1H NOESY NMR Spectra of $d(CGCGAATTCGCG)_2$ in H_2O/ D_2O 9:1 (buffer phosphate 100 mM, pH = 7.0) at 298 K, 500 MHz, t_{mix} = 350 ms.

Figure S18: ^1H NMR Spectra of $d(CGCGAATTCGCG)_2$ upon addition of complex $(4)Cl_4$ at r = 0.5 in H_2O/ D_2O 9:1 (buffer phosphate 100 mM, pH = 7.0) at 298 K, 500 MHz.

Figure S19: ^1H – ^1H COSY NMR Spectra of $d(CGCGAATTCGCG)_2$ upon addition of complex $(4)Cl_4$ at r = 0.5 in H_2O/ D_2O 9:1 (buffer phosphate 100 mM, pH = 7.0) at 298 K, 500 MHz.

Figure S20: ^1H – ^1H NOESY NMR Spectra of $d(CGCGAATTCGCG)_2$ upon addition of complex $(4)Cl_4$ at r = 0.5 in H_2O/ D_2O 9:1 (buffer phosphate 100 mM, pH = 7.0) at 298 K, 500 MHz, t_{mix} = 350 ms.

Figure S21: ^1H NMR Spectra of $d(CGCGAATTCGCG)_2$ upon addition of complex $(4)Cl_4$ at r = 1 in H_2O/ D_2O 9:1 (buffer phosphate 100 mM, pH = 7.0) at 298 K, 500 MHz.

Figure S22: ^1H – ^1H COSY NMR Spectra of $d(CGCGAATTCGCG)_2$ upon addition of complex $(4)Cl_4$ at r = 1 in H_2O/ D_2O 9:1 (buffer phosphate 100 mM, pH = 7.0) at 298 K, 500 MHz.

Figure S23: ^1H – ^1H NOESY NMR Spectra of $d(CGCGAATTCGCG)_2$ upon addition of complex $(4)Cl_4$ at r = 1 in H_2O/ D_2O 9:1 (buffer phosphate 100 mM, pH = 7.0) at 298 K, 500 MHz, t_{mix} = 350 ms.

Figure S24: ^1H NMR Spectra of $d(CGCGAATTCGCG)_2$ upon addition of complex $(4)Cl_4$ at r = 2 in H_2O/ D_2O 9:1 (buffer phosphate 100 mM, pH = 7.0) at 298 K, 500 MHz.

Figure S25: ^1H – ^1H COSY NMR Spectra of $d(CGCGAATTCGCG)_2$ upon addition of complex $(4)Cl_4$ at r = 2 in H_2O/ D_2O 9:1 (buffer phosphate 100 mM, pH = 7.0) at 298 K, 500 MHz.

Figure S26: ^1H – ^1H NOESY NMR Spectra of $d(CGCGAATTCGCG)_2$ upon addition of complex $(4)Cl_4$ at r = 2 in H_2O/ D_2O 9:1 (buffer phosphate 100 mM, pH = 7.0) at 298 K, 500 MHz, t_{mix} = 350 ms.

Table S2: Differences in ^1H chemical shifts of the $d(CGCGAATTCGCG)_2$ (buffer phosphate 100 mM, pH = 7.0) upon the addition of complex $(4)Cl_4$ in various [Ru]/nucleotide ratios at 298 K, 500 MHz. Values in parenthesis denote upfield (-) or downfield (+) shifts from the free oligonucleotide under the same conditions.

Figure S27: ^1H NMR Spectra of $d(CGCGAATTCGCG)_2$ upon addition of complex $(5)Cl_4$ at r = 0.5 in H_2O/ D_2O 9:1 (buffer phosphate 100 mM, pH = 7.0) at 298 K, 500 MHz.

Figure S28: ^1H – ^1H COSY NMR Spectra of $d(CGCGAATTCGCG)_2$ upon addition of complex $(5)Cl_4$ at r = 0.5 in H_2O/ D_2O 9:1 (buffer phosphate 100 mM, pH = 7.0) at 298 K, 500 MHz.

Figure S29: ^1H – ^1H NOESY NMR Spectra of $d(CGCGAATTCGCG)_2$ upon addition of complex $(5)Cl_4$ at r = 0.5 in H_2O/ D_2O 9:1 (buffer phosphate 100 mM, pH = 7.0) at 298 K, 500 MHz, t_{mix} = 350 ms.

Figure S30: ^1H NMR Spectra of $d(CGCGAATTCGCG)_2$ upon addition of complex $(5)Cl_4$ at r = 1 in H_2O/ D_2O 9:1 (buffer phosphate 100 mM, pH = 7.0) at 298 K, 500 MHz.

Figure S31: ^1H – ^1H COSY NMR Spectra of $d(CGCGAATTCGCG)_2$ upon addition of complex $(5)Cl_4$ at r = 1 in H_2O/ D_2O 9:1 (buffer phosphate 100 mM, pH = 7.0) at 298 K, 500 MHz.

Figure S32: ^1H – ^1H NOESY NMR Spectra of $d(CGCGAATTCGCG)_2$ upon addition of complex $(5)Cl_4$ at r = 1 in H_2O/ D_2O 9:1 (buffer phosphate 100 mM, pH = 7.0) at 298 K, 500 MHz, t_{mix} = 350 ms.

Figure S33: ^1H NMR Spectra of $d(CGCGAATTCGCG)_2$ upon addition of complex $(5)Cl_4$ at r = 2 in H_2O/ D_2O 9:1 (buffer phosphate 100 mM, pH = 7.0) at 298 K, 500 MHz.

Figure S34: ^1H – ^1H COSY NMR Spectra of $d(CGCGAATTCGCG)_2$ upon addition of complex $(5)Cl_4$ at r = 2 in H_2O/ D_2O 9:1 (buffer phosphate 100 mM, pH = 7.0) at 298 K, 500 MHz.

Figure S35: ^1H – ^1H NOESY NMR Spectra of $d(CGCGAATTCGCG)_2$ upon addition of complex $(5)Cl_4$ at r = 2 in H_2O/ D_2O 9:1 (buffer phosphate 100 mM, pH = 7.0) at 298 K, 500 MHz, t_{mix} = 350 ms.

Table S3: Differences in ^1H chemical shifts of the d(CGCGAATTCGCG)$_2$ (buffer phosphate 100 mM, pH = 7.0) upon the addition of complex (5)$(Cl)_4$ in various [Ru]/nucleotide ratios at 298 K, 500 MHz. Values in parenthesis denote upfield (-) or downfield (+) shifts from the free oligonucleotide under the same conditions.

Figure S36: ^1H NMR Spectra of d(CGCGAATTCGCG)$_2$ upon addition of complex (6)Cl_4 at r = 0.5 in H_2O/ D_2O 9:1 (buffer phosphate 100 mM, pH = 7.0) at 298 K, 500 MHz.

Figure S37: ^1H – ^1H COSY NMR Spectra of d(CGCGAATTCGCG)$_2$ upon addition of complex (6)Cl_4 at r = 0.5 in H_2O/ D_2O 9:1 (buffer phosphate 100 mM, pH = 7.0) at 298 K, 500 MHz.

Figure S38: ^1H – ^1H NOESY NMR Spectra of d(CGCGAATTCGCG)$_2$ upon addition of complex (6)Cl_4 at r = 0.5 in H_2O/ D_2O 9:1 (buffer phosphate 100 mM, pH = 7.0) at 298 K, 500 MHz, t_{mix} = 350 ms.

Figure S39: ^1H NMR Spectra of d(CGCGAATTCGCG)$_2$ upon addition of complex (6)Cl_4 at r =1 in H_2O/ D_2O 9:1 (buffer phosphate 100 mM, pH = 7.0) at 298 K, 500 MHz.

Figure S40: ^1H – ^1H COSY NMR Spectra of d(CGCGAATTCGCG)$_2$ upon addition of complex (6)Cl_4 at r = 1 in H_2O/ D_2O 9:1 (buffer phosphate 100 mM, pH = 7.0) at 298 K, 500 MHz.

Figure S41: ^1H – ^1H NOESY NMR Spectra of d(CGCGAATTCGCG)$_2$ upon addition of complex (6)Cl_4 at r = 1 in H_2O/ D_2O 9:1 (buffer phosphate 100 mM, pH = 7.0) at 298 K, 500 MHz, t_{mix} = 350 ms.

Figure S42: ^1H NMR Spectra of d(CGCGAATTCGCG)$_2$ upon addition of complex (6)Cl_4 at r =2 in H_2O/ D_2O 9:1 (buffer phosphate 100 mM, pH = 7.0) at 298 K, 500 MHz.

Figure S43: ^1H – ^1H COSY NMR Spectra of d(CGCGAATTCGCG)$_2$ upon addition of complex (6)Cl_4 at r = 2 in H_2O/ D_2O 9:1 (buffer phosphate 100 mM, pH = 7.0) at 298 K, 500 MHz.

Figure S44: ^1H – ^1H NOESY NMR Spectra of d(CGCGAATTCGCG)$_2$ upon addition of complex (6)Cl_4 at r = 2 in H_2O/ D_2O 9:1 (buffer phosphate 100 mM, pH = 7.0) at 298 K, 500 MHz, t_{mix} = 350 ms.

Table S4: Differences in ^1H chemical shifts of the d(CGCGAATTCGCG)$_2$ (buffer phosphate 100 mM, pH = 7.0) upon the addition of complex (6)Cl_4 in various [Ru]/nucleotide ratios at 298 K, 500 MHz. Values in parenthesis denote upfield (-) or downfield (+) shifts from the free oligonucleotide under the same conditions.

Figure S45: ^1H NMR Spectra of d(CGCGAATTCGCG)$_2$ upon addition of the (7)Cl_2 at r =0.5 in H_2O/ D_2O 9:1 (buffer phosphate 100 mM, pH = 7.0) at 298 K, 500 MHz.

Figure S46: ^1H – ^1H COSY NMR Spectra of d(CGCGAATTCGCG)$_2$ upon addition of the (7)Cl_2 at r =0.5 in H_2O/ D_2O 9:1 (buffer phosphate 100 mM, pH = 7.0) at 298 K, 500 MHz.

Figure S47: ^1H – ^1H NOESY NMR Spectra of d(CGCGAATTCGCG)$_2$ upon addition of the (7)Cl_2 at r =0.5 in H_2O/ D_2O 9:1 (buffer phosphate 100 mM, pH = 7.0) at 298 K, 500 MHz, t_{mix} = 350 ms.

Figure S48: Fluorescence emission spectra of DNA–EtBr system with various concentration of complex (**1**) {A}, complex (**2**) {B}, complex (**3**) {C}, complex (**4**) {D}, complex (**5**) {E} and complex (**6**) {F}. [DNA] = 20 µM, [EB] = 5.2 µM, concentration of complexes = 0 – 20.10 µM at 291 K.

Figure S49: Fluorescence emission spectra of DNA–EtBr system with various concentration of complex (**1**) {A}, complex (**2**) {B}, complex (**3**) {C}, complex (**4**) {D}, complex (**5**) {E} and complex (**6**) {F}. [DNA] = 20 µM, [EB] = 5.2 µM, concentration of complexes = 0 – 20.10 µM at 310 K.

Figure S50: Stern–Volmer plots for the interaction of complexes with DNA–EtBr at three different temperatures (291 K, 298 K, and 310 K).

Table S5: Binding parameters of the bimetallic Ru(II) complexes with d(CGCGAATTCGCG)$_2$ at 291 K and 310 K.

Figure S51: The double-log plot of complexes quenching effect on d(CGCGAATTCGCG)$_2$-EtBr system fluorescence at three different temperatures (291 K, 298 K and 310 K) and the van't Hoff plot for the binding of complexes with d(CGCGAATTCGCG)$_2$. (A) for complex **(1)**, (B) for complex **(2)** and (C) for complex **(3)**.

Figure S52: The double-log plot of complexes quenching effect on d(CGCGAATTCGCG)$_2$-EtBr system fluorescence at three different temperatures (291 K, 298 K and 310 K) and the van't Hoff plot for the binding of complexes with d(CGCGAATTCGCG)$_2$. (A) for complex **(4)**, (B) for complex **(5)** and (C) for complex **(6)**.

Figure S53: Fluorescence emission spectra of DNA–EtBr system with various concentration of complex [[η^6-cym)Ru(phen)(py)]$^{2+}$. [DNA] = 20 µM, [EB] = 5.2 µM, and [[η^6-cym)Ru(phen)(py)]$^{2+}$ = 0 – 20.10 µM at 298 K (A). Stern–Volmer plots for the interaction of [[η^6-cym)Ru(phen)(py)]$^{2+}$ with DNA–EtBr at 298 K (B). The double-log plot of complex [[η^6-cym)Ru(phen)(py)]$^{2+}$ quenching effect on d(CGCGAATTCGCG)$_2$-EtBr system fluorescence at 298 K (C).

Table S6: Thermodynamic parameters of the bimetallic Ru(II) complexes with $d(CGCGAATTCGCG)_2$ at 291 K and 310 K.

Figure S54: The van't Hoff plots for the binding of complexes with $d(CGCGAATTCGCG)_2$. (A) for complex **(1)**, (B) for complex **(2)**, (C) for complex **(3)**, (D) for complex **(4)**, (E) for complex **(5)** and (F) for complex **(6)**.

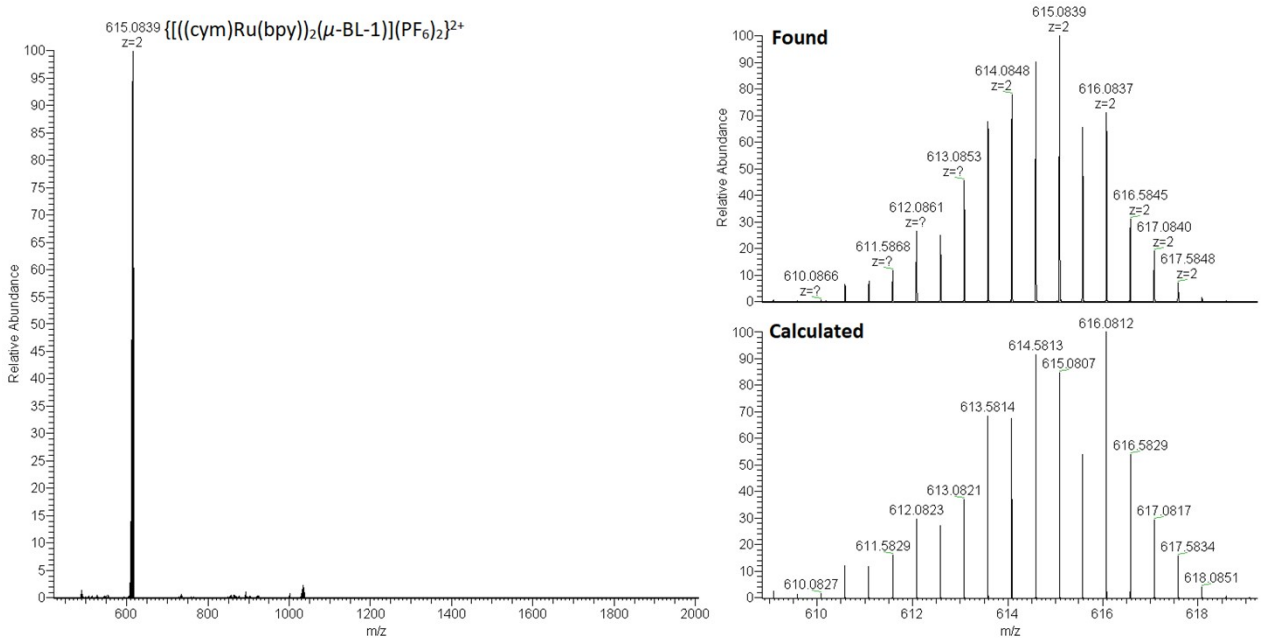

Figure S1: HR-ESI-MS of the complex (1)$(PF_6)_4$ in acetone at 298 K.

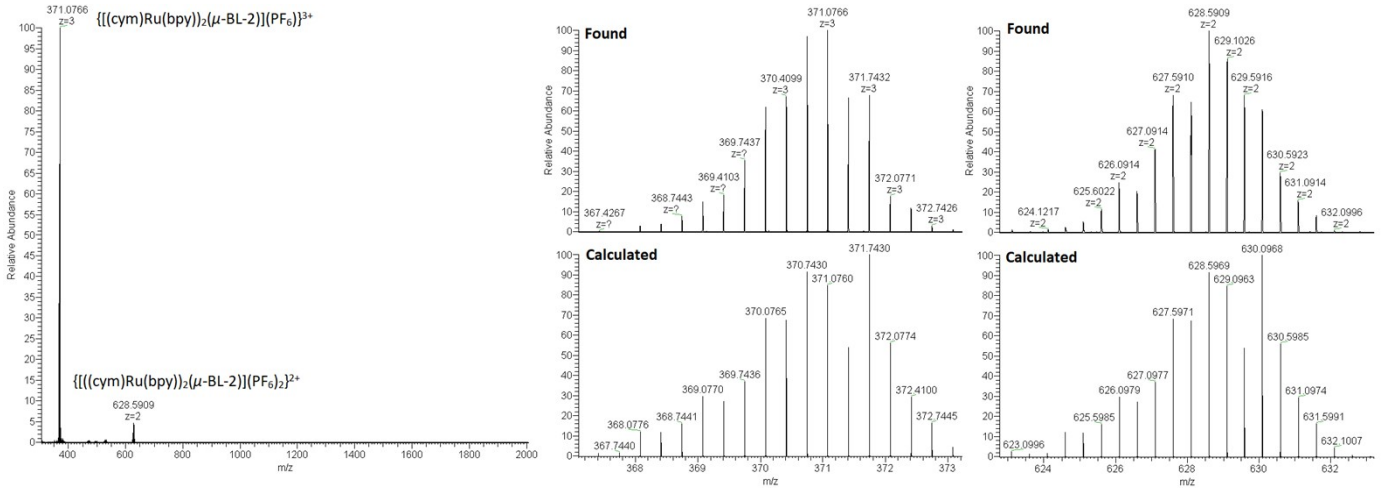

Figure S2: HR-ESI-MS of the complex (2)$(PF_6)_4$ in acetone at 298 K.

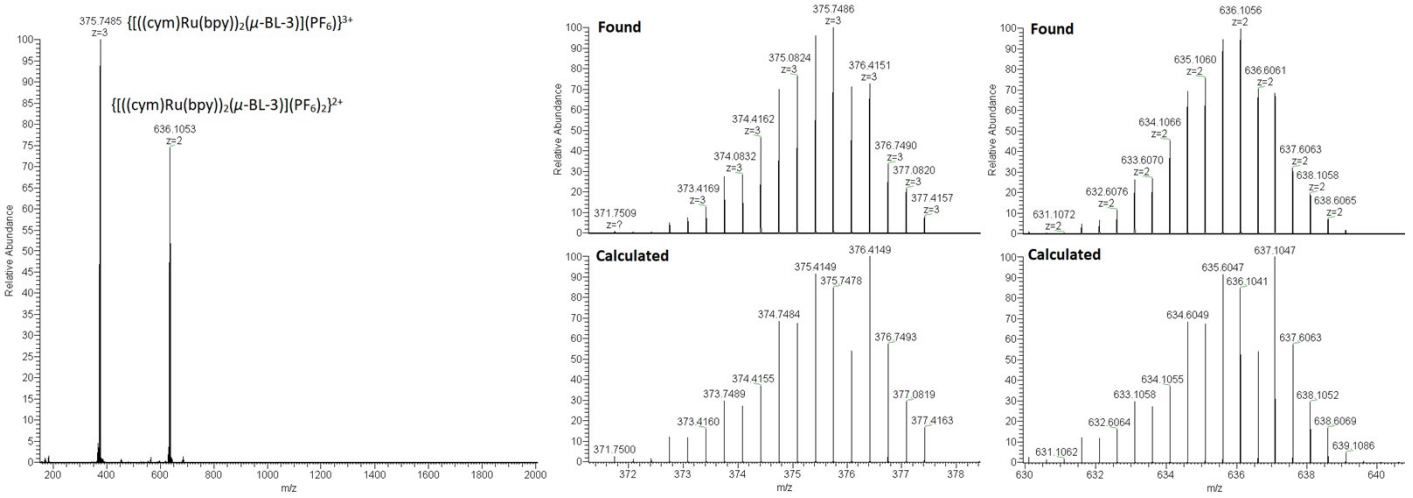

Figure S3: HR-ESI-MS of the complex (3)$(PF_6)_4$ in acetone at 298 K.

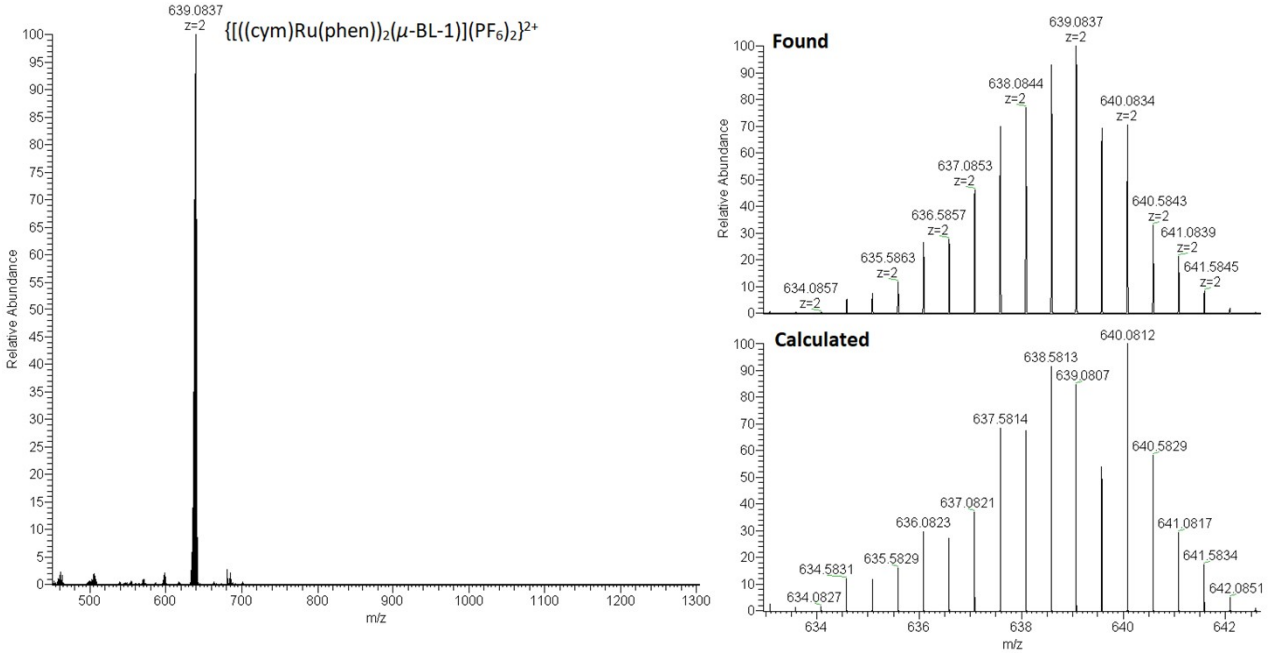

Figure S4: HR-ESI-MS of the complex (4)$(PF_6)_4$ in acetone at 298 K.

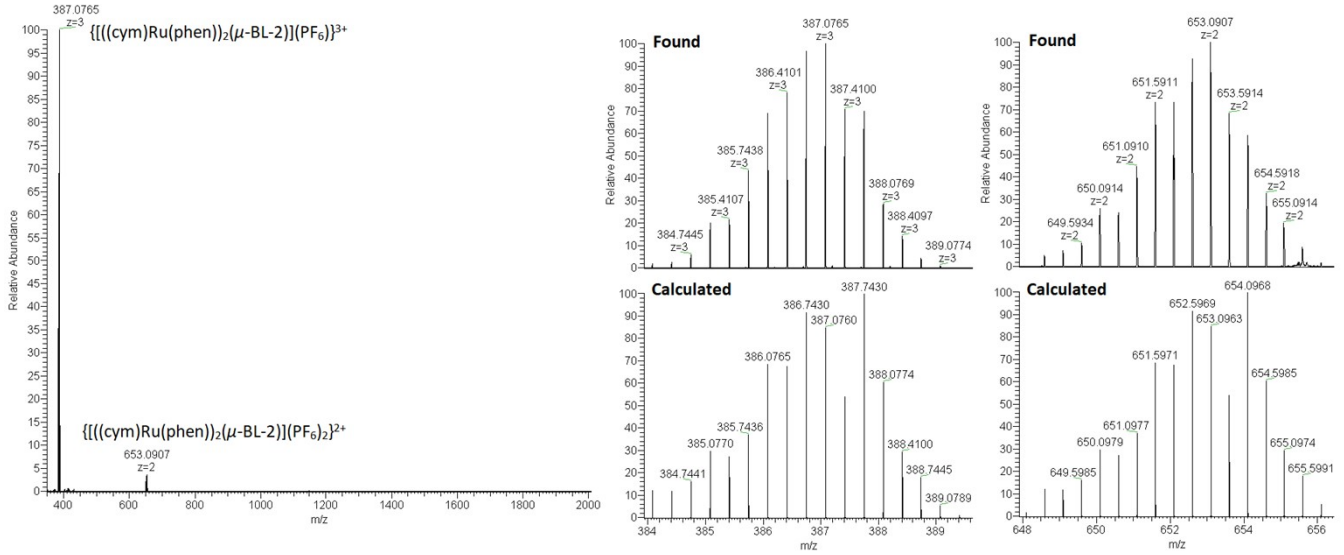

Figure S5: HR-ESI-MS of the complex (5)$(PF_6)_4$ in acetone at 298 K.

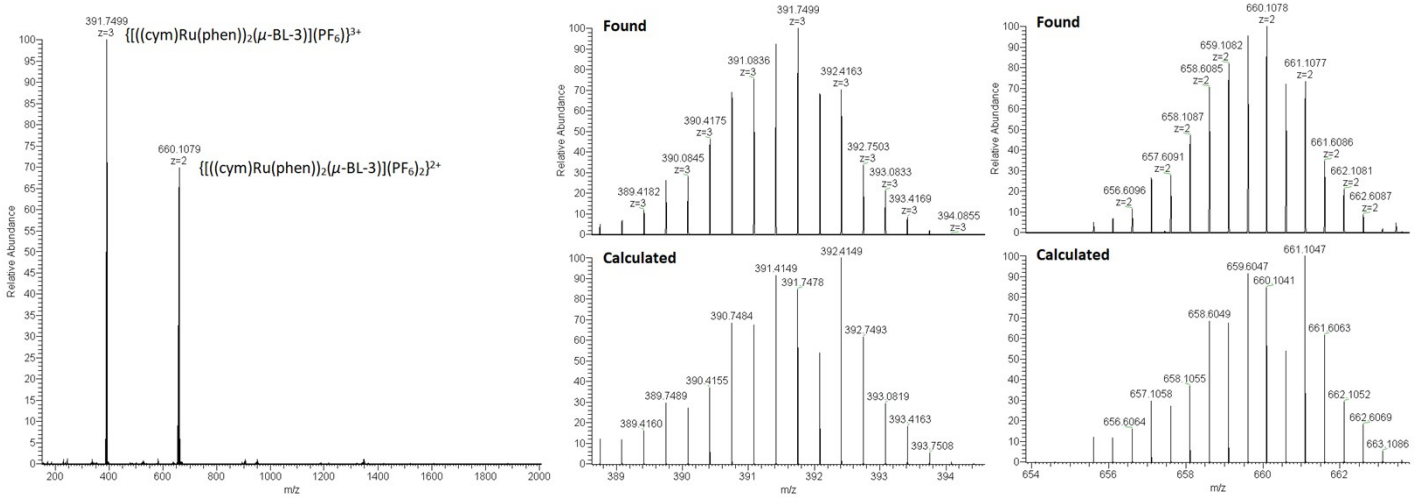

Figure S6: HR-ESI-MS of the complex (6)$(PF_6)_4$ in acetone at 298 K.

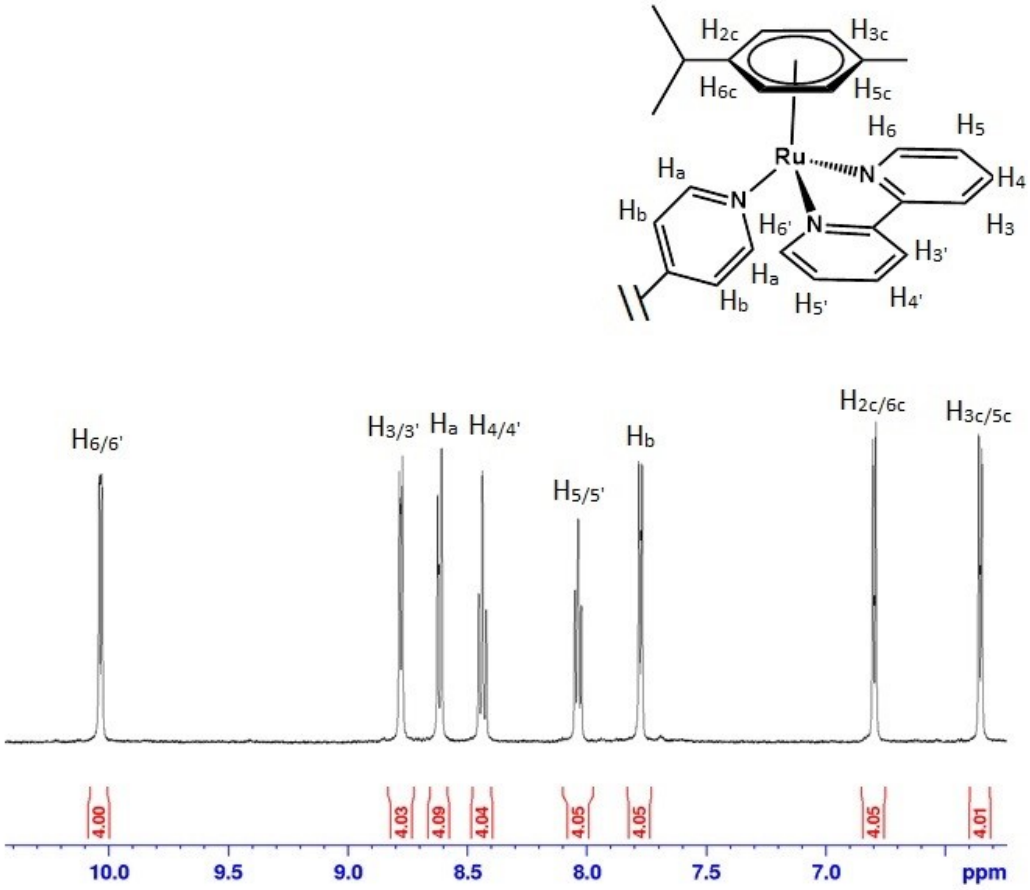

Figure S7a: The aromatic part of the ^{1}H NMR spectrum of the complex $(1)(PF_6)_4$ in acetone-d_6 at 298 K. Half complex shown for clarity.

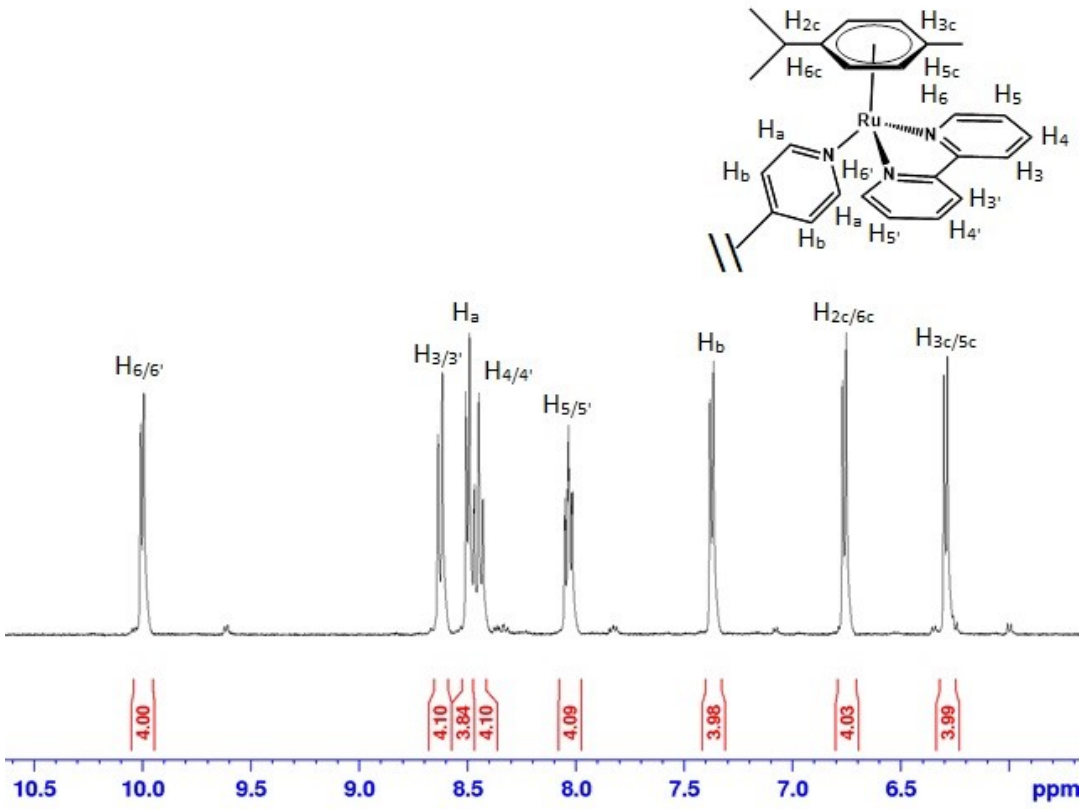

Figure S8a: The aromatic part of the ^{1}H NMR spectrum of the complex (2)$(PF_6)_4$ in acetone-d_6 at 298 K. Half complex shown for clarity.

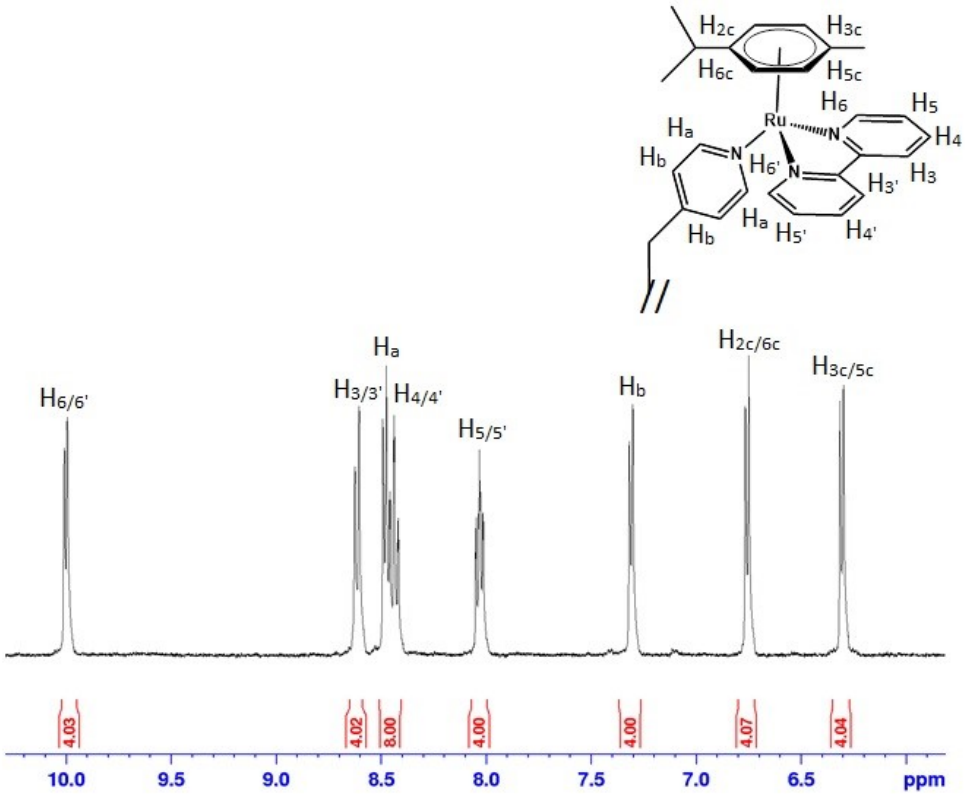

Figure S9a: The aromatic part of the ^{1}H NMR spectrum of the complex (3)$(PF_6)_4$ in acetone-d_6 at 298 K. Half complex shown for clarity.

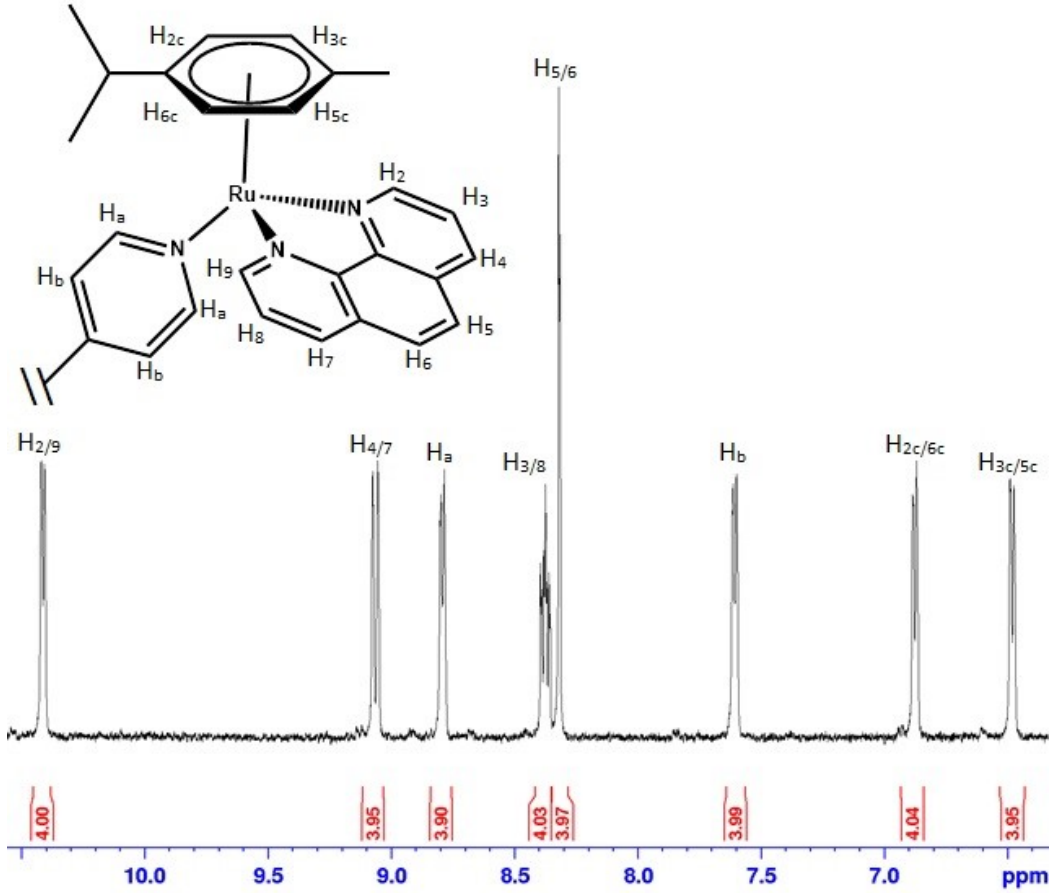

Figure S10a: The aromatic part of the ^{1}H NMR spectrum of the complex (4)$(PF_6)_4$ in acetone-d_6 at 298 K. Half complex shown for clarity.

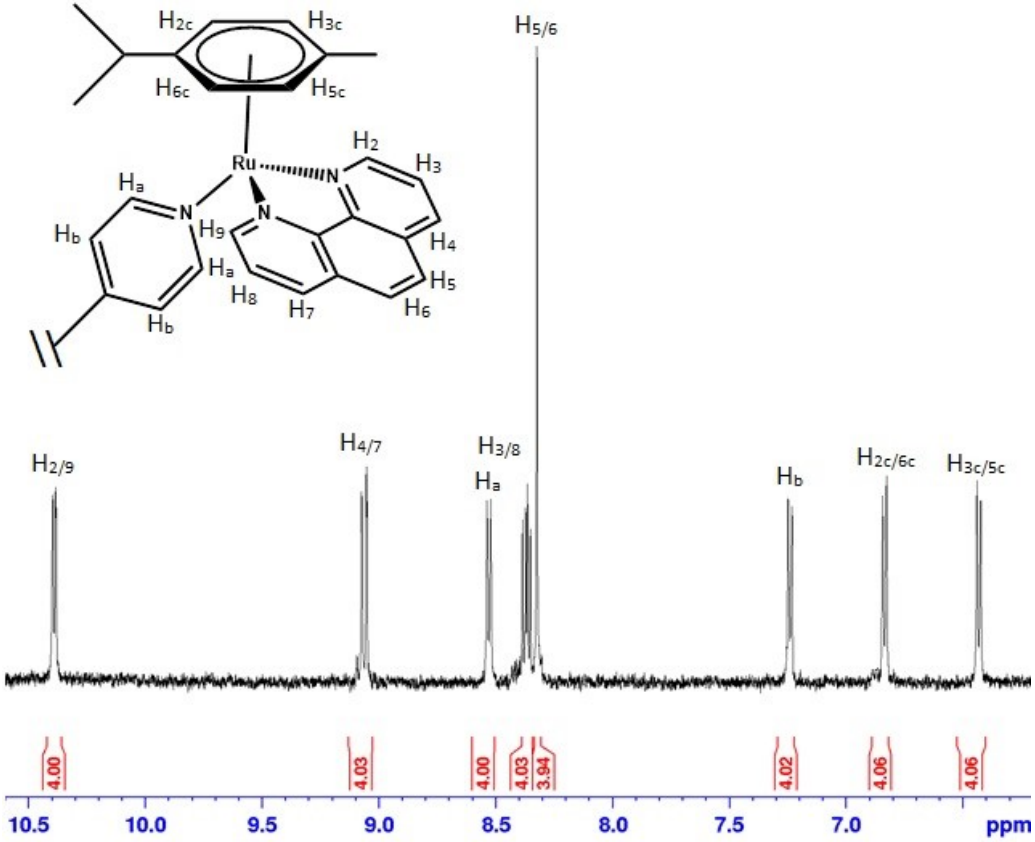

Figure S11a: The aromatic part of the ^{1}H NMR spectrum of the complex (5)$(PF_6)_4$ in acetone-d_6 at 298 K. Half complex shown for clarity.

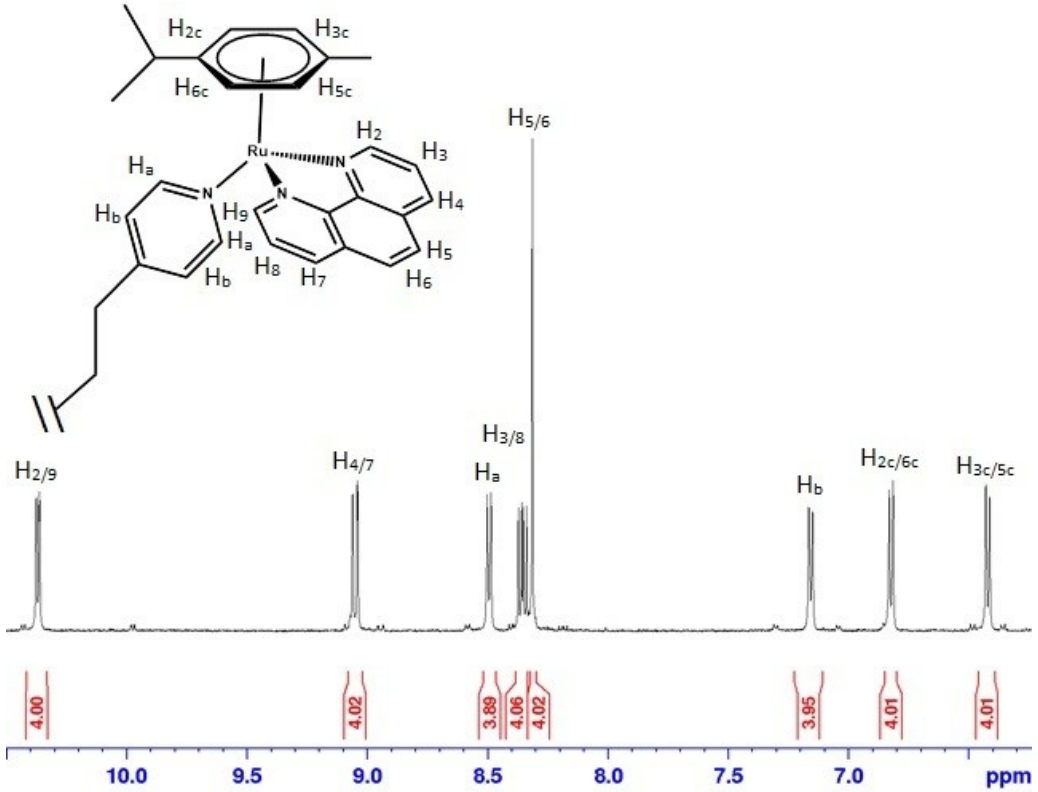

Figure S12a: The aromatic part of the ^{1}H NMR spectrum of the complex (6)$(PF_6)_4$ in acetone-d_6 at 298 K. Half complex shown for clarity.

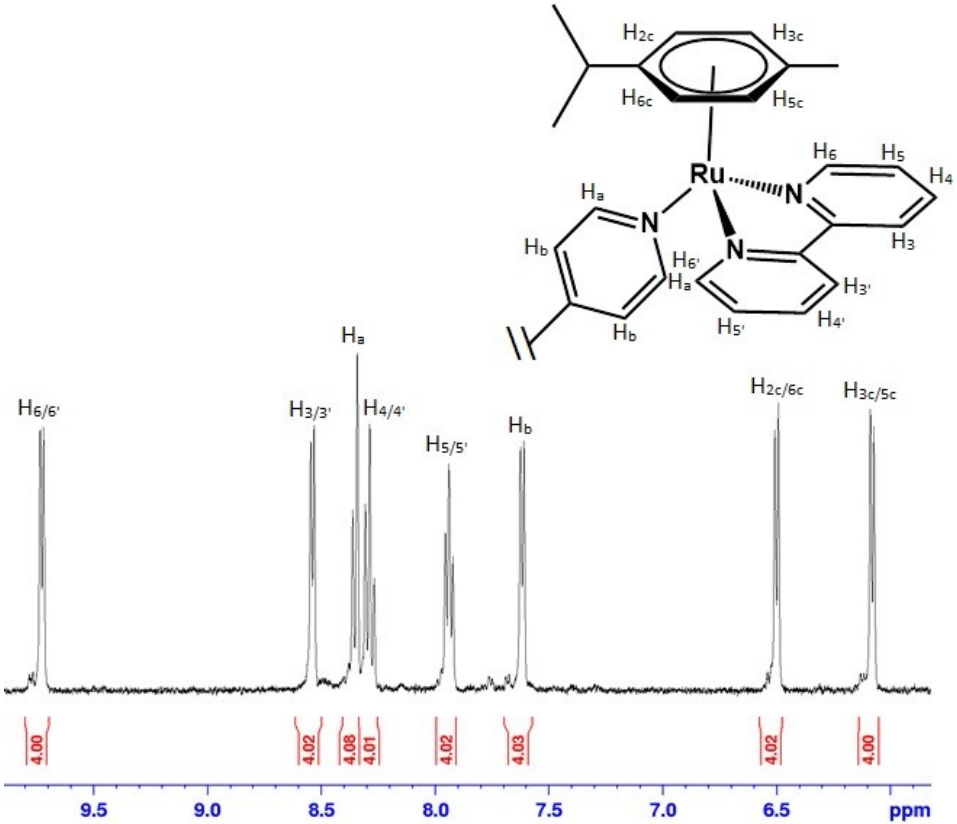

Figure S7b: The aromatic part of the ^{1}H NMR spectrum of the complex $(1)Cl_4$ in D_2O/H_2O (buffer phosphate 100 mM, pH = 7.0) at 298 K. Half complex shown for clarity.

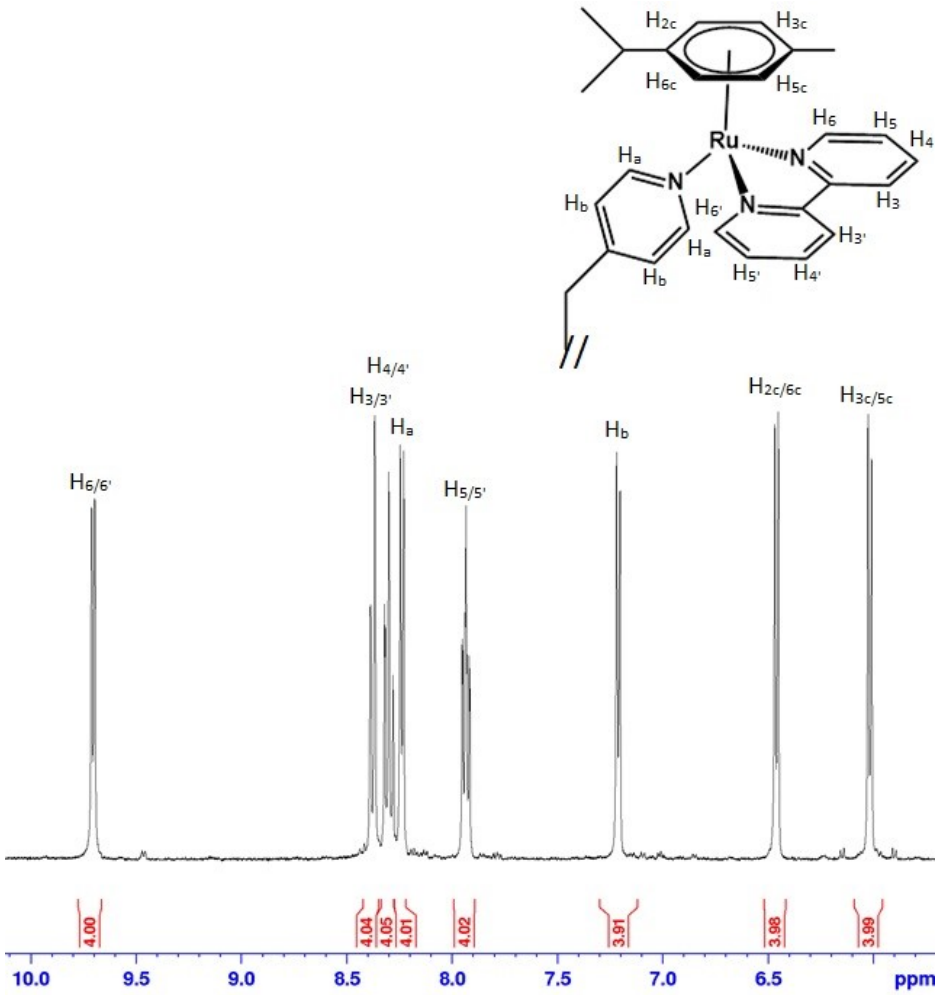

Figure S8b: The aromatic part of the ^{1}H NMR spectrum of the complex (2)Cl_4 in D_2O/H_2O (buffer phosphate 100 mM, pH = 7.0) at 298 K. Half complex shown for clarity.

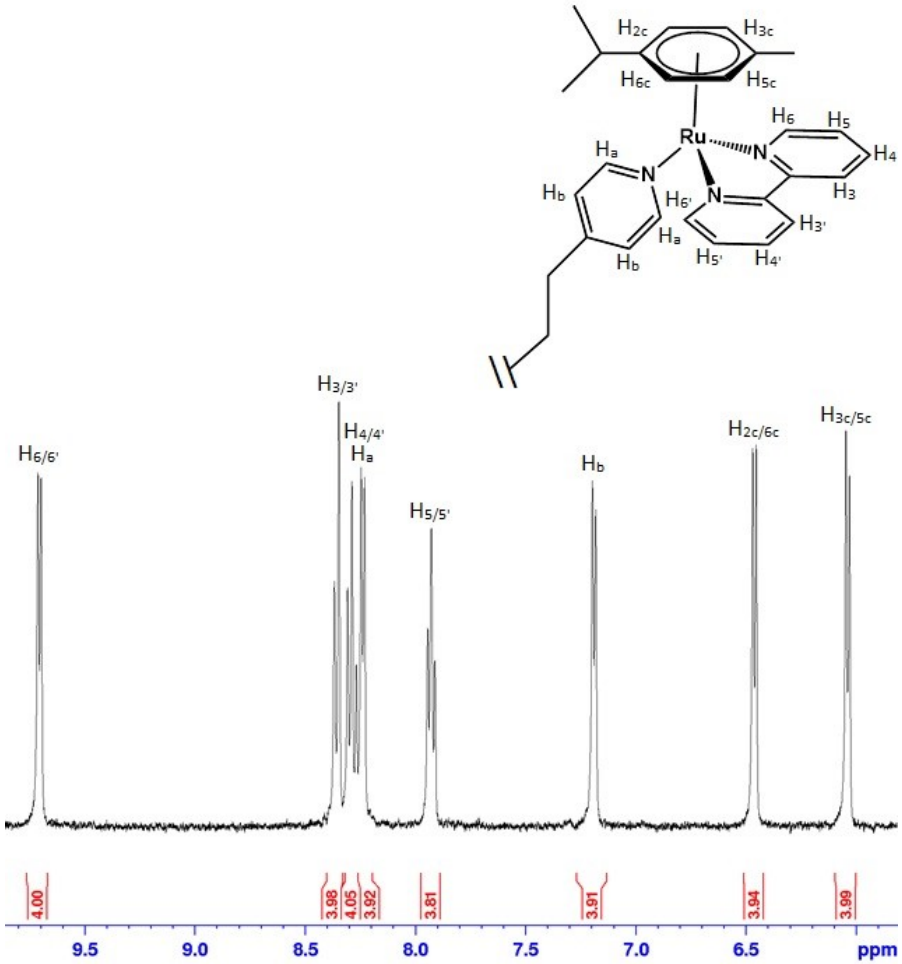

Figure S9b: The aromatic part of the ^{1}H NMR spectrum of the complex (3)Cl_4 in D_2O/H_2O (buffer phosphate 100 mM, pH = 7.0) at 298 K. Half complex shown for clarity.

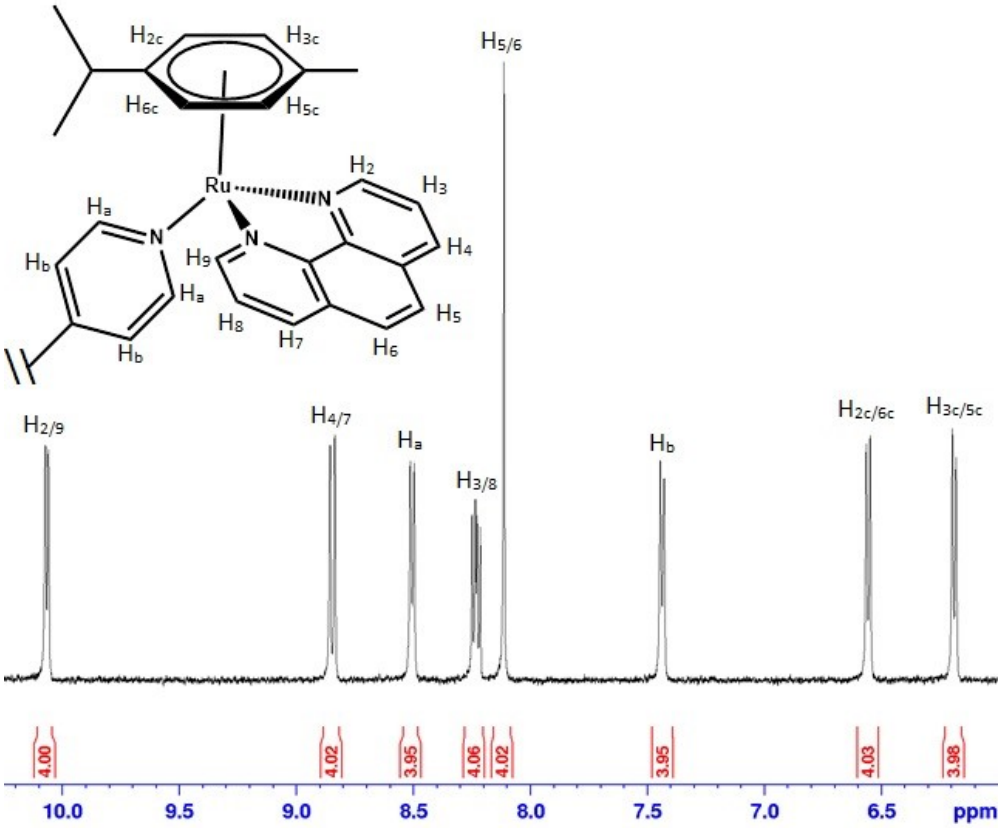

Figure S10b: The aromatic part of the ^{1}H NMR spectrum of the complex (4)Cl_4 in D_2O/H_2O (buffer phosphate 100 mM, pH = 7.0) at 298 K. Half complex shown for clarity.

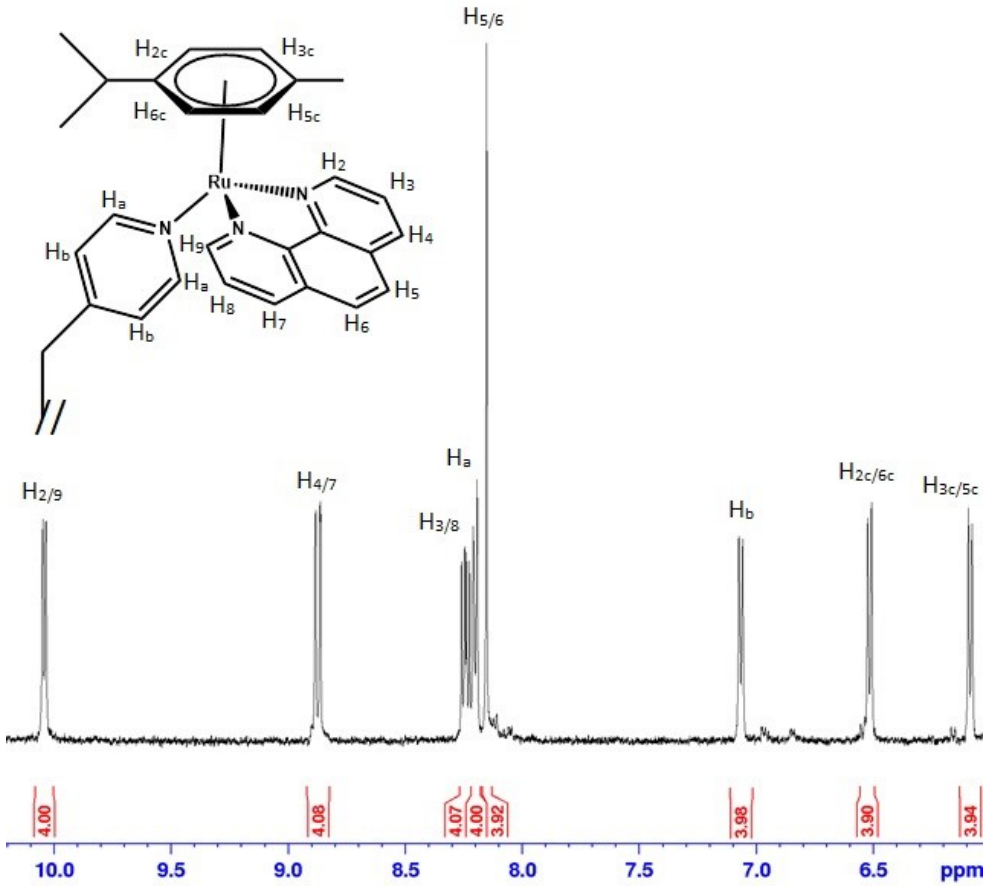

Figure S11b: The aromatic part of the ^{1}H NMR spectrum of the complex (5)Cl_4 in D_2O/H_2O (buffer phosphate 100 mM, pH = 7.0) at 298 K. Half complex shown for clarity.

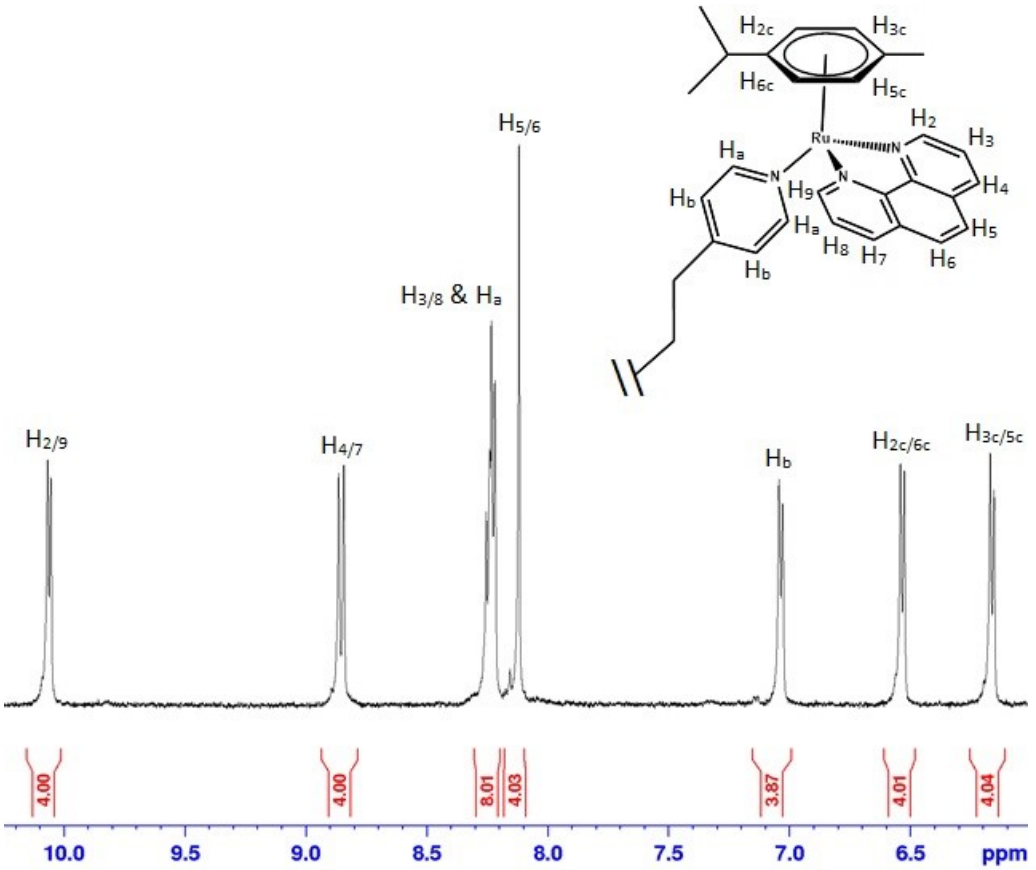

Figure S12b: The aromatic part of the ^{1}H NMR spectrum of the complex (6)Cl_4 in D_2O/H_2O (buffer phosphate 100 mM, pH = 7.0) at 298 K. Half complex shown for clarity.

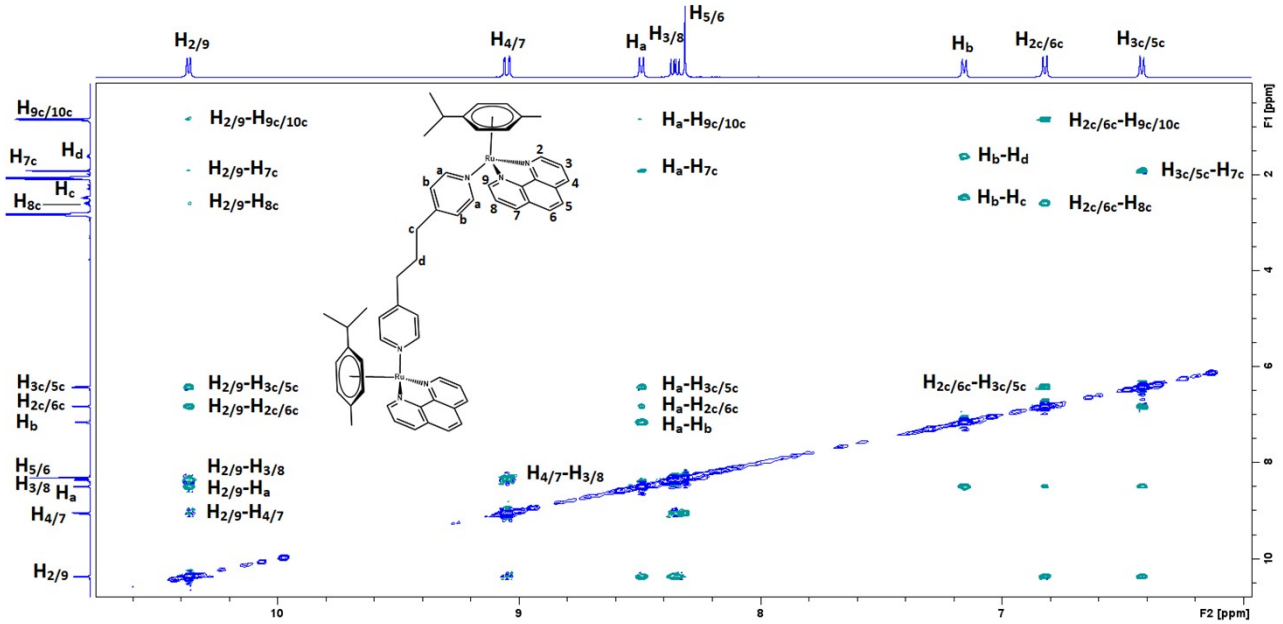

Figure S13: The aromatic part of the ^{1}H - ^{1}H NOESY spectrum of the complex (6)$(PF_6)_4$ in acetone-d_6 at 298 K, 500 MHz, t_{mix} = 350 ms.

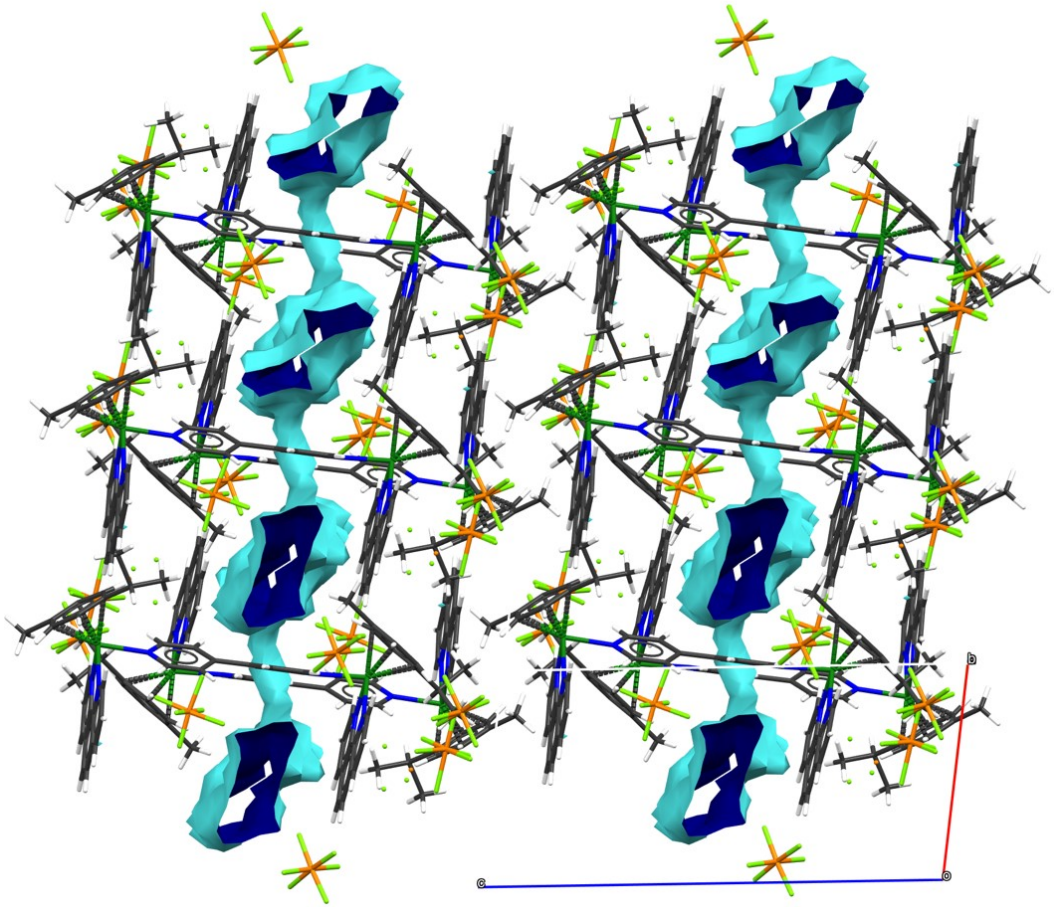

Figure S14: A packing diagram of complex (4)$(PF_6)_4$, viewed down to the {-1, 1, 0) direction of the unit cell, showing the solvent accessible channels present in the crystal structure.

Table S1: Crystal data and structure refinement for complex (4)$(PF_6)_4$.

Empirical formula	$C_{54}H_{52}F_{24}N_6P_4Ru_2$
Formula weight	1567.04
Temperature	296(2) K
Wavelength	0.71073 Å
Crystal system	Triclinic
Space group	$P\bar{1}$
Unit cell dimensions (Å, °)	a = 13.1201(5), α = 92.147(2) b = 13.8478(5), β = 97.737(2) c = 19.2251(7), γ = 96.195(2)
Volume (Å^3)	3436.1(2)
Z	2
Density (calculated)	1.515 g/cm^3
Absorption coefficient	0.636 mm^{-1}
F(000)	1564
Crystal size	0.21 x 0.19 x 0.02 mm^3
θ range for data collection	2.539 to 24.999 °
Index ranges	-15 ≤ h ≤ 15, -16 ≤ k ≤ 16, -22 ≤ l ≤ 22
Reflections collected	193431
Independent reflections	12090 [R_{int} = 0.1329]
Completeness to θ = 24.999°	99.9%
Refinement method	Full-matrix least-squares on F^2
Data / restraints / parameters	12090 / 217 / 854
Goodness-of-fit	1.029
Final R indices [I > 2σ(I)]	R_{obs} = 0.0566, wR_{obs} = 0.1502
R indices [all data]	R_{all} = 0.1029, wR_{all} = 0.1697
Largest diff. peak and hole	0.456 and -0.565 e·Å^{-3}

$R = \Sigma||F_o|-|F_c|| / \Sigma|F_o|$, $wR = \{\Sigma[w(|F_o|^2 - |F_c|^2)^2] / \Sigma[w(|F_o|^4)]\}^{1/2}$ and $w=1/[\sigma^2(Fo^2)+(0.1000P)^2]$ where $P=(Fo^2+2Fc^2)/3$

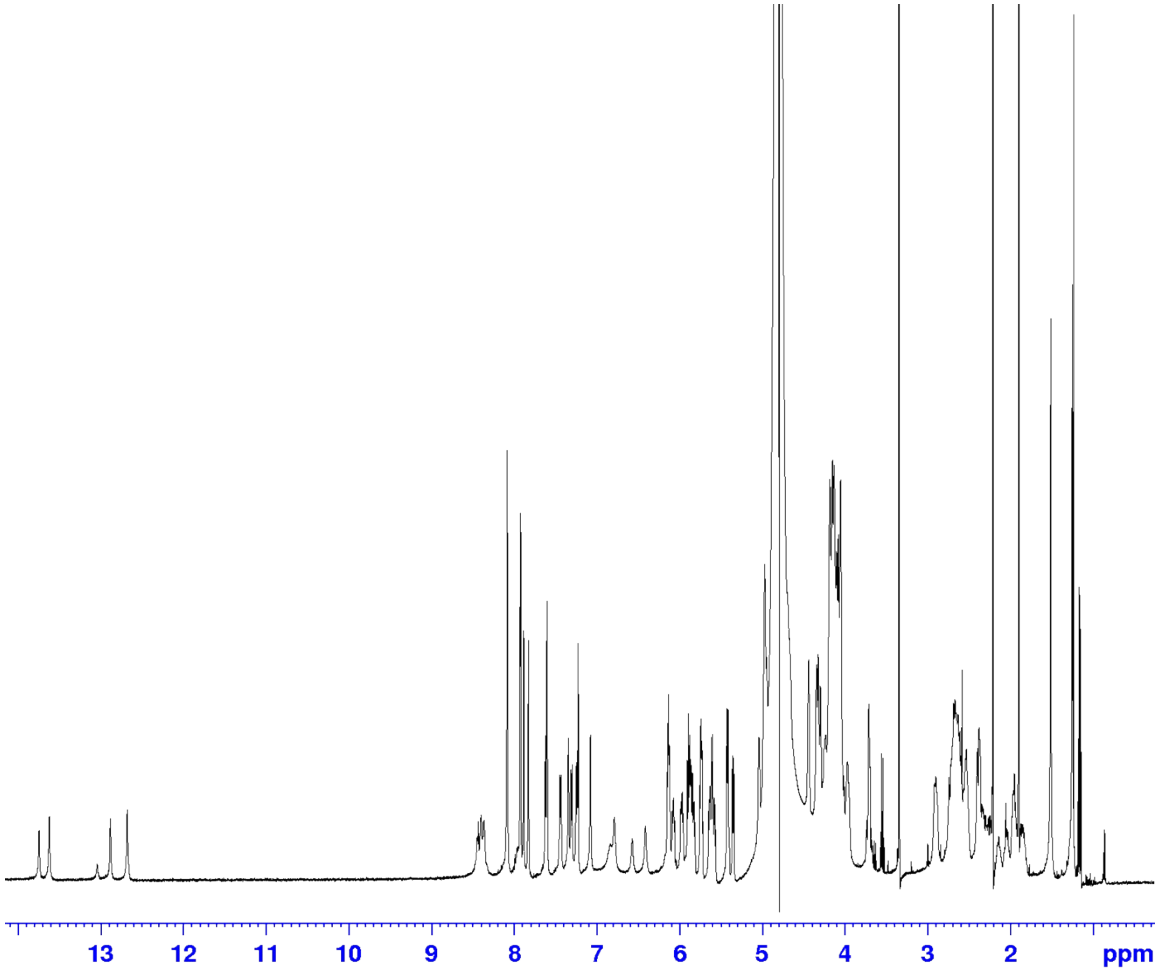

Figure S15: ^{1}H NMR Spectra of d(CGCGAATTCGCG)$_2$ in H_2O/ D_2O 9:1 (buffer phosphate 100 mM, pH = 7.0) at 298 K, 500 MHz.

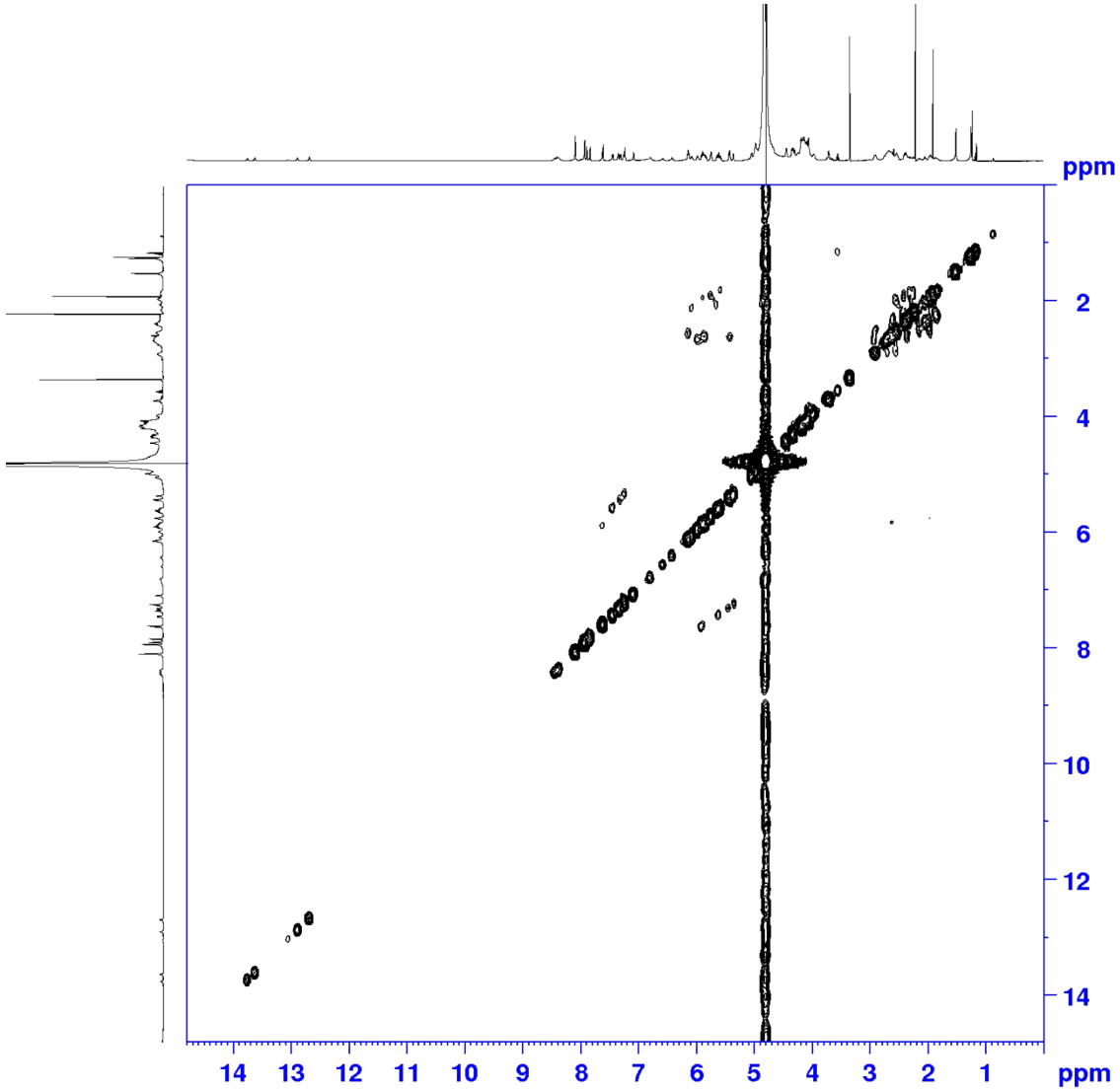

Figure S16: ^{1}H – ^{1}H COSY NMR Spectra of d(CGCGAATTCGCG)$_2$ in H_2O/ D_2O 9:1 (buffer phosphate 100 mM, pH = 7.0) at 298 K, 500 MHz.

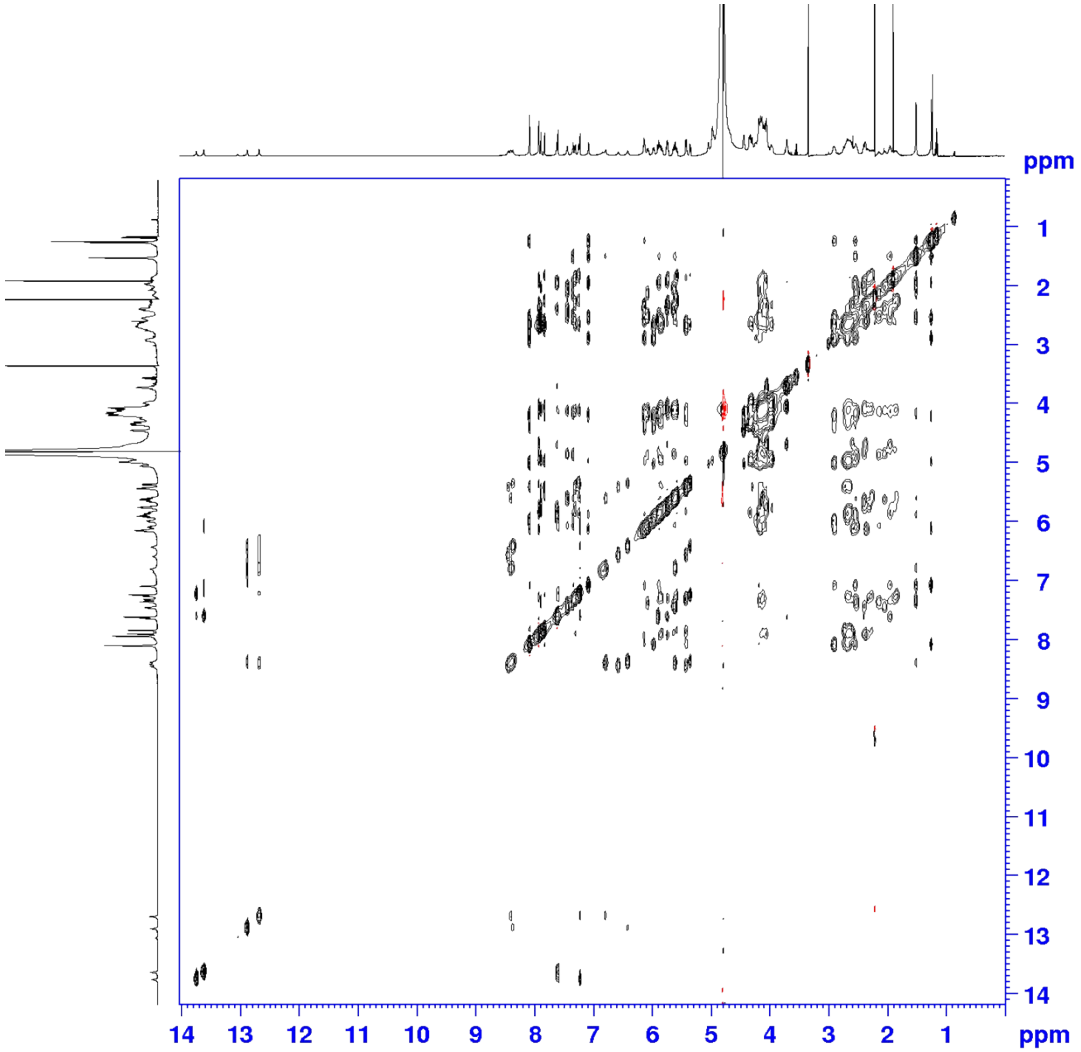

Figure S17: $^{1}H - {}^{1}H$ NOESY NMR Spectra of d(CGCGAATTCGCG)$_2$ in H_2O/ D_2O 9:1 (buffer phosphate 100 mM, pH = 7.0) at 298 K, 500 MHz, t_{mix} = 350 ms.

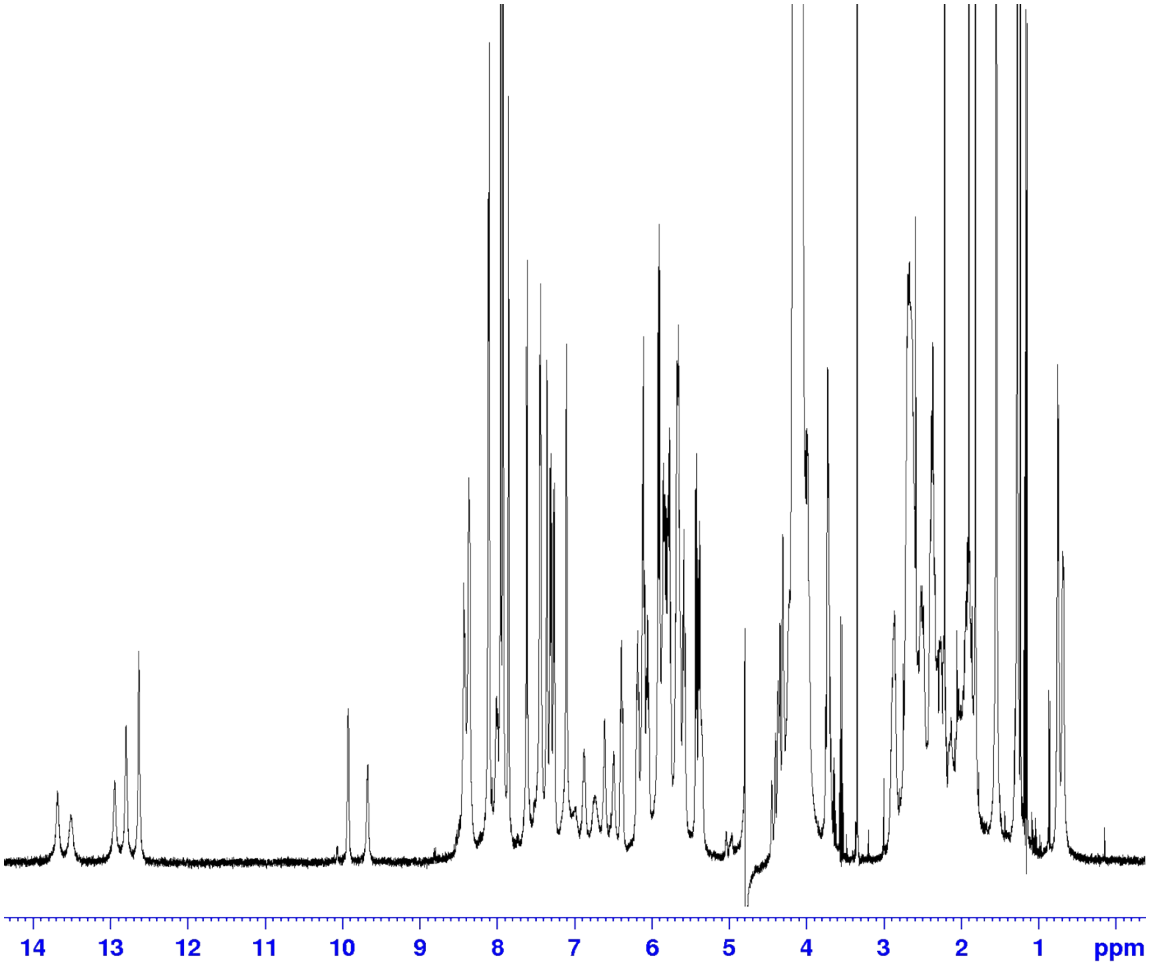

Figure S18: ^{1}H NMR Spectra of d(CGCGAATTCGCG)$_2$ upon addition of complex (4)Cl_4 at r = 0.5 in H_2O/ D_2O 9:1 (buffer phosphate 100 mM, pH = 7.0) at 298 K, 500 MHz.

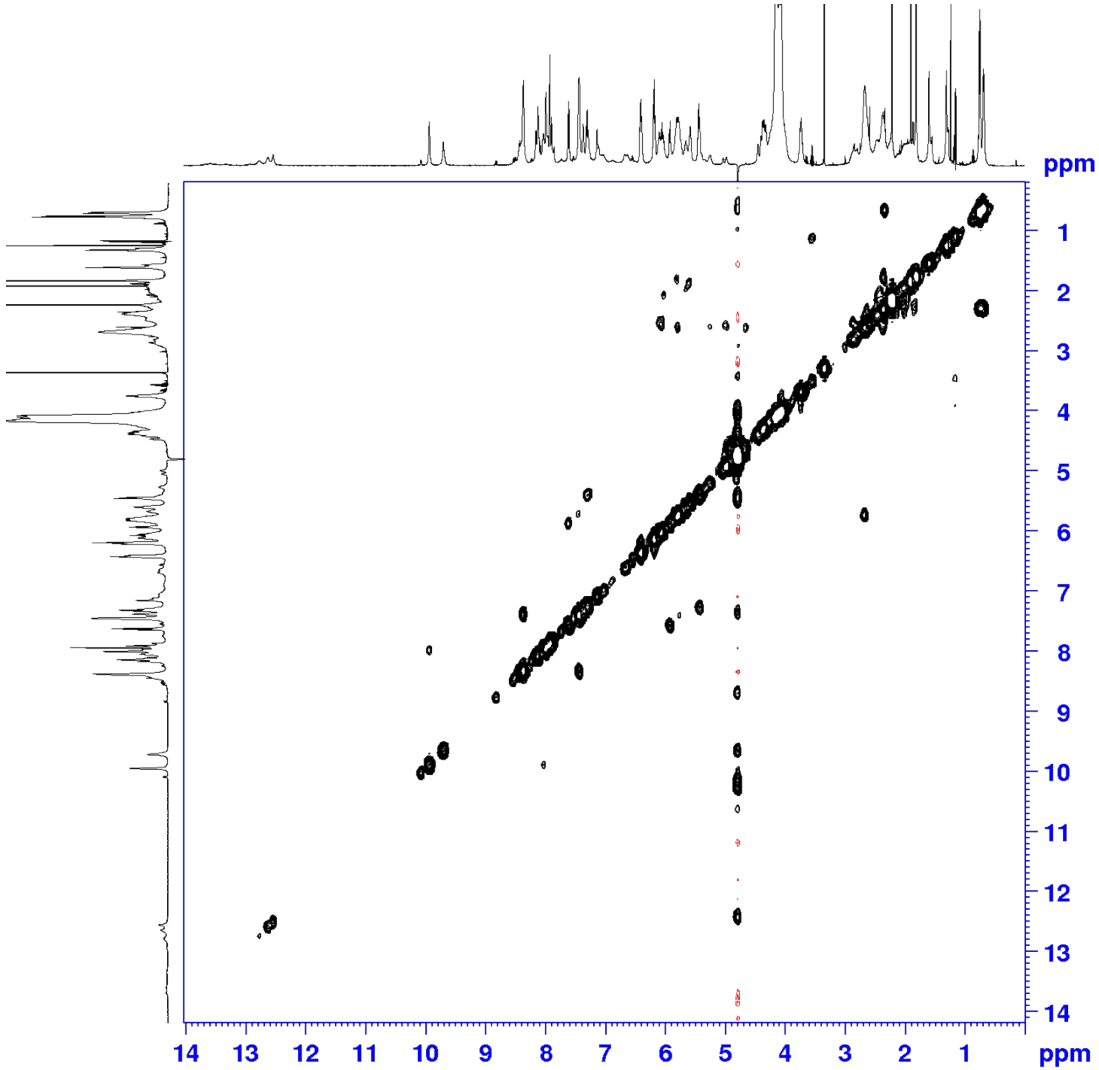

Figure S19: $^{1}H - {}^{1}H$ COSY NMR Spectra of $d(CGCGAATTCGCG)_2$ upon addition of complex $(4)Cl_4$ at r = 0.5 in H_2O/ D_2O 9:1 (buffer phosphate 100 mM, pH = 7.0) at 298 K, 500 MHz.

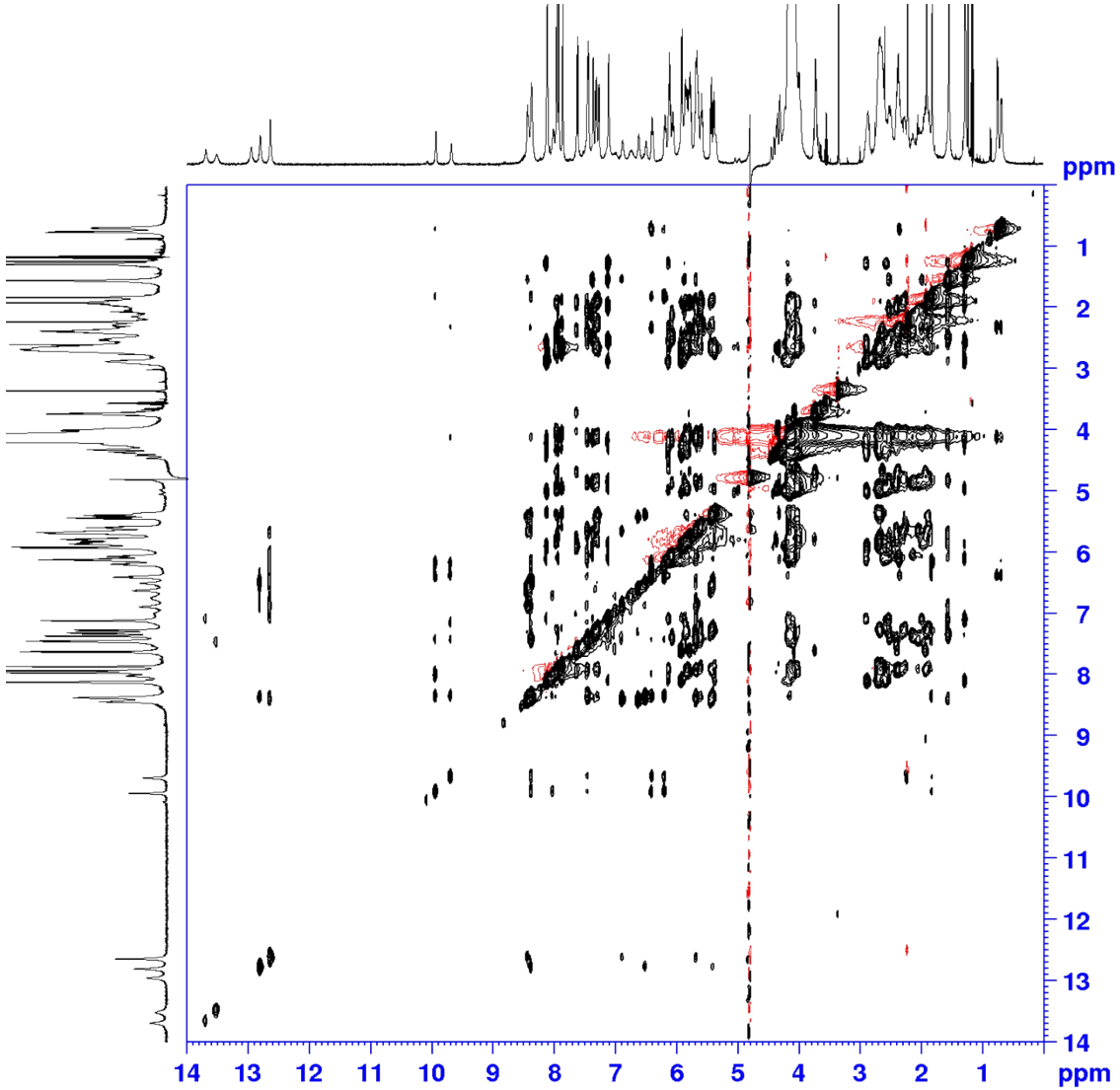

Figure S20: $^{1}H - {}^{1}H$ NOESY NMR Spectra of d(CGCGAATTCGCG)$_2$ upon addition of complex (4)Cl_4 at r = 0.5 in H_2O/ D_2O 9:1 (buffer phosphate 100 mM, pH = 7.0) at 298 K, 500 MHz, t_{mix} = 350 ms.

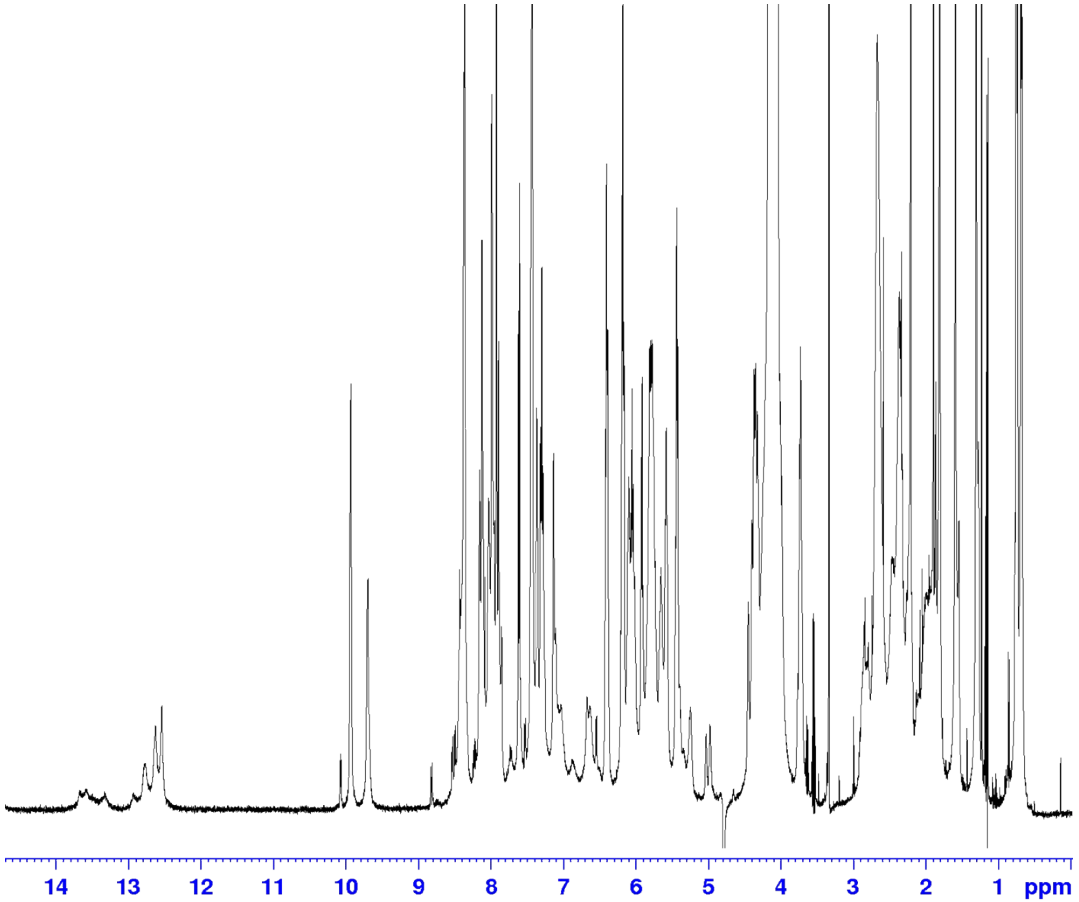

Figure S21: ^{1}H NMR Spectra of d(CGCGAATTCGCG)$_2$ upon addition of complex (4)Cl_4 at r = 1 in H_2O/ D_2O 9:1 (buffer phosphate 100 mM, pH = 7.0) at 298 K, 500 MHz.

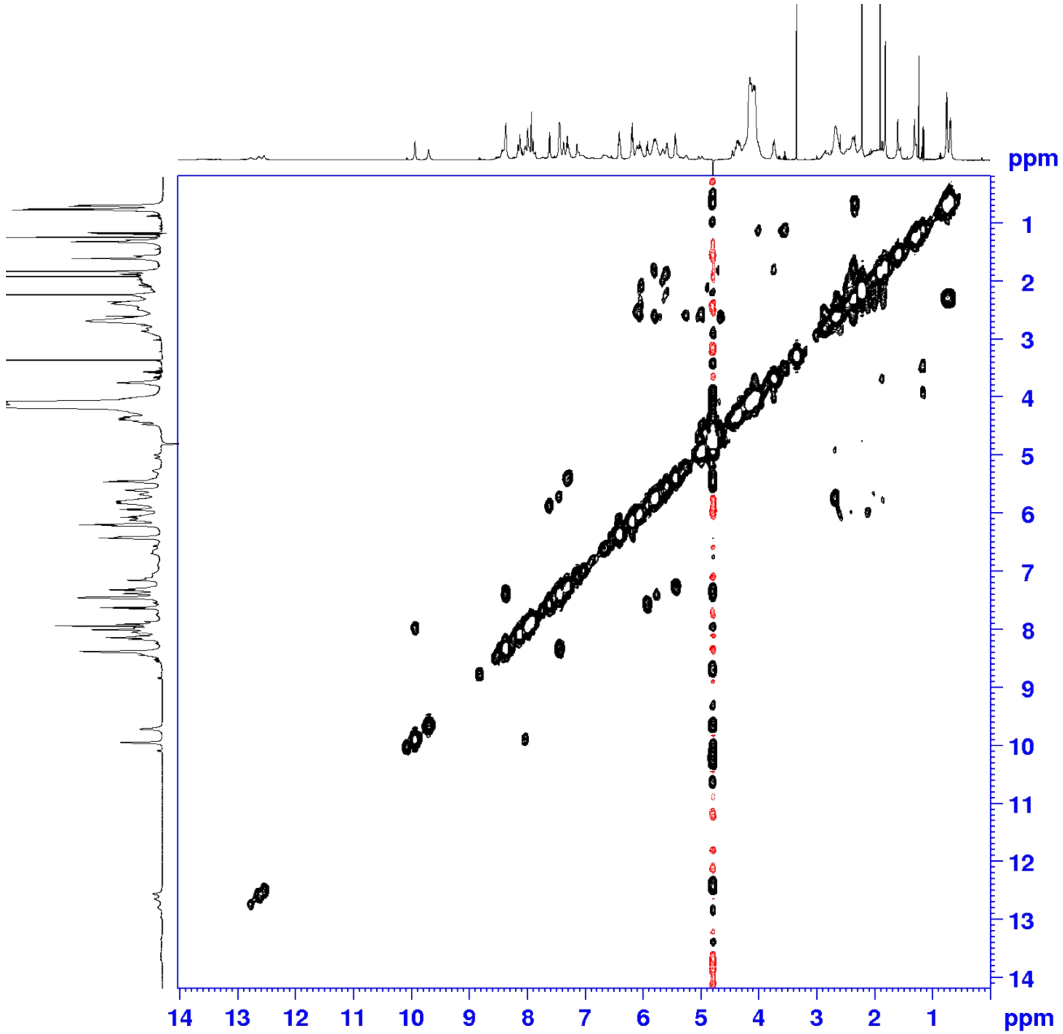

Figure S22: $^{1}H - {}^{1}H$ COSY NMR Spectra of $d(CGCGAATTCGCG)_2$ upon addition of complex $(4)Cl_4$ at r = 1 in H_2O/ D_2O 9:1 (buffer phosphate 100 mM, pH = 7.0) at 298 K, 500 MHz.

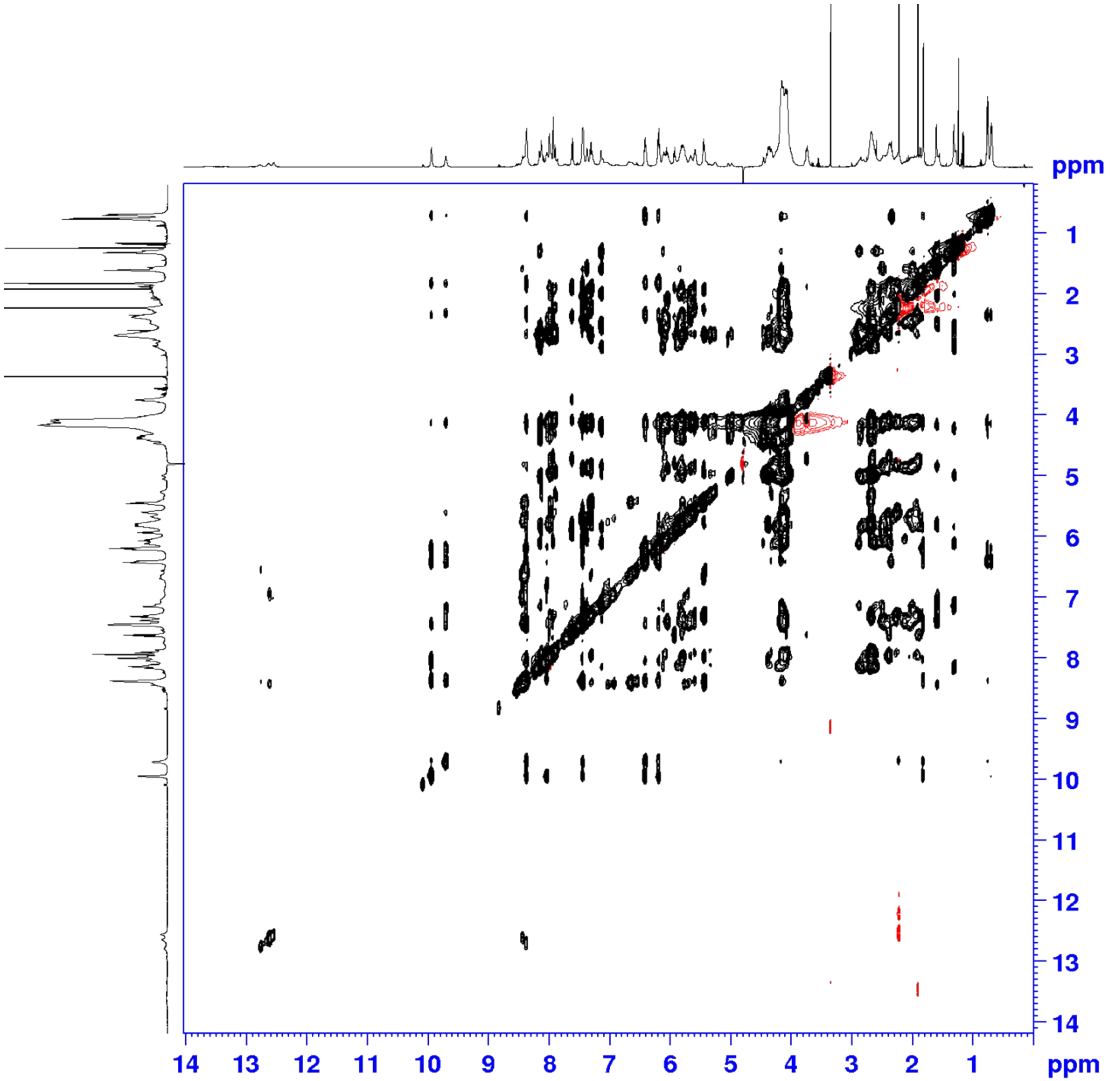

Figure S23: $^{1}H - ^{1}H$ NOESY NMR Spectra of d(CGCGAATTCGCG)$_2$ upon addition of complex (4)Cl_4 at r = 1 in H_2O/ D_2O 9:1 (buffer phosphate 100 mM, pH = 7.0) at 298 K, 500 MHz, t_{mix} = 350 ms.

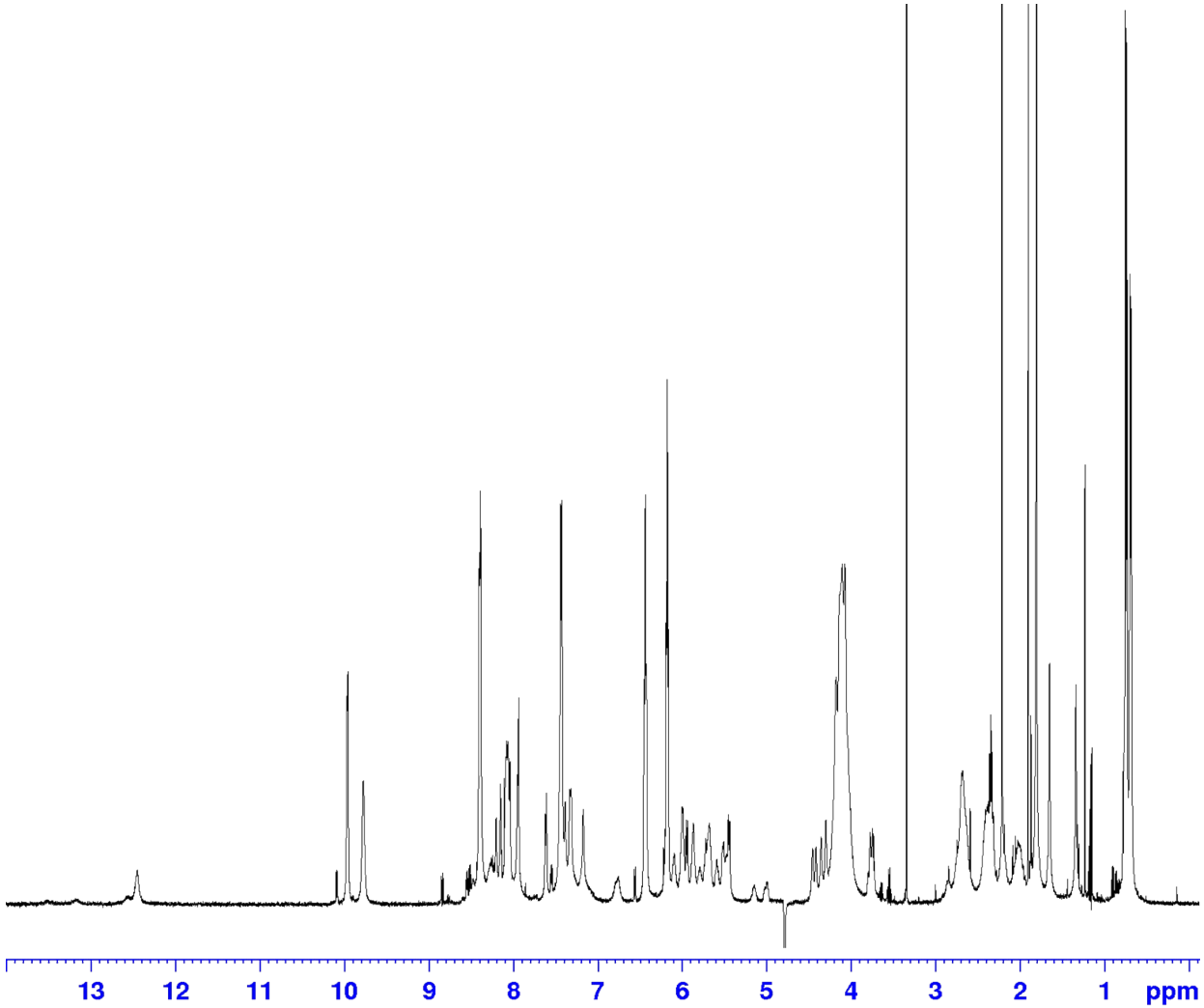

Figure S24: ^{1}H NMR Spectra of d(CGCGAATTCGCG)$_2$ upon addition of complex (4)Cl$_4$ at r = 2 in H_2O/ D_2O 9:1 (buffer phosphate 100 mM, pH = 7.0) at 298 K, 500 MHz.

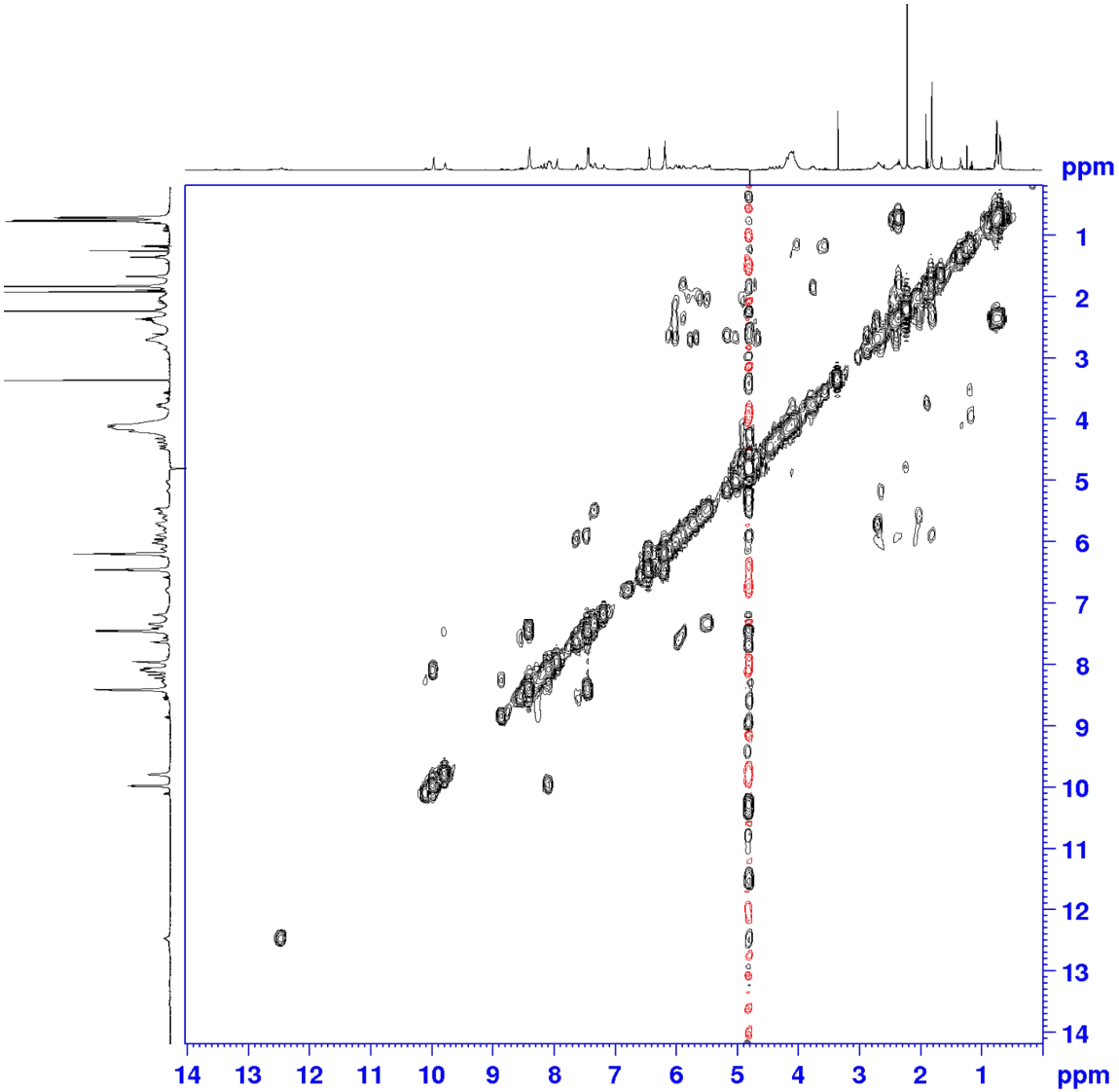

Figure S25: $^{1}H - {}^{1}H$ COSY NMR Spectra of d(CGCGAATTCGCG)$_2$ upon addition of complex (4)Cl_4 at r = 2 in H_2O/ D_2O 9:1 (buffer phosphate 100 mM, pH = 7.0) at 298 K, 500 MHz.

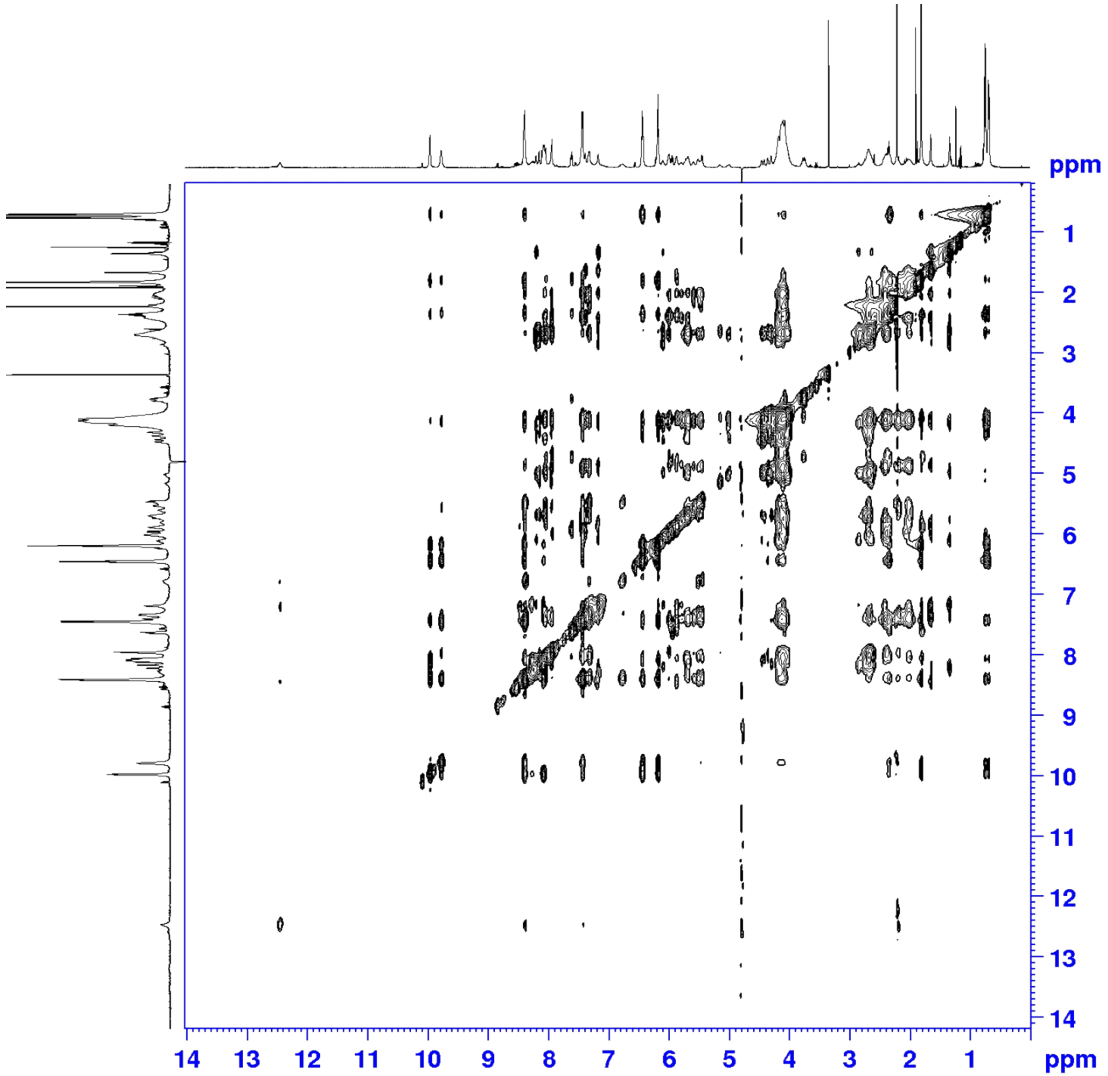

Figure S26: ^{1}H – ^{1}H NOESY NMR Spectra of d(CGCGAATTCGCG)$_2$ upon addition of complex (4)Cl_4 at r = 2 in H_2O/ D_2O 9:1 (buffer phosphate 100 mM, pH = 7.0) at 298 K, 500 MHz, t_{mix} = 350 ms.

Table S2: Differences in ^{1}H chemical shifts of the $d(CGCGAATTCGCG)_2$ (buffer phosphate 100 mM, pH = 7.0) upon the addition of complex $(4)Cl_4$ in various [Ru]/nucleotide ratios at 298 K, 500 MHz. Values in parenthesis denote upfield (-) or downfield (+) shifts from the free oligonucleotide under the same conditions.

	r = 0								r = 0.5								r = 1								r = 2							
	H8/6	**H5/H2 -CH$_3$**	**H1'**	**H2'**	**H2''**	**H3'**	**H4'**	**H5'5''**	**H8/6**	**H5/H2 -CH$_3$**	**H1'**	**H2'**	**H2''**	**H3'**	**H4'**	**H5'5''**	**H8/6**	**H5/H2 -CH$_3$**	**H1'**	**H2'**	**H2''**	**H3'**	**H4'**	**H5'5''**	**H8/6**	**H5/H2 -CH$_3$**	**H1'**	**H2'**	**H2''**	**H3'**	**H4'**	**H5'5''**
C1	7.60	5.88	5.72	1.89	2.37	4.60	3.91	3.69 3.72	7.60 0.00	5.91 +0.03	**5.77** **+0.05**	1.90 +0.01	**2.36** **-0.01**	**4.66** **+0.06**	**4.06** **+0.15**	3.68 -0.01 3.72 0.00	7.60 0.00	5.91 +0.03	5.79 +0.07	1.85 -0.04	2.36 -0.01	4.64 +0.04	4.04 +0.13	3.63 -0.06 3.73 +0.01	7.61 +0.01	5.93 +0.05	n.o.	n.o.	n.o.	n.o.	n.o.	n.o. n.o.
G2	7.93		5.88	2.53	2.65	4.97	4.36	3.97 4.08	7.95 +0.02		**5.78** **-0.10**	**2.48** **-0.05**	2.65 0.00	4.95 -0.02	4.33 -0.03	3.97 0.00 4.06 -0.02	7.98 +0.05		5.76 -0.12	2.62 +0.09	2.67 +0.02	4.93 -0.04	4.34 -0.02	3.98 +0.01 4.06 -0.02	7.94 +0.01		n.o.	n.o.	n.o.	n.o.	n.o.	n.o. n.o.
C3	7.25	5.35	5.56	1.81	2.22	4.77	4.10	4.12 4.15	7.29 +0.04	5.31 -0.04	5.57 +0.01	1.81 0.00	2.22 0.00	4.73 -0.04	4.09 -0.01	n.o. n.o.	7.29 +0.04	5.42 +0.07	5.56 0.00	1.83 +0.02	2.21 -0.01	4.76 -0.01	4.10 0.00	n.o. n.o.	7.34 +0.09	5.50 +0.15	5.59 +0.03	1.83 +0.02	2.21 -0.01	4.76 -0.01	4.10 0.00	n.o. n.o.
G4	7.83		5.42	2.63	2.74	4.97	4.39	3.97 4.06	7.85 +0.02		**5.33** **-0.09**	**2.58** **-0.05**	2.70 -0.04	4.96 -0.01	4.31 -0.08	3.99 +0.02 4.06 0.00	7.88 +0.05		5.32 -0.10 5.25* -0.17	2.63 0.00	2.86 +0.12	4.97 0.00	4.34 -0.05	3.99 +0.02 4.06 0.00	7.94 +0.11		5.13 -0.43 4.99* -0.57	2.63 0.00	2.67 -0.07	4.93 -0.04	4.35 -0.04	n.o. n.o.
A5	8.09	7.21	6.13	2.67	2.89	5.03	4.45	4.15 4.19	8.11 +0.02	**7.07** **-0.14**	**6.09** **-0.06**	2.64 -0.03	n.o.	5.03 0.00	4.45 0.00	**4.10** **-0.05** 4.18 -0.01	8.12 +0.03	7.11 -0.10	5.86 -0.27	2.65 -0.02	2.84 -0.05	5.03 0.00	4.45 0.00	4.11 -0.04 4.19 0.00	8.15 +0.06	7.15 -0.06	5.86 -0.27	2.64 -0.03	2.85 -0.04	5.00 -0.03	4.45 0.00	n.o. n.o.
A6	8.09	7.60	5.97	2.57	2.90	4.99	4.45	n.o. 4.25	8.12 +0.03	**7.44** **-0.16**	**5.88** **-0.09**	**2.52** **-0.05**	**3.00** **+0.10**	5.00 +0.01	4.44 -0.01	n.o 4.23 -0.02	8.12 +0.03	7.42 -0.18	6.10 -0.13	2.60 +0.03	2.85 -0.05	4.99 0.00	4.45 0.00	n.o. 4.24 -0.01	8.18 +0.09	7.41 -0.19	6.09 +0.12	2.59 +0.02	2.84 -0.06	4.99 0.00	4.43 -0.02	n.o. 4.30 +0.05
T7	7.09	1.24	5.88	1.95	2.53	4.81	4.14	4.15	7.11 +0.02	1.27 +0.03	5.84 -0.04	1.97 +0.02	2.58 +0.05	4.86 +0.05	4.16 +0.02	n.o. n.o.	7.12 +0.03	1.28 +0.04	5.81 -0.07	1.94 -0.01	2.54 +0.01	4.82 +0.01	4.14 0.00	n.o. n.o.	7.15 +0.06	1.34 +0.10	5.87 -0.01	1.81 -0.14	2.56 +0.03	4.68 -0.13	n.o.	n.o. n.o.
T8	7.35	1.51	6.12	2.14	2.53	4.88	4.19	4.09	7.36 +0.01	1.54 +0.03	**6.05** **-0.07**	2.13 +0.01	2.52 +0.01	4.88 0.00	4.21 +0.02	**3.99** **-0.10**	7.38 +0.03	1.58 +0.07	6.03 -0.09	2.13 -0.01	2.60 +0.07	4.88 0.00	4.15 -0.04	n.o. n.o.	7.39 +0.04	1.65 +0.14	5.99 -0.13	2.08 -0.06	2.63 -0.10	4.93 +0.05	4.17 -0.02	n.o. n.o.
C9	7.44	5.60	5.64	2.04	2.39	4.86	4.14	4.10 4.17	7.44 0.00	**5.66** **+0.06**	5.66 +0.02	2.03 -0.01	2.42 +0.03	**4.92** **+0.06**	4.13 -0.01	4.12 +0.02 n.o	7.42 -0.02	5.75 +0.15	5.65 +0.01	2.05 +0.01	2.34 -0.05	4.91 +0.05	4.15 +0.01	4.12 +0.02	7.44 0.00	5.88 +0.28	5.57 -0.07	2.05 +0.01	2.31 -0.08	4.90 +0.04	4.14 0.00	4.13 +0.03 n.o.
G10	7.89		5.83	2.54	2.67	4.97	4.41	4.04 4.15	7.92 +0.03		5.82 -0.01	2.59 +0.05	**2.62** **-0.05**	4.97 0.00	4.41 0.00	4.06 +0.02 4.15 0.00	7.95 +0.06		5.80 -0.03	2.57 +0.03	2.66 -0.01	4.92 -0.05	4.40 -0.01	4.06 +0.02 n.o.	7.97 +0.08		n.o.	n.o.	n.o.	n.o.	n.o.	n.o. n.o.
C11	7.31	5.42	5.72	1.85	2.31	4.78	4.18	4.09 n.o.	7.29 -0.02	5.40 -0.02	5.69 -0.03	1.86 +0.01	2.32 +0.01	4.78 +0.01	4.16 -0.02	n.o. n.o.	7.29 -0.02	5.42 0.00	5.65 -0.07	1.85 0.00	2.36 +0.05	4.76 -0.02	4.15 -0.03	n.o. n.o.	7.31 0.00	5.45 +0.03	5.61 -0.11	2.02 -0.17	2.22 -0.09	4.87 +0.09	4.18 0.00	n.o. n.o.
G12	7.92		6.13	2.37	2.58	4.66	4.19	n.o. n.o.	7.92 0.00		6.11 -0.02	2.38 +0.01	**2.53** **-0.05**	4.66 +0.03	4.18 -0.01	n.o. n.o.	7.95 +0.03		6.07 -0.06	2.36 -0.01	2.65 +0.07	4.67 +0.01	4.13 +0.06	n.o. n.o.	7.94 +0.02		6.00 -0.13	2.36 -0.01	2.67 +0.09	4.67 +0.01	4.13 -0.06	n.o. n.o.

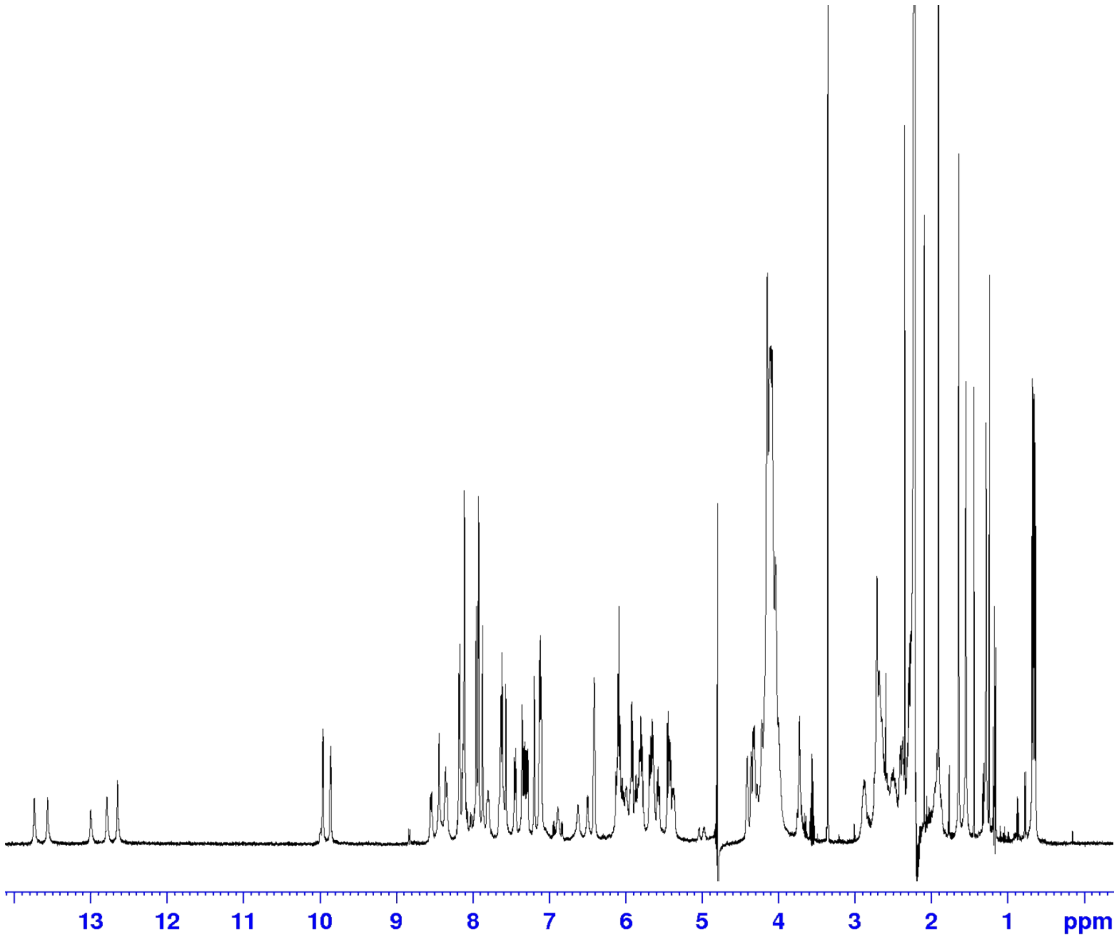

Figure S27: ^{1}H NMR Spectra of d(CGCGAATTCGCG)$_2$ upon addition of complex (5)Cl_4 at r = 0.5 in H_2O/ D_2O 9:1 (buffer phosphate 100 mM, pH = 7.0) at 298 K, 500 MHz.

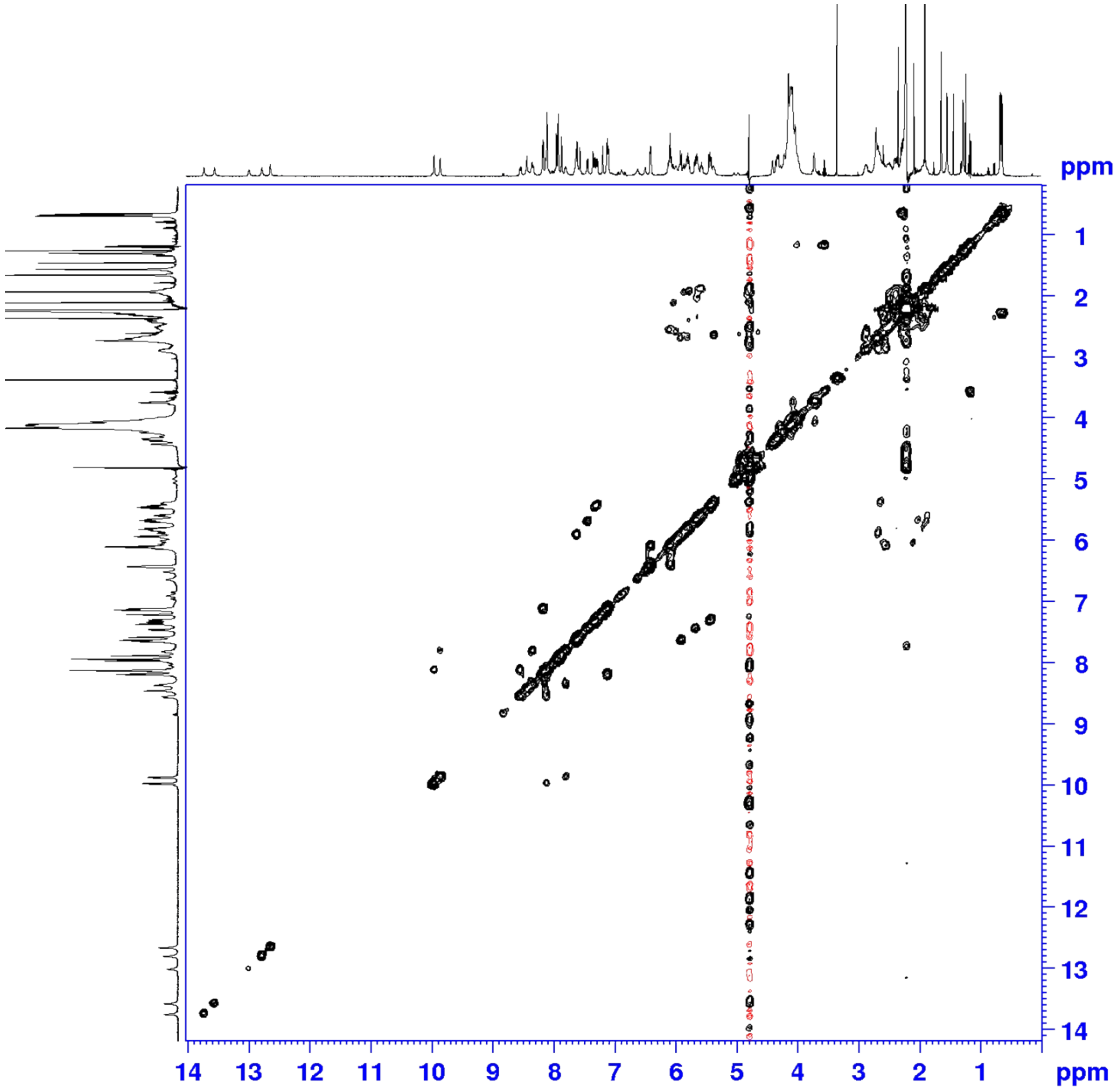

Figure S28: $^{1}H - {}^{1}H$ COSY NMR Spectra of $d(CGCGAATTCGCG)_2$ upon addition of complex $(5)Cl_4$ at r = 0.5 in H_2O/ D_2O 9:1 (buffer phosphate 100 mM, pH = 7.0) at 298 K, 500 MHz.

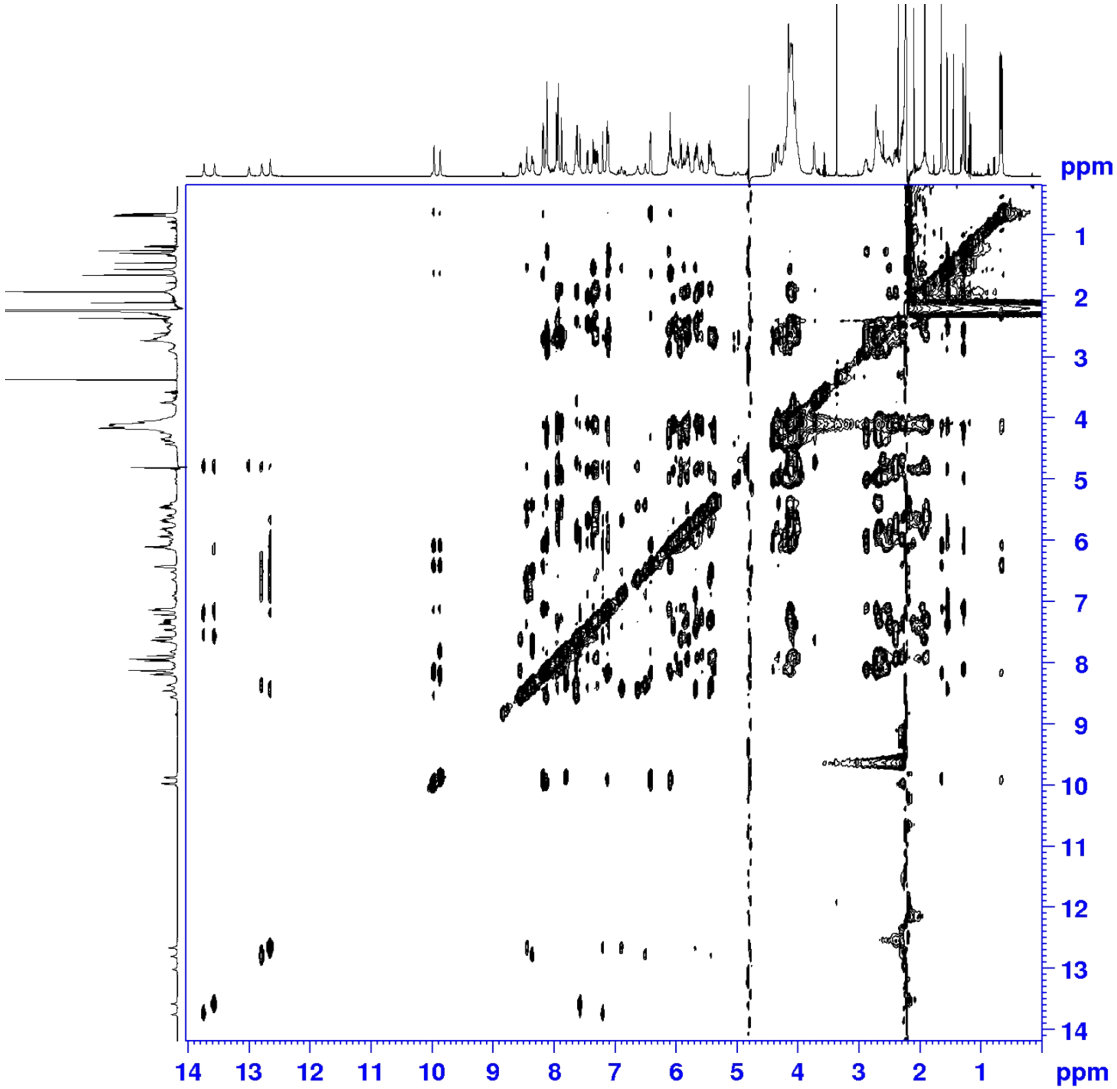

Figure S29: ^{1}H – ^{1}H NOESY NMR Spectra of d(CGCGAATTCGCG)$_2$ upon addition of complex (5)Cl_4 at r = 0.5 in H_2O/ D_2O 9:1 (buffer phosphate 100 mM, pH = 7.0) at 298 K, 500 MHz, t_{mix} = 350 ms.

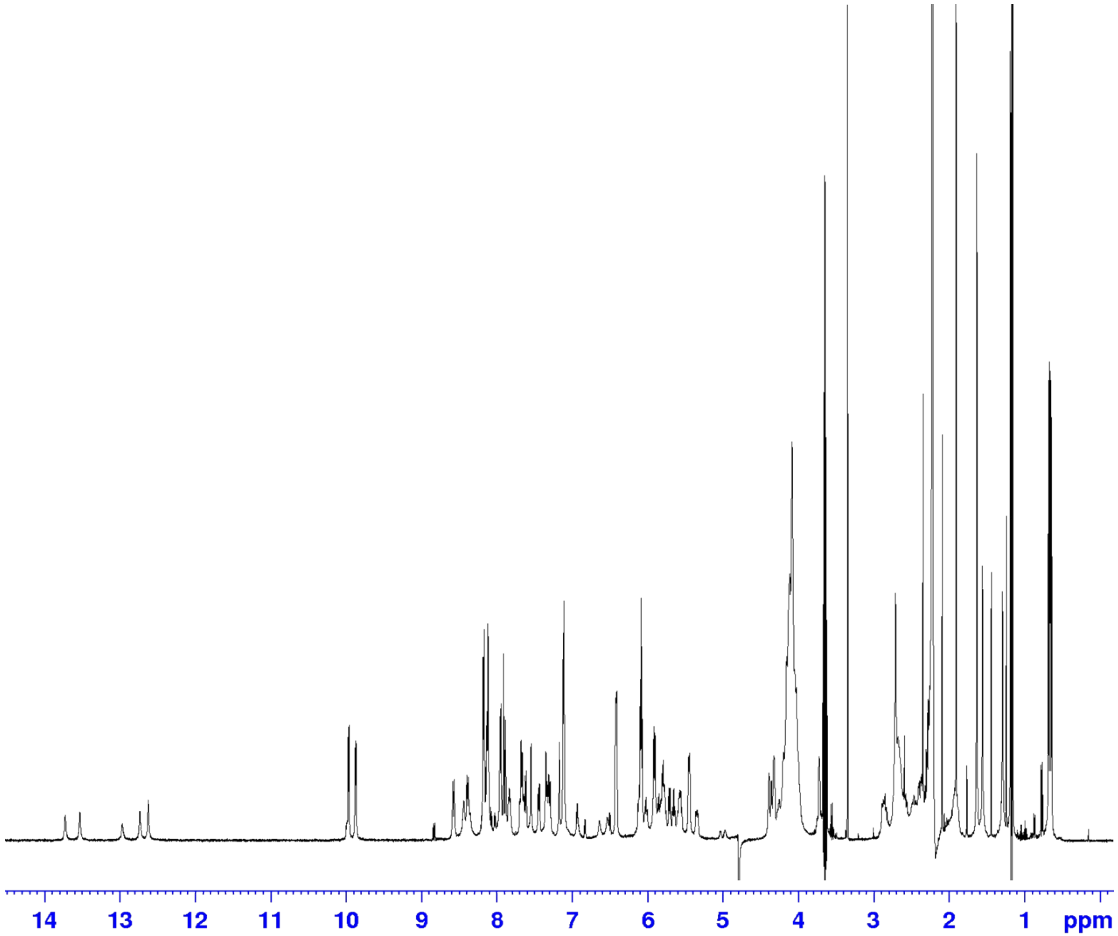

Figure S30: ^{1}H NMR Spectra of d(CGCGAATTCGCG)$_2$ upon addition of complex (5)Cl_4 at r = 1 in H_2O/ D_2O 9:1 (buffer phosphate 100 mM, pH = 7.0) at 298 K, 500 MHz.

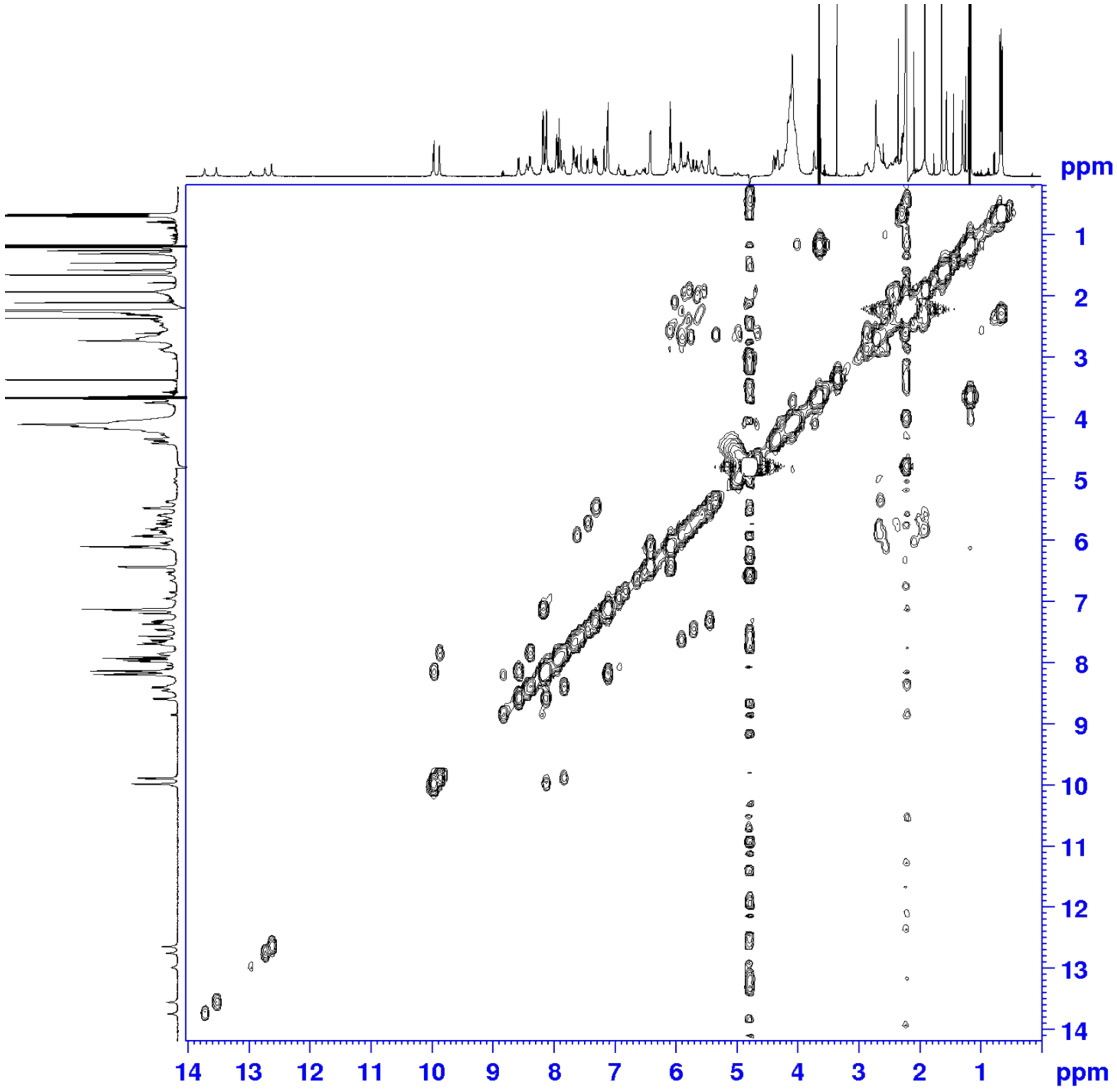

Figure S31: ^{1}H – ^{1}H COSY NMR Spectra of d(CGCGAATTCGCG)$_2$ upon addition of complex (5)Cl_4 at r = 1 in H_2O/ D_2O 9:1 (buffer phosphate 100 mM, pH = 7.0) at 298 K, 500 MHz.

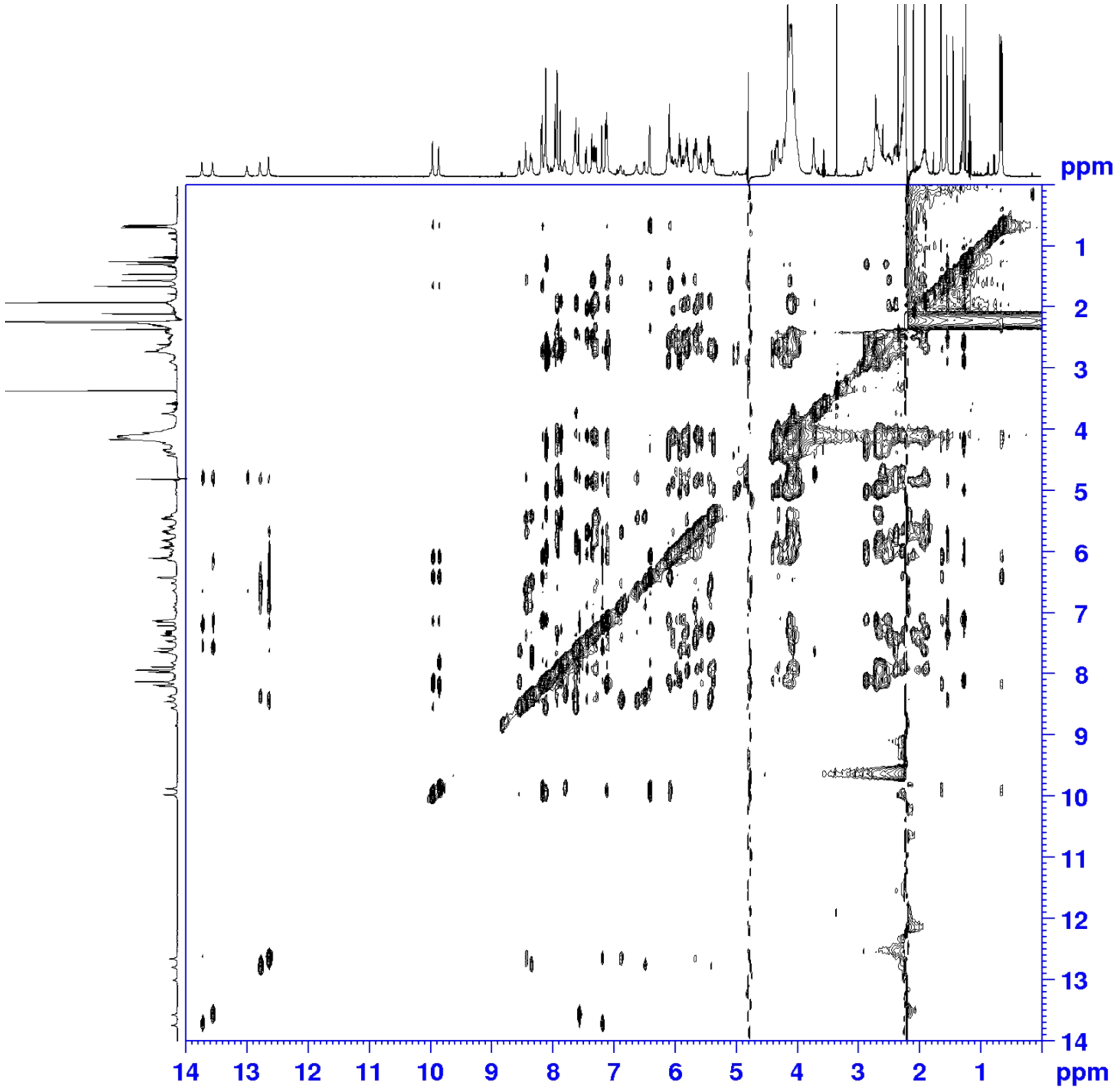

Figure S32: $^{1}H - {}^{1}H$ NOESY NMR Spectra of d(CGCGAATTCGCG)$_2$ upon addition of complex (5)Cl_4 at r = 1 in H_2O/ D_2O 9:1 (buffer phosphate 100 mM, pH = 7.0) at 298 K, 500 MHz, t_{mix} = 350 ms.

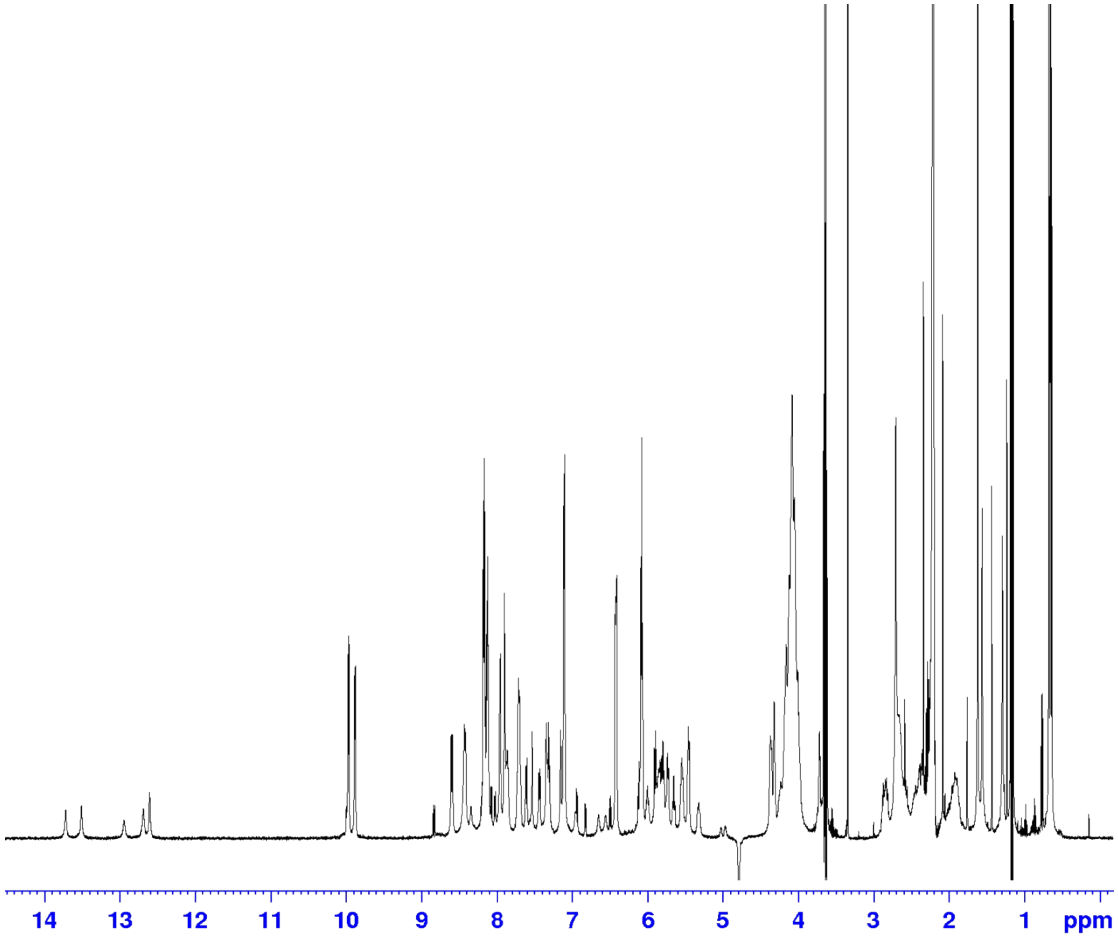

Figure S33: ^{1}H NMR Spectra of d(CGCGAATTCGCG)$_2$ upon addition of complex (5)Cl_4 at r = 2 in H_2O/ D_2O 9:1 (buffer phosphate 100 mM, pH = 7.0) at 298 K, 500 MHz.

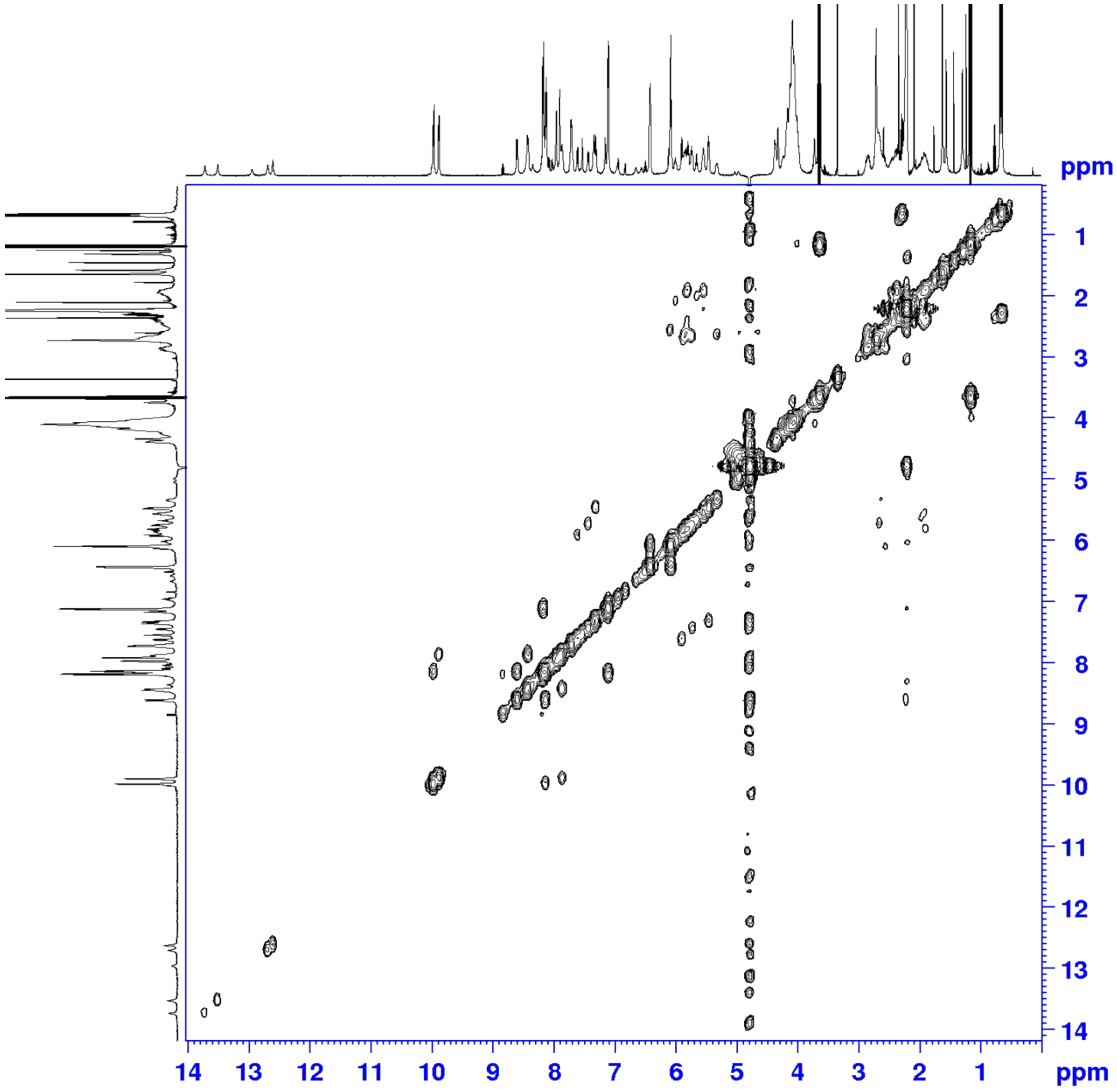

Figure S34: $^{1}H - {}^{1}H$ COSY NMR Spectra of d(CGCGAATTCGCG)$_2$ upon addition of complex (5)Cl_4 at r = 2 in H_2O/ D_2O 9:1 (buffer phosphate 100 mM, pH = 7.0) at 298 K, 500 MHz.

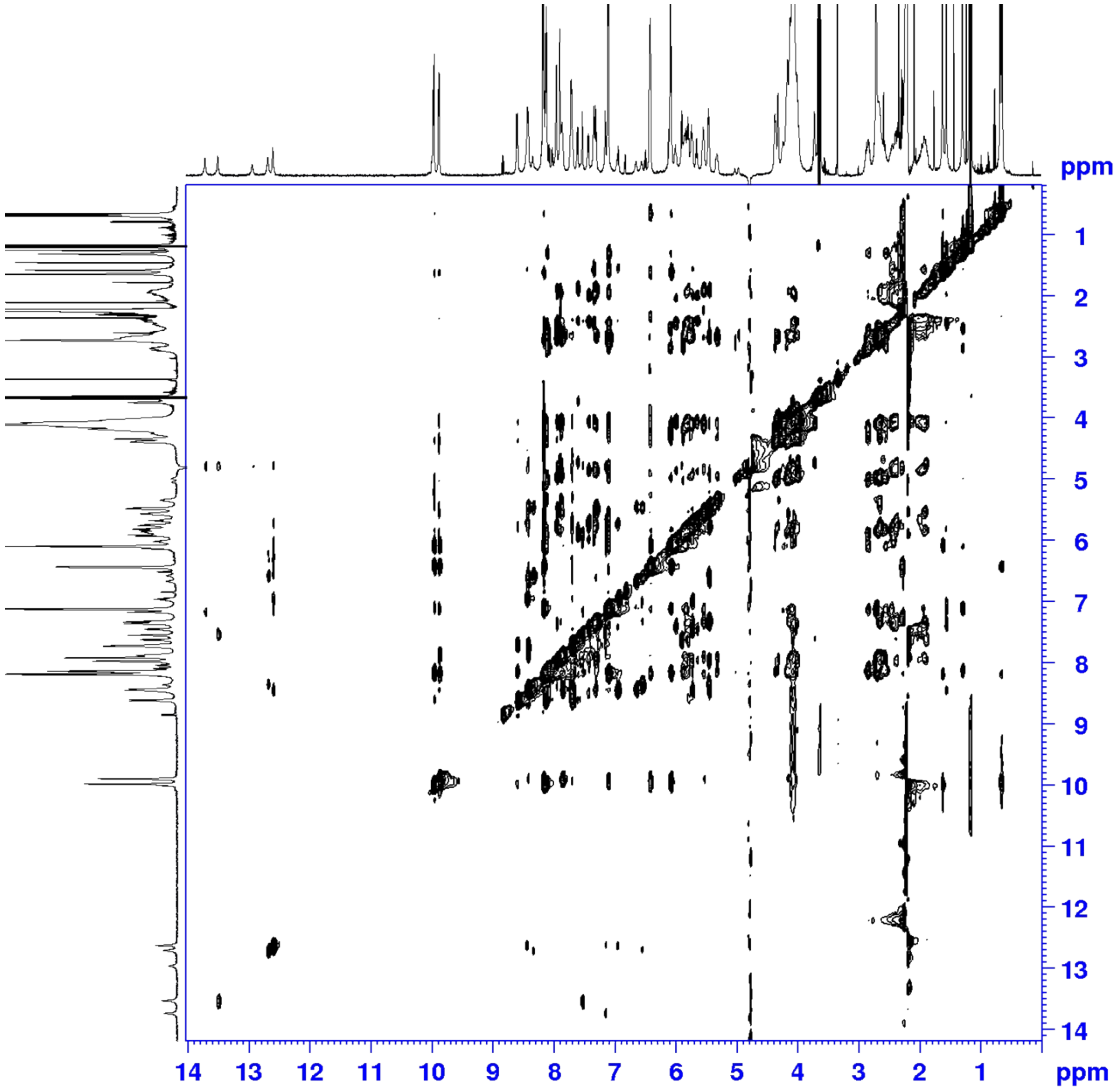

Figure S35: $^{1}H - {}^{1}H$ NOESY NMR Spectra of d(CGCGAATTCGCG)$_2$ upon addition of complex (5)Cl_4 at r = 2 in H_2O/ D_2O 9:1 (buffer phosphate 100 mM, pH = 7.0) at 298 K, 500 MHz, t_{mix} = 350 ms.

Table S3: Differences in ^{1}H chemical shifts of the $d(CGCGAATTCGCG)_2$ (buffer phosphate 100 mM, pH = 7.0) upon the addition of complex $(5)(Cl)_4$ in various [Ru]/nucleotide ratios at 298 K, 500 MHz. Values in parenthesis denote upfield (-) or downfield (+) shifts from the free oligonucleotide under the same conditions.

	r = 0								r = 0.5								r = 1								r = 2							
	H8/6	**H5/H2 -CH_3**	**H1'**	**H2'**	**H2''**	**H3'**	**H4'**	**H5'5''**	**H8/6**	**H5/H2 -CH_3**	**H1'**	**H2'**	**H2''**	**H3'**	**H4'**	**H5'5''**	**H8/6**	**H5/H2 -CH_3**	**H1'**	**H2'**	**H2''**	**H3'**	**H4'**	**H5'5''**	**H8/6**	**H5/H2 -CH_3**	**H1'**	**H2'**	**H2''**	**H3'**	**H4'**	**H5'5''**
C1	7.60	5.88	5.72	1.89	2.37	4.60	3.91	3.69 3.72	7.61 +0.01	5.90 +0.02	**5.78** **+0.06**	1.92 +0.03	2.41 +0.04	**4.66** **+0.06**	**4.04** **+0.13**	3.59 +0.10 3.71 -0.01	7.62 +0.02	5.91 +0.03	5.79 +0.07	1.91 +0.02	2.37 0.00	4.69 +0.09	4.08 +0.17	3.57 -0.12 3.71 -0.01	7.63 +0.03	5.93 +0.05	5.80 -0.08	1.89 0.00	2.39 +0.02	4.63 +0.03	4.08 +0.17	3.57 -0.12 3.71 -0.01
G2	7.93	-	5.88	2.53	2.65	4.97	4.36	3.97 4.08	7.95 +0.02	-	5.80 -0.08	**2.47** **-0.06**	2.66 +0.01	4.97 0.00	4.32 -0.04	3.93 -0.04 4.08 0.00	7.96 +0.03	-	5.76 -0.12	n.o.	2.67 +0.02	4.97 0.00	4.32 -0.04	3.93 -0.04 4.08 0.00	7.98 +0.05	-	5.75 -0.13	n.o.	2.65 0.00	4.32 -0.04	3.93 -0.04 4.08 0.00	4.32 -0.04
C3	7.25	5.35	5.56	1.81	2.22	4.77	4.10	4.12 4.15	7.28 +0.03	5.40 +0.05	5.57 +0.01	**1.89** **+0.08**	2.24 +0.02	4.77 0.00	n.o.	n.o. n.o.	7.29 +0.04	5.43 +0.08	5.58 0.02	**1.90** **+0.09**	2.24 +0.02	4.78 +0.01	n.o.	n.o. n.o.	7.34 +0.09	5.53 +0.18	5.54 -0.02	**1.90** **+0.09**	2.22 0.00	4.70 -0.07	n.o	n.o. n.o.
G4	7.83	-	5.42	2.63	2.74	4.97	4.39	3.97 4.06	7.88 +0.05	-	**5.37** **-0.05**	2.64 +0.01	2.77 +0.03	4.98 +0.01	4.31 -0.08	3.93 -0.04 4.09 +0.03	7.88 +0.05	-	5.37 -0.05	2.65 +0.02	n.o.	4.99 +0.02	4.32 -0.07	3.93 -0.04 4.08 +0.02	7.85 +0.02	-	5.32 -0.10	2.65 +0.02	n.o.	4.96 -0.01	4.36 -0.03	n.o. n.o.
A5	8.09	7.21	5.97	2.67	2.89	5.03	4.45	4.15 4.19	8.10 +0.01	7.19 -0.02	5.93 -0.04	2.70 +0.03	2.87 -0.02	5.04 +0.01	4.42 -0.03	4.11 **-0.04** n.o.	8.12 +0.03	7.20 -0.01	5.93 -0.04	2.67 0.00	2.87 -0.02	5.04 +0.01	n.o.	n.o.	8.12 +0.03	7.17 -0.04	5.86 -0.11	2.67 0.00	2.85 -0.04	5.03 0.00	n.o.	n.o. n.o.
A6	8.09	7.60	6.13	2.57	2.90	4.99	4.45	n.o. 4.25	8.10 +0.02	7.57 -0.03	6.12 -0.01	2.58 -0.01	2.88 -0.02	4.98 -0.01	4.42 -0.03	n.o 4.24 -0.01	8.12 +0.03	7.55 -0.05	6.11 -0.02	2.59 0.00	2.89 -0.01	4.98 -0.01	n.o.	n.o.	8.12 +0.03	7.56 -0.04	6.08 -0.05	2.59 +0.02	2.84 -0.06	4.96 -0.03	n.o.	n.o. n.o.
T7	7.09	1.24	5.88	1.95	2.53	4.81	4.14	4.15	7.10 +0.01	1.27 +0.03	5.87 -0.01	1.94 -0.01	2.51 -0.02	4.80 -0.01	4.13 -0.01	n.o. n.o.	7.12 +0.03	1.29 +0.05	5.86 -0.02	n.o.	2.53 +0.00	4.80 -0.01	4.12 -0.02	n.o. n.o.	7.11 +0.02	1.27 +0.03	5.84 -0.04	1.94 -0.01	n.o.	4.83 +0.02	n.o.	n.o. n.o.
T8	7.35	1.51	6.12	2.14	2.53	4.88	4.19	4.09	7.35 0.00	1.54 +0.03	**6.04** **-0.08**	2.13 +0.01	2.54 +0.01	4.87 -0.01	**4.26** **+0.07**	**n.o**	7.35 0.00	1.55 +0.04	**6.04** **-0.08**	2.06 -0.08	2.50 -0.07	4.87 -0.01	n.o.	n.o. n.o.	7.35 0.00	1.55 +0.04	6.00 -0.12	2.06 -0.08	2.42 -0.15	4.87 -0.01	n.o.	n.o. n.o.
C9	7.44	5.60	5.64	2.04	2.39	4.86	4.14	4.10 4.17	7.45 +0.01	**5.66** **+0.06**	5.62 -0.02	2.02 -0.02	2.37 -0.02	4.86 0.00	4.11 -0.03	n.o. n.o.	7.44 0.00	5.70 +0.10	5.63 -0.01	2.02 -0.02	n.o.	4.86 0.00	4.08 -0.06	4.12 +0.02 n.o.	7.45 +0.01	5.70 +0.10	5.66 +0.02	2.01 -0.03	2.38 -0.01	4.84 -0.02	4.08 -0.06	4.12 +0.02 n.o.
G10	7.89	-	5.83	2.54	2.67	4.97	4.41	4.04 4.15	7.94 +0.05	-	5.82 -0.01	2.56 +0.02	2.68 +0.01	4.98 +0.01	4.36 -0.05	4.04 0.00 4.11 -0.04	7.93 +0.04	-	5.81 -0.02	2.59 +0.05	2.68 +0.01	4.98 +0.01	4.35 -0.06	4.06 +0.02 n.o.	7.91 +0.02	-	5.84 +0.01	2.59 +0.05	2.68 +0.01	4.98 +0.01.	n.o.	n.o. n.o.
C11	7.31	5.42	5.72	1.85	2.31	4.78	4.18	4.09 n.o.	7.33 +0.02	5.44 +0.02	5.67 -0.05	1.90 +0.05	2.32 +0.01	4.77 -0.01	n.o. n.o	n.o. n.o.	7.31 0.00	5.44 +0.02	5.65 -0.07	1.91 +0.06	2.33 +0.02	n.o.	n.o.	n.o. n.o.	7.37 +0.06	5.53 +0.11	5.62 -0.10	1.94 +0.09	2.39 +0.08	n.o.	n.o.	n.o. n.o.
G12	7.92	-	6.13	2.37	2.58	4.66	4.19	n.o. n.o.	7.92 0.00	-	6.10 -0.03	2.37 0.00	2.59 +0.01	4.67 +0.01	**4.15** **-0.04**	n.o. n.o.	7.91 -0.01	-	6.09 -0.05	n.o.	n.o.	n.o.	n.o.	n.o. n.o.	7.96 +0.04	-	6.07 -0.06	n.o.	n.o.	n.o.	n.o.	n.o. n.o..

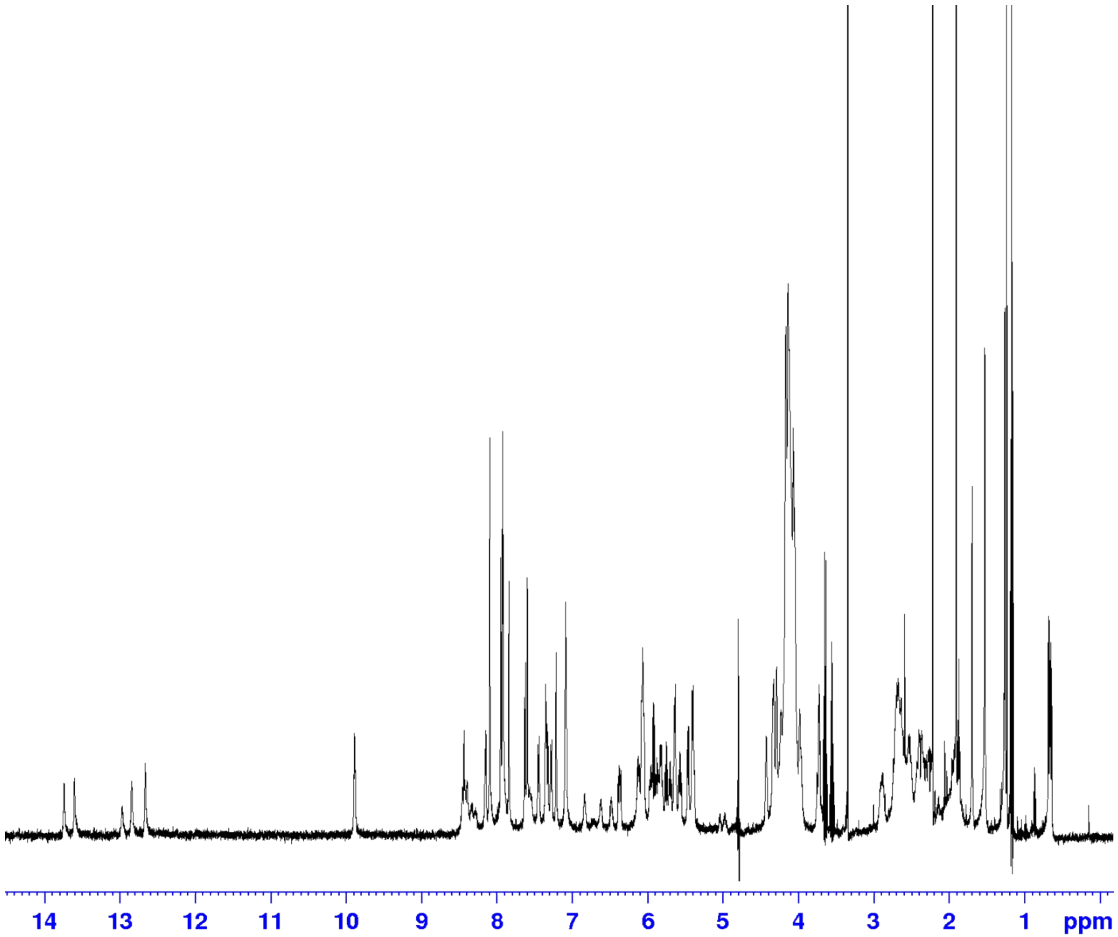

Figure S36: ^{1}H NMR Spectra of d(CGCGAATTCGCG)$_2$ upon addition of complex (6)Cl_4 at r = 0.5 in H_2O/ D_2O 9:1 (buffer phosphate 100 mM, pH = 7.0) at 298 K, 500 MHz.

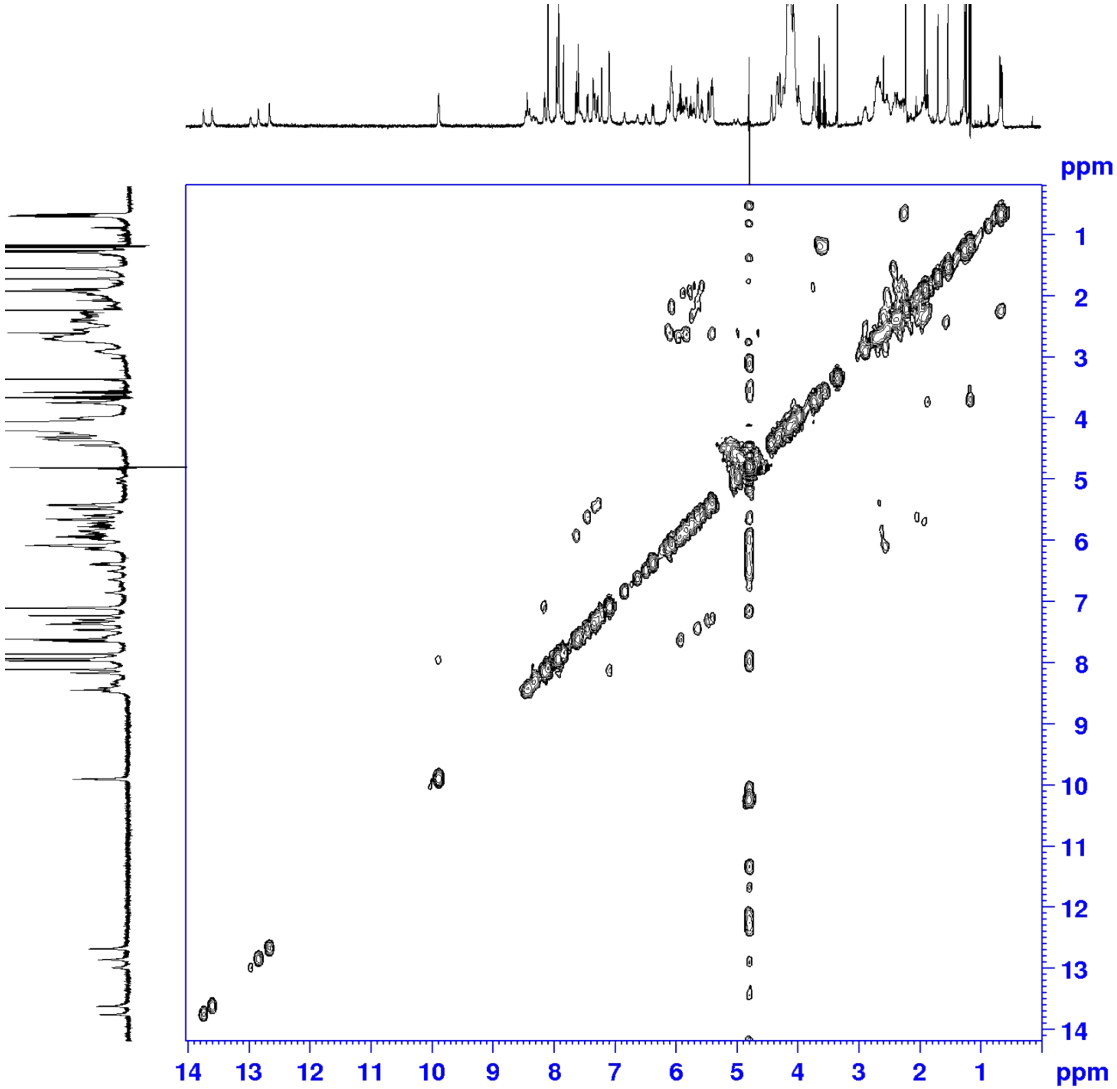

Figure S37: ^{1}H – ^{1}H COSY NMR Spectra of d(CGCGAATTCGCG)$_2$ upon addition of complex (6)Cl_4 at r = 0.5 in H_2O/ D_2O 9:1 (buffer phosphate 100 mM, pH = 7.0) at 298 K, 500 MHz.

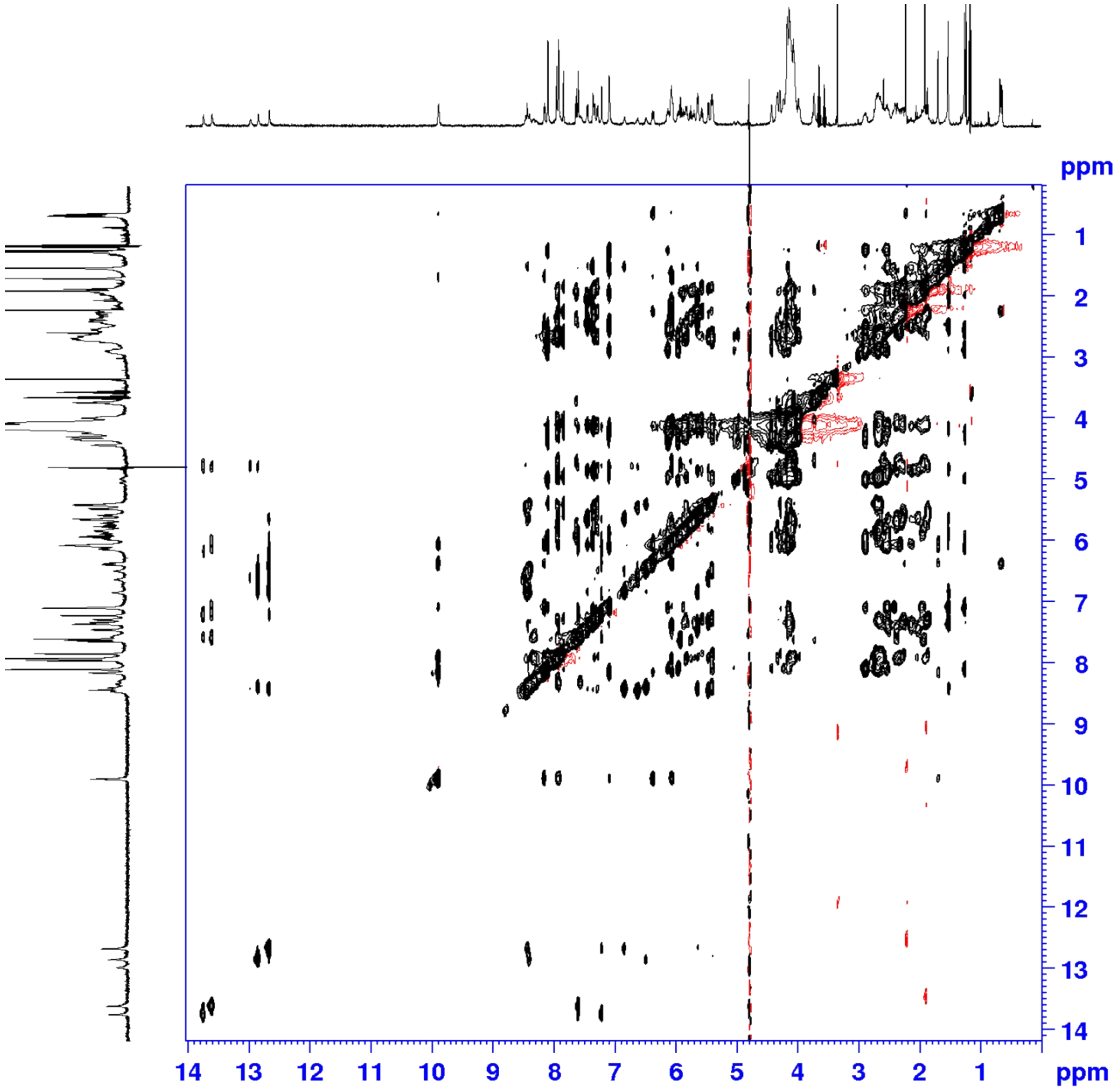

Figure S38: $^{1}H - {}^{1}H$ NOESY NMR Spectra of d(CGCGAATTCGCG)$_2$ upon addition of complex (6)Cl_4 at r = 0.5 in H_2O/ D_2O 9:1 (buffer phosphate 100 mM, pH = 7.0) at 298 K, 500 MHz, t_{mix} = 350 ms.

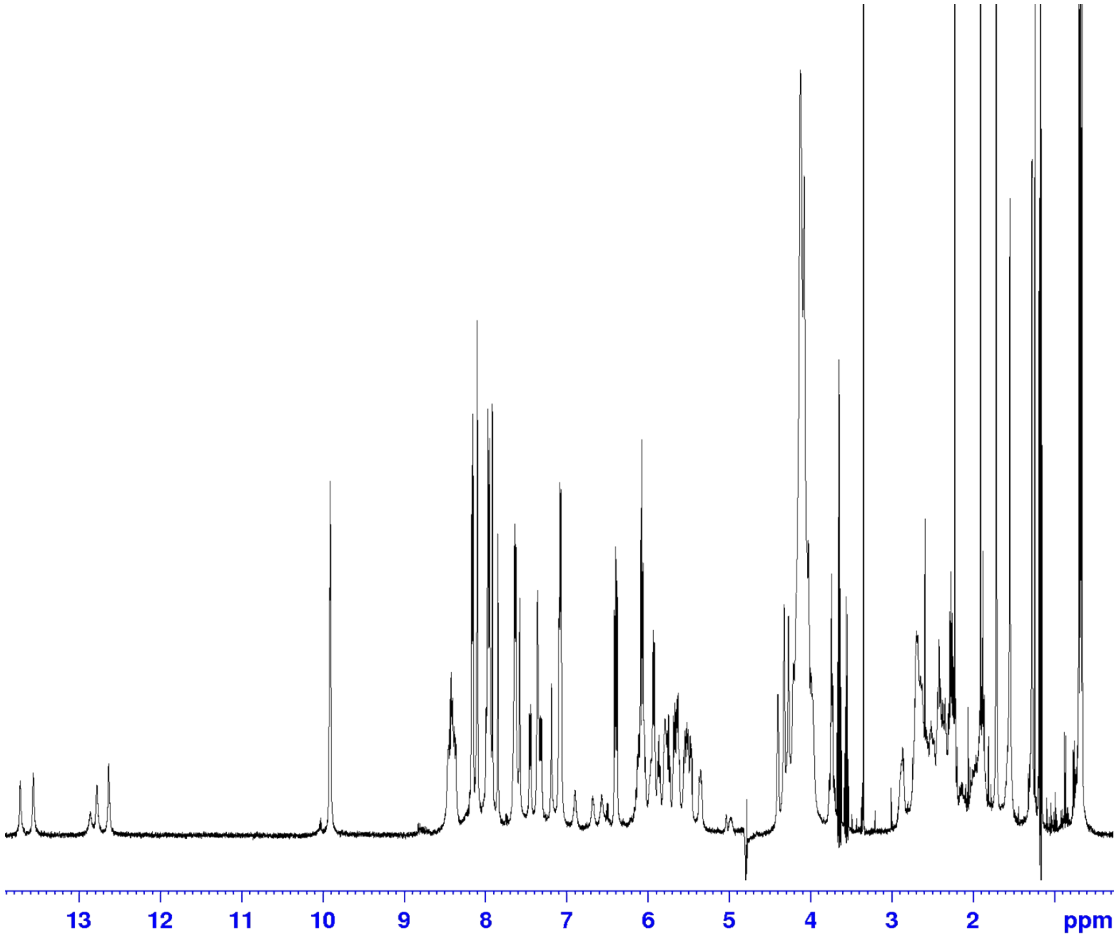

Figure S39: ^{1}H NMR Spectra of d(CGCGAATTCGCG)$_2$ upon addition of complex (6)Cl_4 at r =1 in H_2O/ D_2O 9:1 (buffer phosphate 100 mM, pH = 7.0) at 298 K, 500 MHz.

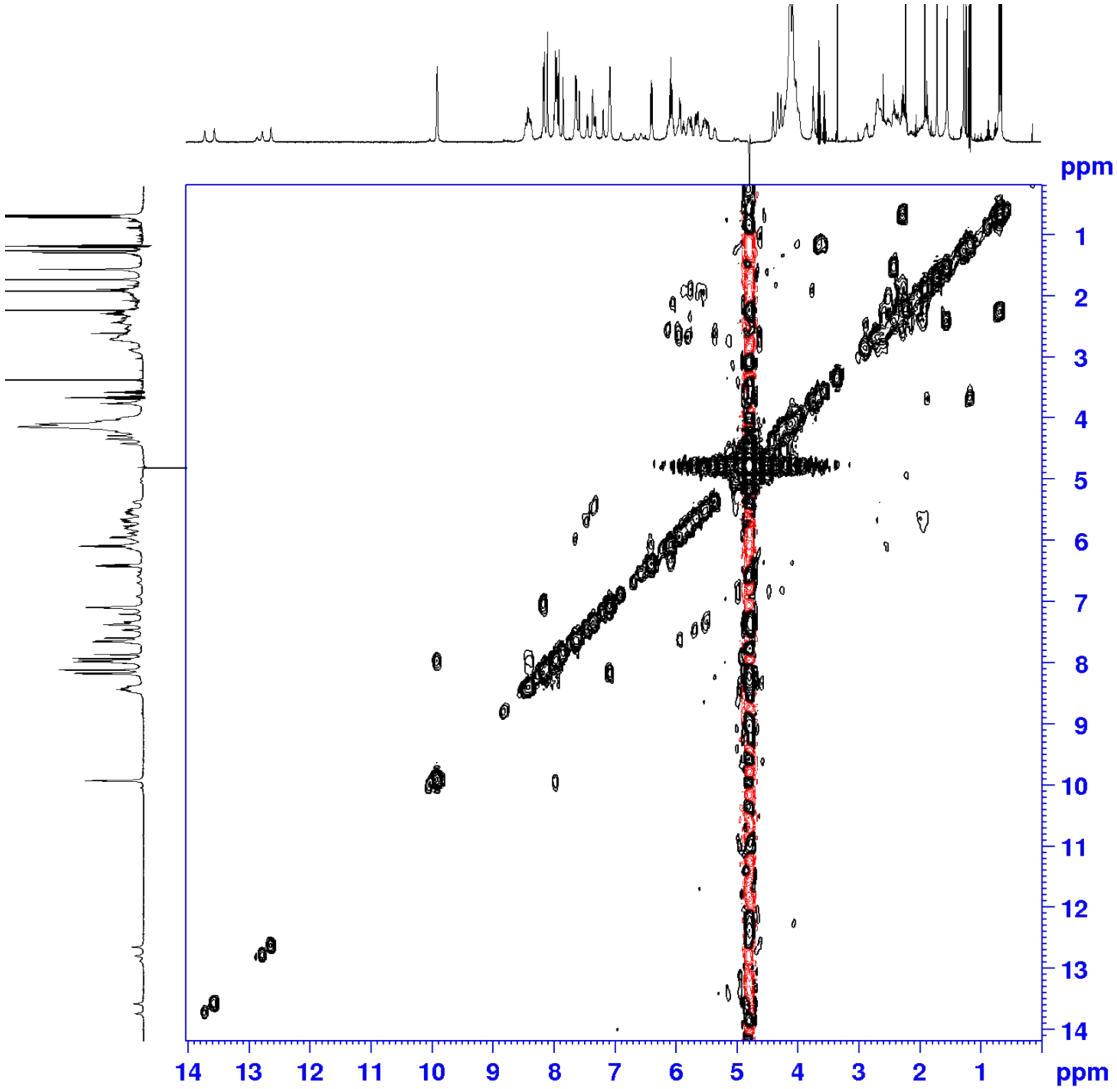

Figure S40: ^{1}H – ^{1}H COSY NMR Spectra of d(CGCGAATTCGCG)$_2$ upon addition of complex (6)Cl_4 at r = 1 in H_2O/ D_2O 9:1 (buffer phosphate 100 mM, pH = 7.0) at 298 K, 500 MHz.

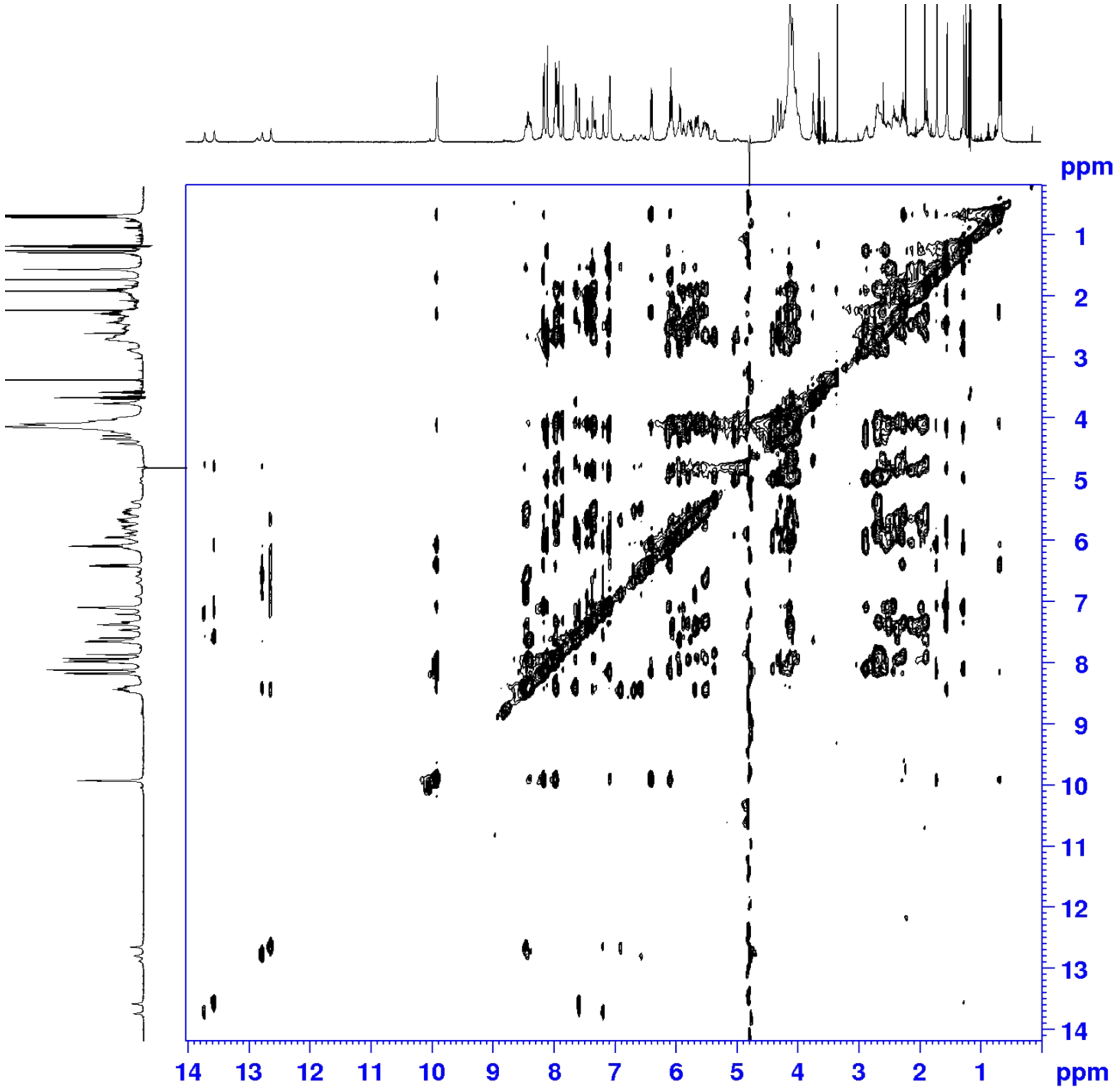

Figure S41: $^{1}H - ^{1}H$ NOESY NMR Spectra of d(CGCGAATTCGCG)$_2$ upon addition of complex (6)Cl_4 at r = 1 in H_2O/ D_2O 9:1 (buffer phosphate 100 mM, pH = 7.0) at 298 K, 500 MHz, t_{mix} = 350 ms.

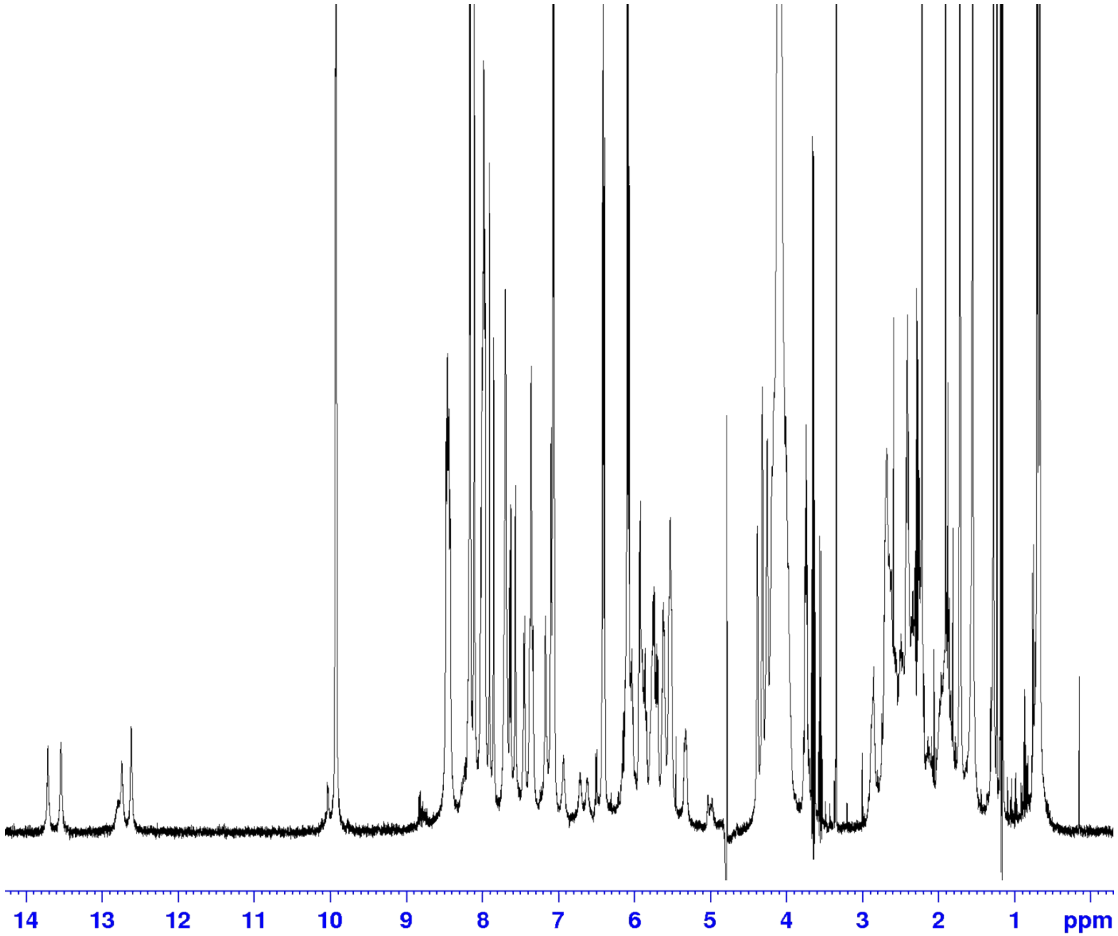

Figure S42: ^{1}H NMR Spectra of d(CGCGAATTCGCG)$_2$ upon addition of complex (6)Cl_4 at r =2 in H_2O/ D_2O 9:1 (buffer phosphate 100 mM, pH = 7.0) at 298 K, 500 MHz.

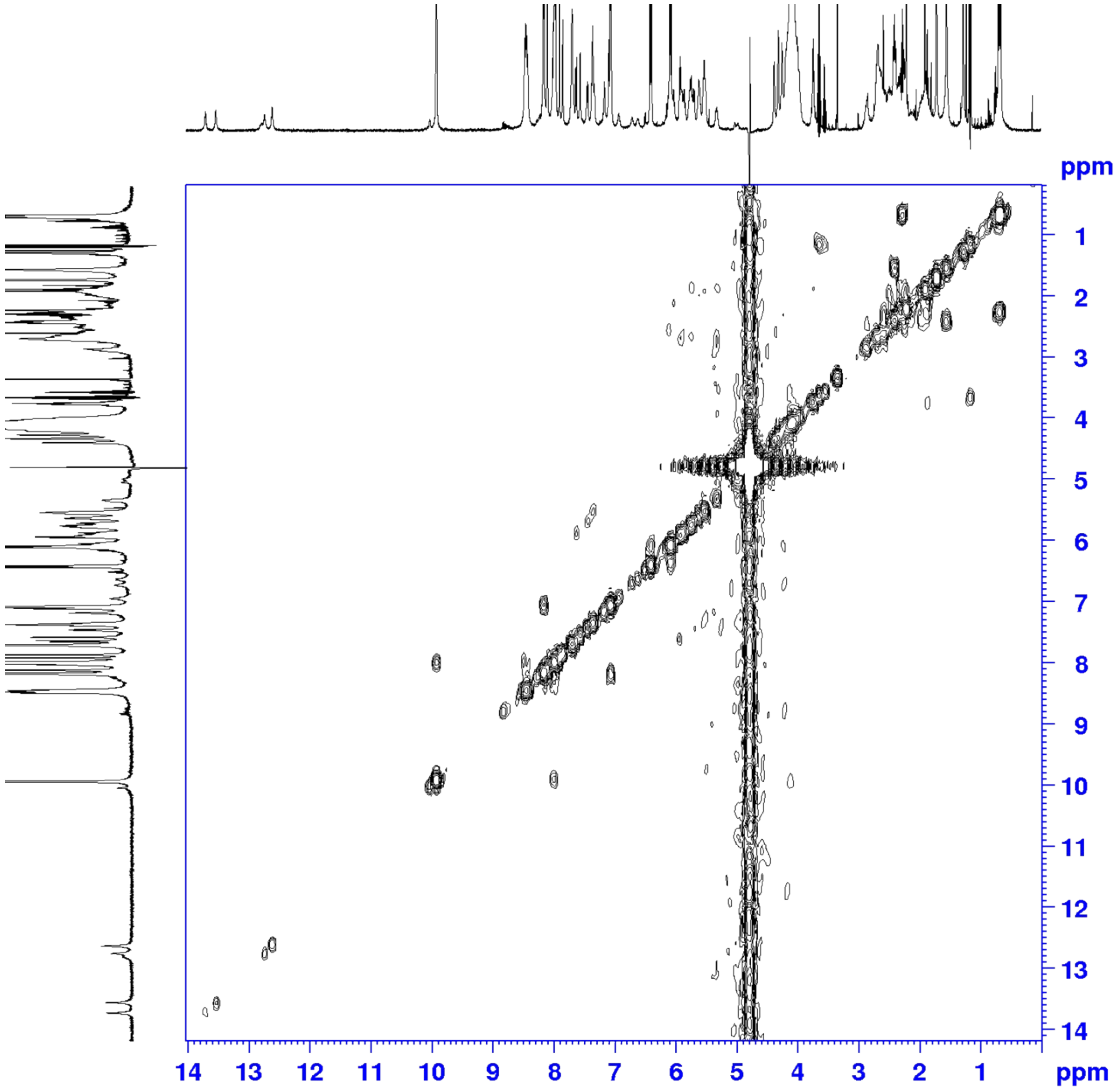

Figure S43: ^{1}H – ^{1}H COSY NMR Spectra of d(CGCGAATTCGCG)$_2$ upon addition of complex (6)Cl_4 at r = 2 in H_2O/ D_2O 9:1 (buffer phosphate 100 mM, pH = 7.0) at 298 K, 500 MHz.

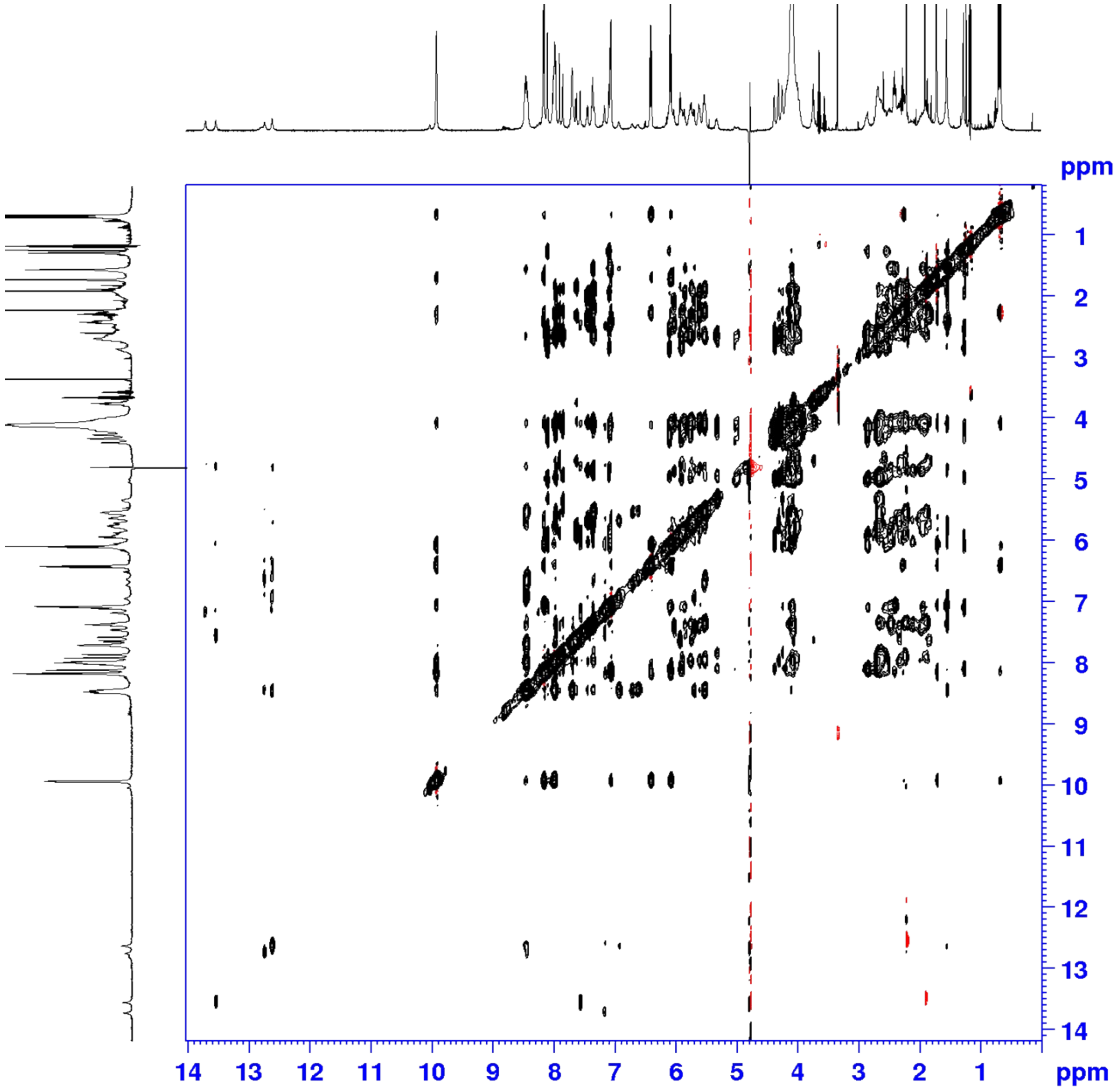

Figure S44: $^{1}H - ^{1}H$ NOESY NMR Spectra of d(CGCGAATTCGCG)$_2$ upon addition of complex (6)Cl_4 at r = 2 in H_2O/ D_2O 9:1 (buffer phosphate 100 mM, pH = 7.0) at 298 K, 500 MHz, t_{mix} = 350 ms.

Table S4: Differences in ^{1}H chemical shifts of the d(CGCGAATTCGCG)$_2$ (buffer phosphate 100 mM, pH = 7.0) upon the addition of complex (6)Cl_4 in various [Ru]/nucleotide ratios at 298 K, 500 MHz. Values in parenthesis denote upfield (-) or downfield (+) shifts from the free oligonucleotide under the same conditions.

	r = 0								r = 0.5								r = 1								r = 2							
	H8/6	H5/H2 -CH_3	H1'	H2'	H2''	H3'	H4'	H5'5''	H8/6	H5/H2 -CH_3	H1'	H2'	H2''	H3'	H4'	H5'5''	H8/6	H5/H2 -CH_3	H1'	H2'	H2''	H3'	H4'	H5'5''	H8/6	H5/H2 -CH_3	H1'	H2'	H2''	H3'	H4'	H5'5''
C1	7.60	5.88	5.72	1.89	2.37	4.60	3.91	3.69 3.72	7.63 +0.03	5.93 +0.05	5.76 +0.04	1.90 +0.01	2.39 +0.02	4.65 +0.05	3.98 +0.07	3.65 +0.04 3.73 +0.01	7.63 +0.03	5.97 +0.05	5.76 +0.04	1.90 +0.01	2.37 0.00	n.o.	n.o.	n.o. n.o.	7.63 +0.03	5.93 +0.05	5.74 +0.02	1.90 +0.01	n.o.	n.o.	n.o.	n.o. n.o.
G2	7.93	-	5.88	2.53	2.65	4.97	4.36	3.97 4.08	7.95 +0.02	-	5.89 +0.01	2.53 0.00	2.63 -0.02	4.97 0.00	4.32 -0.04	3.98 +0.01 4.08 0.00	7.97 +0.04	-	5.92 +0.04	n.o.	2.63 -0.02	4.97 0.00	4.33 -0.03	3.98 +0.01 4.07 -0.01	7.98 +0.05	-	5.90 -0.02	n.o.	2.67 +0.02	4.97 0.00	4.31 -0.05	n.o. 4.08 0.00
C3	7.25	5.35	5.56	1.81	2.22	4.77	4.10	4.12 4.15	7.28 +0.03	5.40 +0.05	5.57 +0.01	1.85 +0.04	2.21 -0.01	n.o.	n.o.	n.o. n.o.	7.31 +0.06	5.48 +0.13	5.51 -0.05	1.87 +0.06	2.22 0.00	n.o.	n.o.	n.o. n.o.	7.34 +0.09	5.53 +0.18	5.52 -0.04	1.88 +0.07	2.22 0.00	n.o.	n.o.	n.o. n.o.
G4	7.83	-	5.42	2.63	2.74	4.97	4.39	3.97 4.06	7.84 +0.01	-	5.40 -0.02	2.63 0.00	2.72 -0.02	4.97 0.00	4.34 -0.05	3.98 +0.01 4.08 +0.02	7.84 +0.01	-	5.35 -0.07	2.63 0.00	2.74 0.00	4.97 0.00	4.33 -0.06	3.98 +0.01 4.07 -0.01	7.85 +0.02	-	5.32 -0.10	2.60 -0.03	2.69 -0.05	4.97 0.00	4.31 -0.08	n.o. 4.08 +0.02
A5	8.09	7.21	5.97	2.67	2.89	5.03	4.45	4.15 4.19	8.09 0.00	7.21 0.00	5.96 -0.01	2.67 0.00	2.89 0.00	5.04 +0.01	4.42 -0.03	4.13 -0.02 n.o.	8.10 +0.01	7.18 -0.03	5.92 -0.05	2.67 0.00	2.88 -0.01	5.03 0.00	4.41 -0.04	4.14 -0.01 n.o.	8.10 +0.01	7.17 -0.04	5.93 -0.04	2.64 -0.03	2.87 -0.02	5.04 +0.00	4.38 -0.07	4.11 -0.04 n.o.
A6	8.09	7.60	6.13	2.57	2.90	4.99	4.45	n.o. 4.25	8.09 0.00	7.60 0.00	6.13 0.00	2.57 0.00	2.89 -0.01	4.98 -0.01	4.42 -0.03	n.o 4.23 -0.02	8.10 +0.01	7.58 -0.02	6.10 -0.03	2.58 +0.01	2.88 -0.02	4.97 -0.02	4.41 -0.04	n.o. 4.27 +0.02	8.10 +0.01	7.58 -0.02	6.10 -0.03	2.55 -0.02	2.87 -0.03	4.97 -0.02	4.38 -0.07	n.o. 4.26 +0.01
T7	7.09	1.24	5.88	1.95	2.53	4.81	4.14	4.15	7.08 -0.01	1.26 +0.02	5.88 0.00	1.95 0.00	2.54 +0.01	4.89 +0.08	4.14 0.00	n.o. n.o.	7.08 -0.01	1.27 +0.03	5.86 -0.02	1.95 0.00	2.52 -0.01	4.90 +0.10	n.o.	n.o. n.o.	7.08 -0.01	1.28 +0.04	5.86 -0.02	1.95 0.00	2.52 -0.01	4.89 +0.08	n.o.	n.o. n.o.
T8	7.35	1.51	6.12	2.14	2.53	4.88	4.19	4.09	7.35 0.00	1.53 +0.02	6.06 -0.06	2.18 +0.04	2.63 +0.10	4.92 +0.04	4.16 -0.03	3.98	7.35 0.00	1.54 +0.03	6.05 -0.07	2.14 0.00	n.o.	4.88 0.00	4.14 -0.05	n.o. n.o.	7.34 -0.01	1.55 +0.04	6.03 -0.09	2.10 -0.04	n.o.	4.91 +0.03	4.20 +0.01	n.o. n.o.
C9	7.44	5.60	5.64	2.04	2.39	4.86	4.14	4.10 4.17	7.44 0.00	5.64 +0.04	5.64 0.00	2.07 +0.03	2.39 0.00	4.88 +0.02	4.14 0.00	n.o. n.o.	7.45 +0.01	5.68 +0.04	5.65 +0.01	2.05 +0.01	2.39 0.00	4.90 +0.04	n.o	n.o	7.44 0.00	5.70 +0.10-	5.70 +0.06	2.05 +0.01	2.40 +0.01	4.90 -0.07	4.13 -0.01	n.o. n.o
G10	7.89	-	5.83	2.54	2.67	4.97	4.41	4.04 4.15	7.91 +0.02	-	5.82 -0.01	2.53 -0.01	2.63 -0.04	4.97 0.00	4.42 +0.01	4.05 +0.01 4.16 +0.01	7.91 +0.02	-	5.79 -0.04	2.55 +0.01	2.68 +0.01	4.97 0.00	4.42 +0.01	4.07 +0.03 4.14	7.91 +0.02	-	5.78 -0.05	n.o.	2.64 -0.03	4.97 0.00	4.38 -0.03	4.08 +0.04 4.11 -0.05
C11	7.31	5.42	5.72	1.85	2.31	4.78	4.18	4.09 n.o.	7.33 +0.02	5.47 +0.05	5.69 -0.03	1.85 0.00	2.30 -0.01	4.68 -0.10	4.17 -0.01	n.o. n.o.	7.36 +0.05	5.51 +0.09	5.64 -0.08	1.87 +0.02	2.33 +0.02	4.76 -0.02	4.64 +0.14	n.o. n.o.	7.37 +0.06	5.53 +0.11	5.62 -0.10	1.88 +0.03	2.33 +0.02	n.o	n.o	n.o. n.o.
G12	7.92	-	6.13	2.37	2.58	4.66	4.19	n.o. n.o.	7.92 0.00	-	6.07 -0.06	2.37 0.00	2.58 0.00	4.66 0.00	4.17 -0.02	n.o. n.o.	7.92 0.00	-	6.06 -0.07	n.o.	2.58 0.00	4.70 +0.04	4.13 +0.06	n.o. n.o.	7.96 +0.04	-	6.07 -0.06	2.41 +0.04	2.54 -0.04	4.70 +0.04	4.13 -0.06	n.o. n.o.

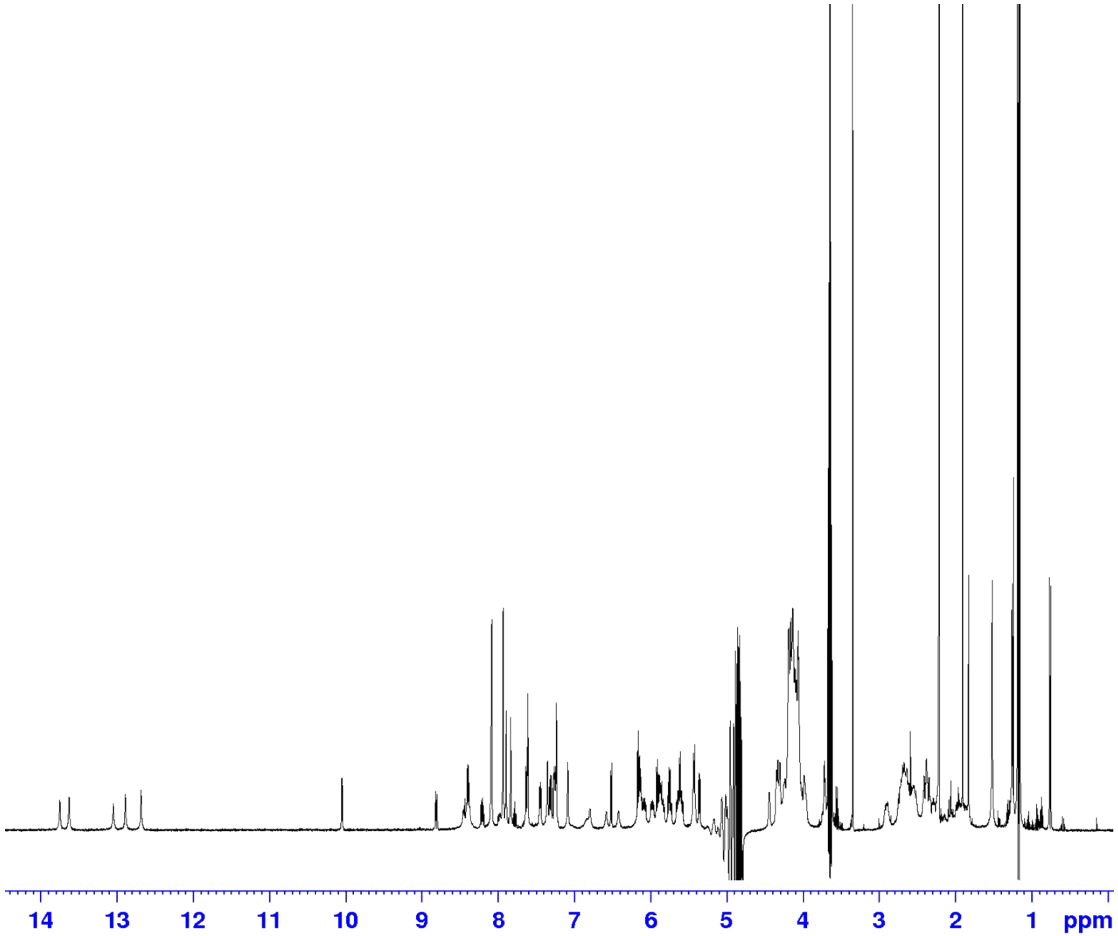

Figure S45: ^{1}H NMR Spectra of d(CGCGAATTCGCG)$_2$ upon addition of the (7)Cl_2 at r =0.5 in H_2O/ D_2O 9:1 (buffer phosphate 100 mM, pH = 7.0) at 298 K, 500 MHz.

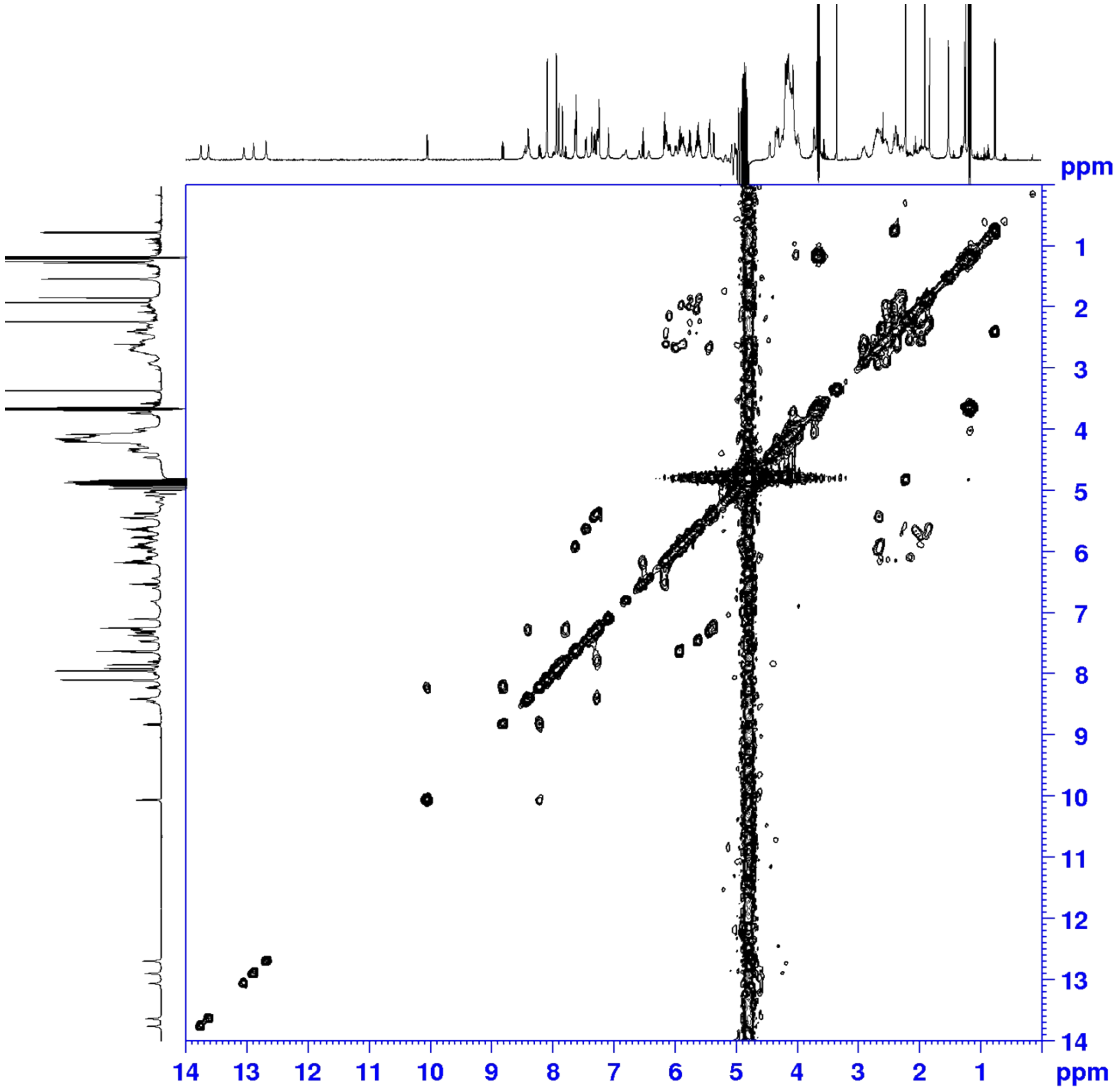

Figure S46: $^{1}H - {}^{1}H$ COSY NMR Spectra of d(CGCGAATTCGCG)$_2$ upon addition of the (7)Cl_2 at r =0.5 in H_2O/ D_2O 9:1 (buffer phosphate 100 mM, pH = 7.0) at 298 K, 500 MHz.

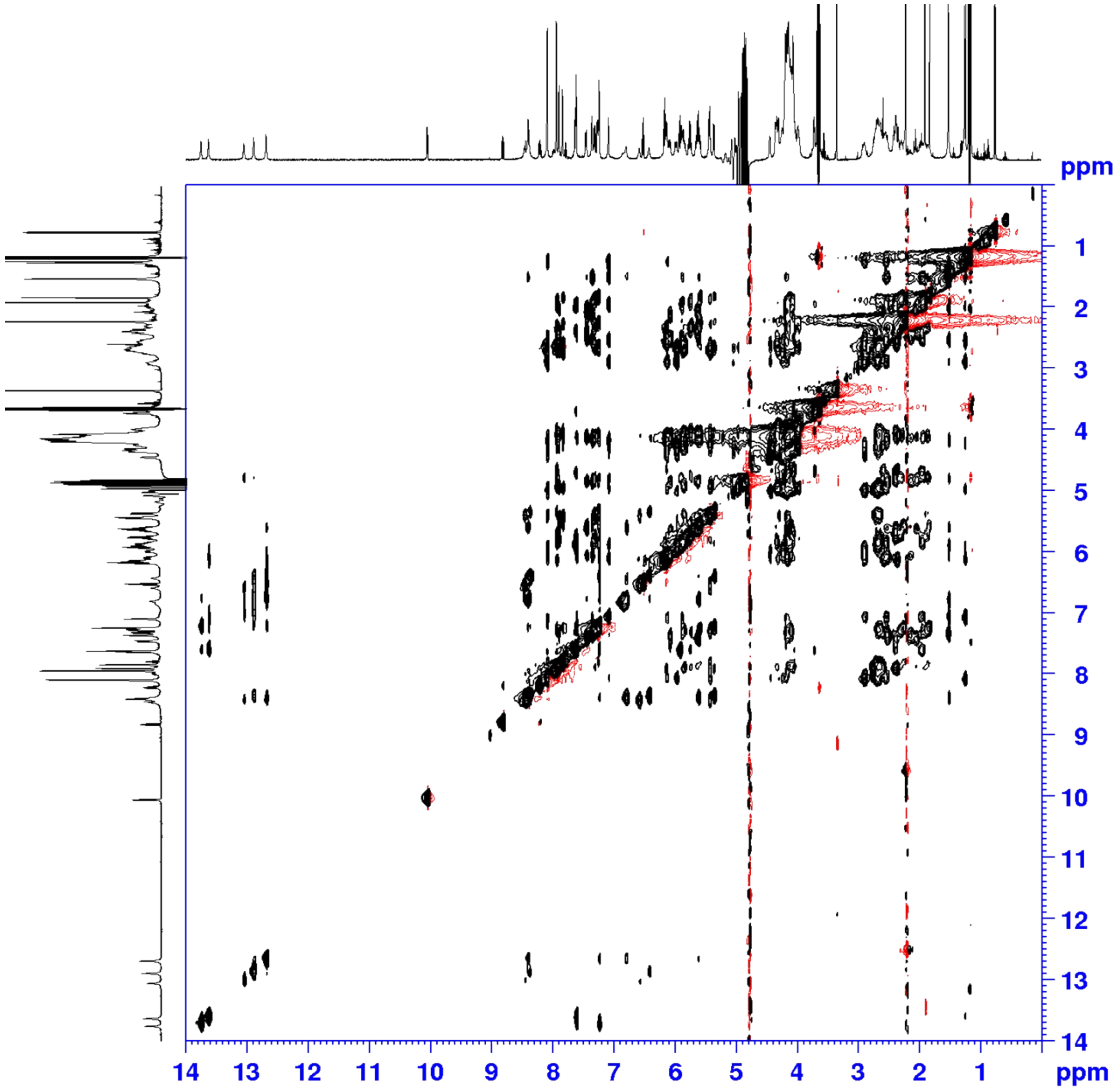

Figure S47: $^{1}H - ^{1}H$ NOESY NMR Spectra of d(CGCGAATTCGCG)$_2$ upon addition of the (7)Cl_2 at r =0.5 in H_2O/ D_2O 9:1 (buffer phosphate 100 mM, pH = 7.0) at 298 K, 500 MHz, t_{mix} = 350 ms.

Calculation of complexes Binding Parameters.

Fluorescence quenching property described by the Stern-Volmer equation [1]:

$$F_0/F = 1 + K_{SV}[Q] = 1 + k_q\tau_0[Q]$$

where F_0 and F are the fluorescence intensities in the absence and the presence of quencher, respectively. K_{SV} is the Stern-Volmer quenching constant and [Q] is the concentration of complex. The slope of the linear plot of F_0/F versus [Q] shows the value of K_{SV}.

According to the equation:

$$K_{SV} = k_q\tau_0$$

where K_q is the biomolecular quenching rate constant, τ_0 is the average lifetime of the molecule without the quencher that is equal to 10^{-8} s [2], can be found if quenching mechanism is static (the ground-state complex formation between a quencher and a fluorophore) or dynamic (a collisional process) [3].

The number of binding sites (n) and binding constant (K_b) between the complexes and $d(CGCGAATTCGCG)_2$ determined using the following double logarithmic equation [4]:

$$\log[(F_O\text{-}F)/F] = n\log[Q] + \log K_b$$

The plot $\log[F_O\text{-}F/F]$ versus log[Q] is a straight line and the values of n and K_b can be found from slope and the intercept of the plot respectively, at three different temperatures.

The thermodynamic parameters calculated from the Van't Hoff equation [5]:

$$lnK = -\frac{\Delta H^\circ}{R}\frac{1}{T} + \frac{\Delta S^\circ}{R}$$

where K is the binding constant, R is the gas constant, and T is the temperature. The free energy of Gibbs is obtained from the equation [6]:

$$\Delta G^\circ = \Delta H^\circ - T\Delta S^\circ = -RT\ln K$$

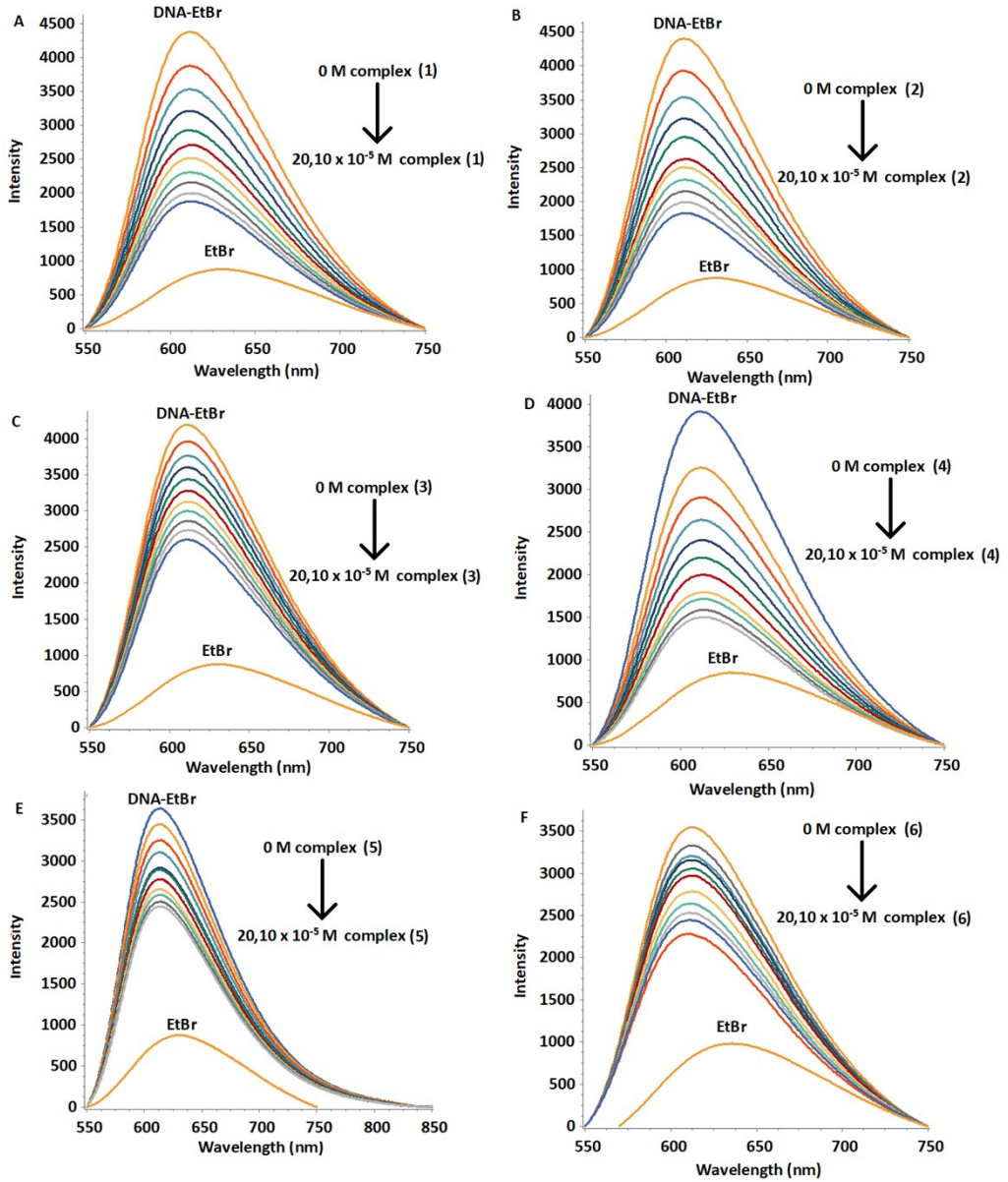

Figure S48: Fluorescence emission spectra of DNA–EtBr system with various concentration of complex (**1**) {A}, complex (**2**) {B}, complex (**3**) {C}, complex (**4**) {D}, complex (**5**) {E} and complex (**6**) {F}. [DNA] = 20 µM, [EB] = 5.2 µM, concentration of complexes = 0 – 20.10 µM at 291 K.

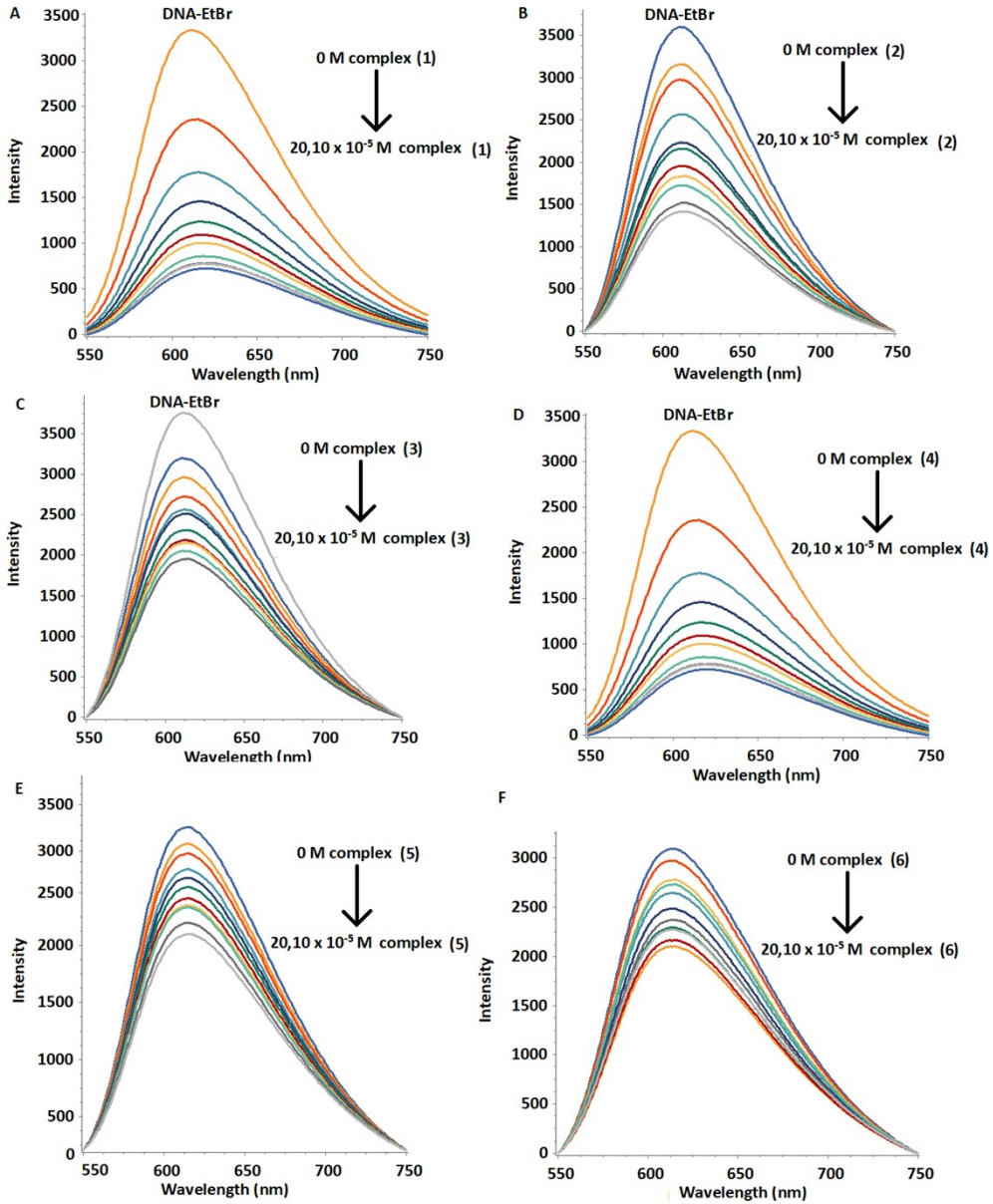

Figure S49: Fluorescence emission spectra of DNA–EtBr system with various concentration of complex (**1**) {A}, complex (**2**) {B}, complex (**3**) {C}, complex (**4**) {D}, complex (**5**) {E} and complex (**6**) {F}. [DNA] = 20 µM, [EB] = 5.2 µM, concentration of complexes = 0 – 20.10 µM at 310 K.

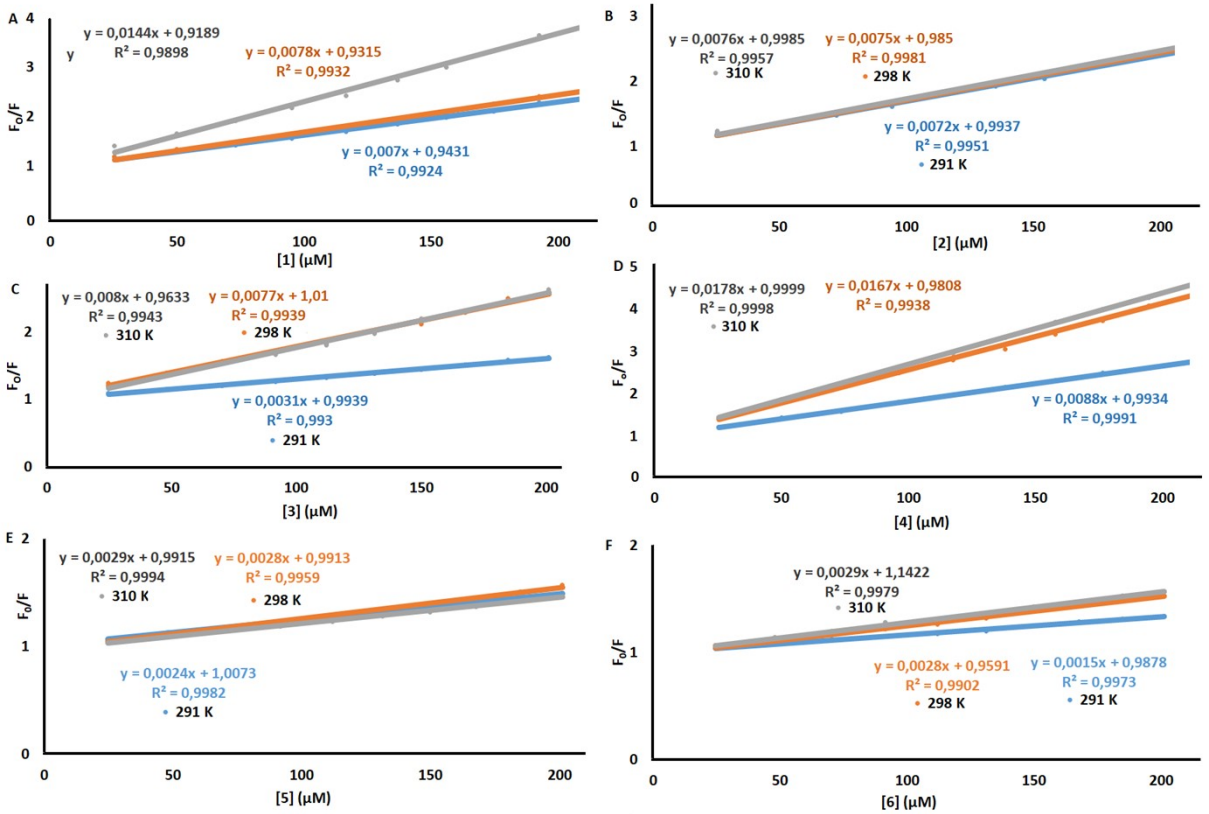

Figure S50: Stern–Volmer plots for the interaction of complexes with DNA–EtBr at three different temperatures (291 K, 298 K, and 310 K).

Table S5: Binding parameters of the bimetallic Ru(II) complexes with $d(CGCGAATTCGCG)_2$ at 291 K and 310 K.

Complex	K_{sv} (10^4 M^{-1})	K_q (10^{11} M^{-1} s^{-1})	K_b (10^3 M^{-1})	n	percentage quenching
(1)	0.7018 ± 0.081 (291 K) 1,4423 ± 0.076 (310 K)	7.018 (291 K) 14.423 (310 K)	6.894 ± 0.001 (291 K) 19.124 ± 0.001 (310 K)	1.00 (291 K) 1.04 (310 K)	73.12 84.38
(2)	0.7233 ± 0.034 (291 K) 0.7572 ± 0.029 (310 K)	7.233 (291 K) 7.572 (310 K)	3.173 ± 0.001 (291 K) 16.195 ± 0.001 (310 K)	0.92 (291 K) 1.10 (310 K)	65,45 69.19
(3)	0.3057 ± 0.027 (291 K) 0.8038 ± 0.029 (310 K)	3.057 (291 K) 8.038 (310 K)	1.567 ± 0.001 (291 K) 8.179 ± 0.001 (310 K)	0.96 (291 K) 1.00 (310 K)	48.66 70.41
(4)	8.7854 ± 0.085 (291 K) 17.807 ± 0.078 (310 K)	87.854 (291 K) 178.07 (310 K)	8.970 ± 0.001 (291 K) 18.352 ± 0.001 (310 K)	1.00 (291 K) 1.00 (310 K)	81,67 91.29
(5)	0.2415 ± 0.017 (291 K) 0.2899 ± 0.020 (310 K)	2.415 (291 K) 2.899 (310 K)	1.718 ± 0.001 (291 K) 4.106 ± 0.001 (310 K)	0.96 (291 K) 1.04 (310 K)	37.92 52.03
(6)	0.1673 ± 0.026 (291 K) 0.2863 ± 0.024 (310 K)	1.485 (291 K) 2.877 (310 K)	1.663 ± 0.001 (291 K) 15.114 ± 0.001 (310 K)	1.00 (291 K) 1.21 (310 K)	34.20 41.68

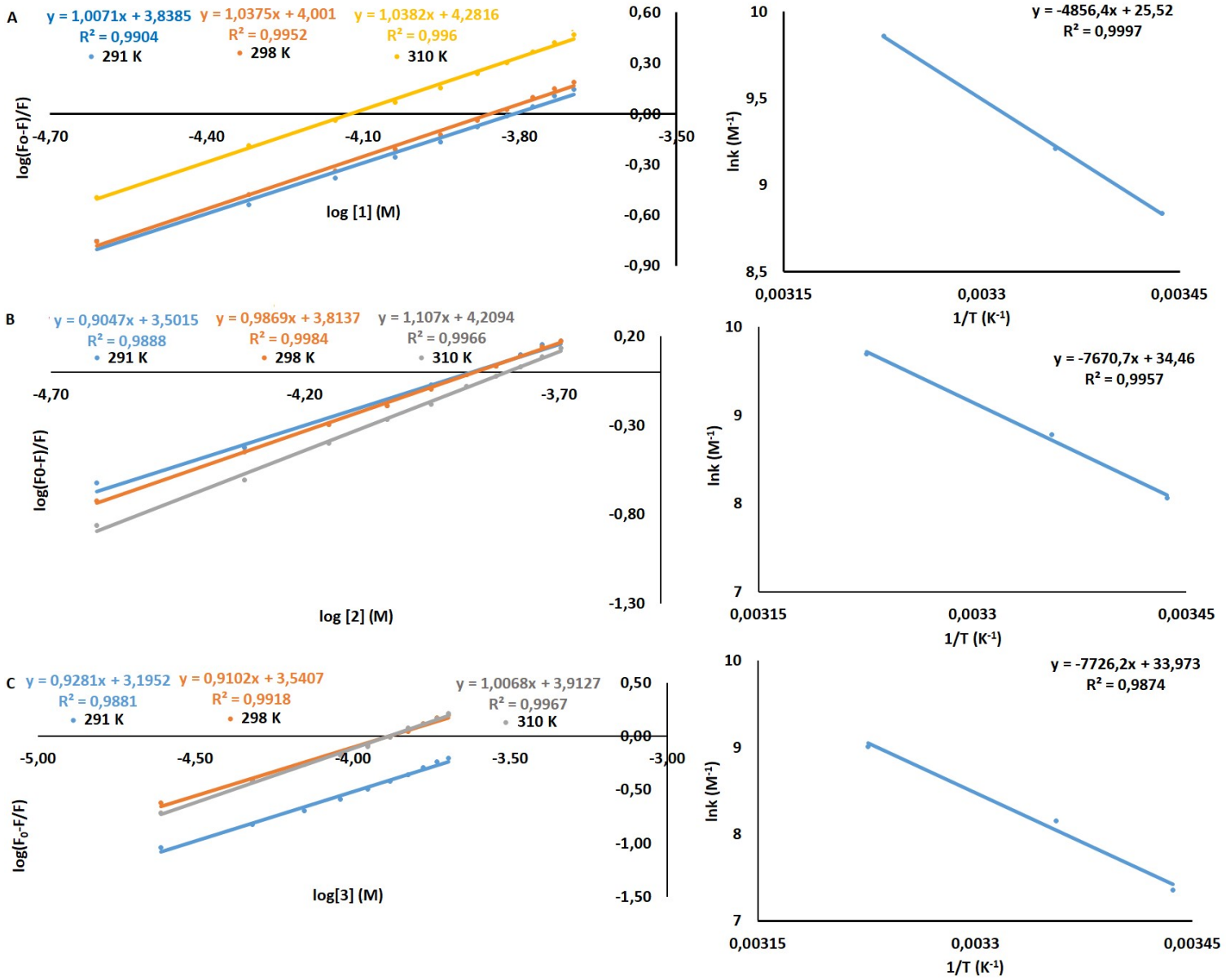

Figure S51: The double-log plot of complexes quenching effect on d(CGCGAATTCGCG)$_2$-EtBr system fluorescence at three different temperatures (291 K, 298 K and 310 K) and the van't Hoff plot for the binding of complexes with d(CGCGAATTCGCG)$_2$. (A) for complex **(1)**, (B) for complex **(2)** and (C) for complex **(3)**.

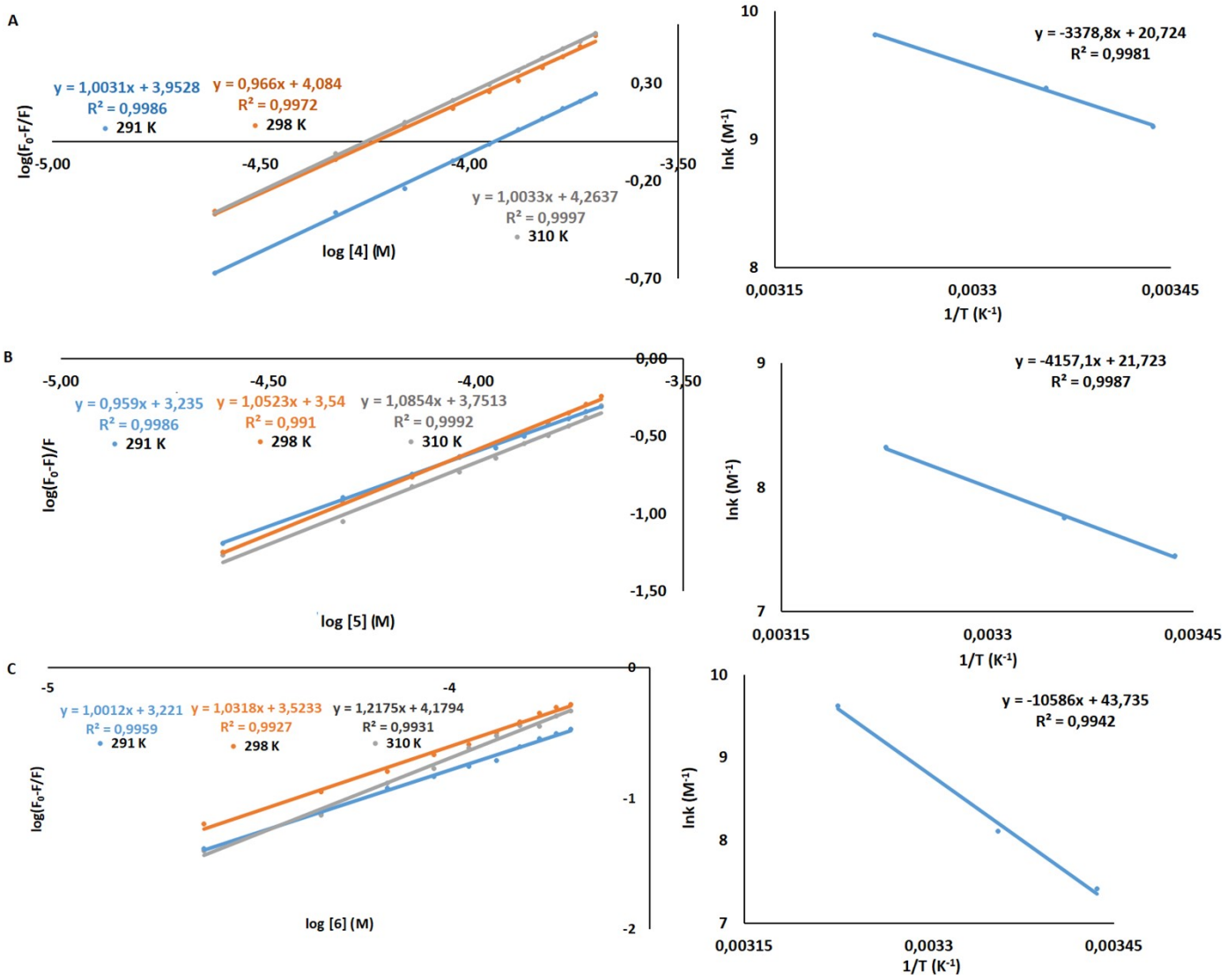

Figure S52: The double-log plot of complexes quenching effect on d(CGCGAATTCGCG)$_2$-EtBr system fluorescence at three different temperatures (291 K, 298 K and 310 K) and the van't Hoff plot for the binding of complexes with d(CGCGAATTCGCG)$_2$. (A) for complex **(4)**, (B) for complex **(5)** and (C) for complex **(6)**.

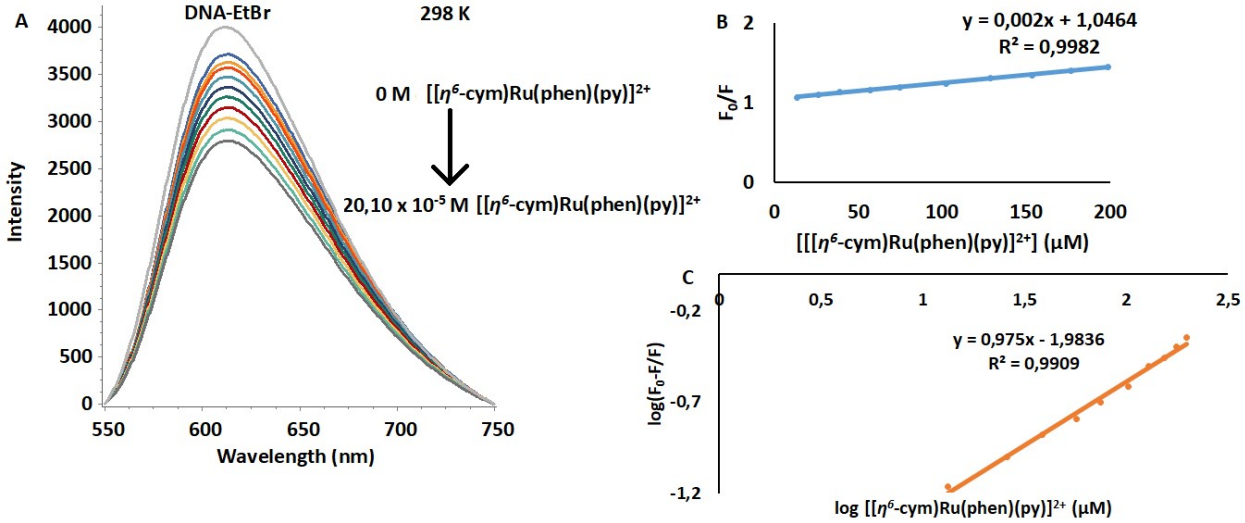

Figure S53: Fluorescence emission spectra of DNA–EtBr system with various concentration of complex $[[\eta^6\text{-cym})Ru(phen)(py)]^{2+}$. [DNA] = 20 μM, [EB] = 5.2 μM, and $[[\eta^6\text{-cym})Ru(phen)(py)]^{2+}$ = 0 – 20.10 μM at 298 K (A). Stern–Volmer plots for the interaction of $[[\eta^6\text{-cym})Ru(phen)(py)]^{2+}$ with DNA–EtBr at 298 K (B). The double-log plot of complex $[[\eta^6\text{-cym})Ru(phen)(py)]^{2+}$ quenching effect on $d(CGCGAATTCGCG)_2$-EtBr system fluorescence at 298 K (C).

Table S6: Thermodynamic parameters of the bimetallic Ru(II) complexes with $d(CGCGAATTCGCG)_2$ at 291 K and 310 K.

Complex	ΔH° (kJ/mol)	ΔS°(J/mol)	ΔG° (kJ/mol)
(1)	40.38 ± 0.019	212.18 ± 0.065	-21.37 ± 0.034 (291 K) -25.40 ± 0.033 (310 K)
(2)	63.77 ± 0.108	286.51 ± 0.366	-19.59 ± 0.221 (291 K) -25.04 ± 0.222 (310 K)
(3)	64.24 ± 0.187	282.46 ± 0.630	-17.96 ± 0.376 (291 K) -23.32 ± 0.372 (310 K)
(4)	40.38 ± 0.032	212.18 ± 0.107	-22.05 ± 0.063 (291 K) --25.32 ± 0.068 (310 K)
(5)	34.56 ± 0.032	180.61 ± 0.108	-17.99 ± 0.063 (291 K) -21.42 ± 0.067 (310 K)
(6)	88.01 ± 0.172	363.63 ± 0.581	-17.80 ± 0.341 (291 K) -24.71 ± 0.348 (310 K)

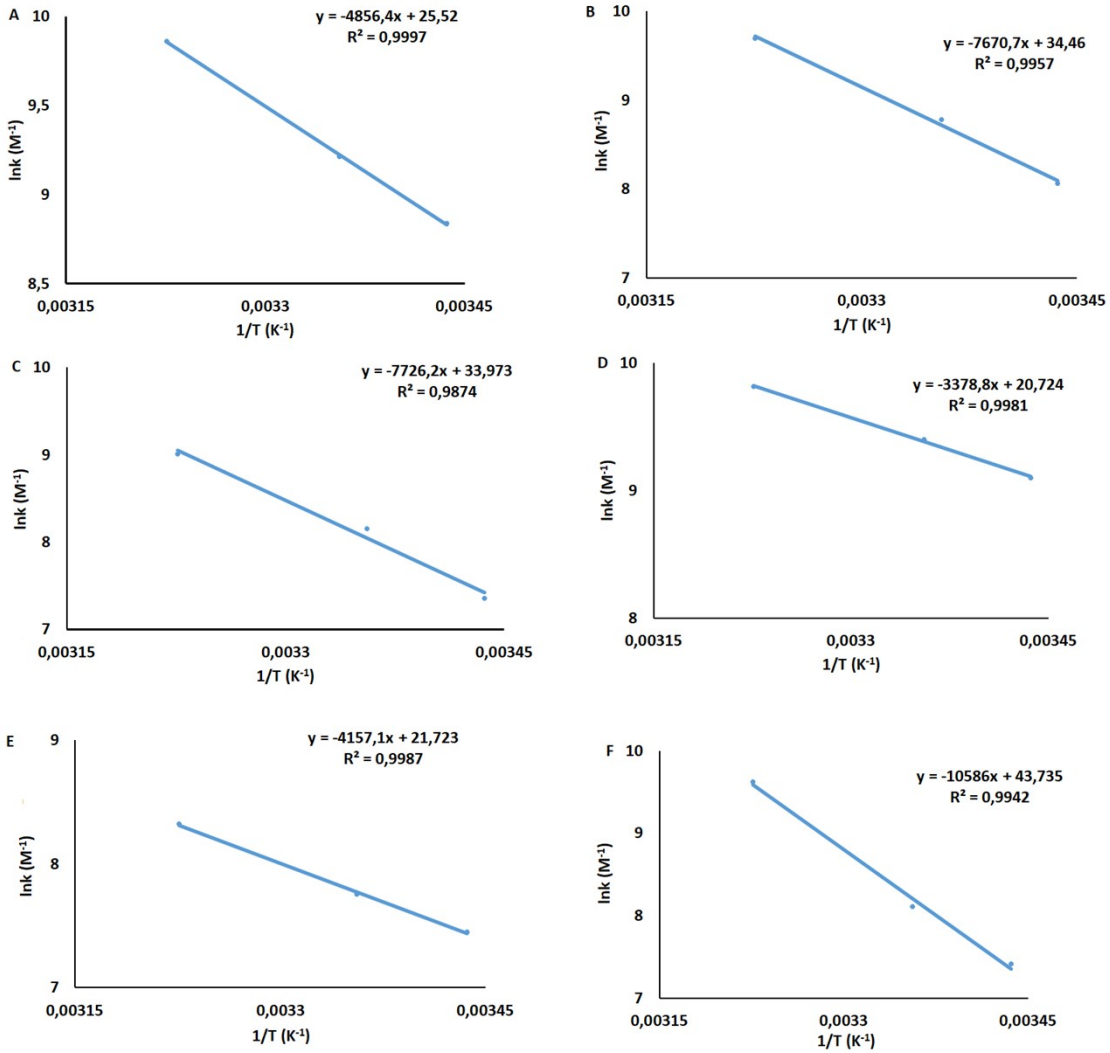

Figure S54: The van't Hoff plots for the binding of complexes with d(CGCGAATTCGCG)$_2$. (A) for complex **(1)**, (B) for complex **(2)**, (C) for complex **(3)**, (D) for complex **(4)**, (E) for complex **(5)** and (F) for complex **(6)**.